

PDF hosted at the Radboud Repository of the Radboud University Nijmegen

The following full text is a publisher's version.

For additional information about this publication click this link.

<http://hdl.handle.net/2066/82964>

Please be advised that this information was generated on 2017-12-06 and may be subject to change.

**Novel tools for tissue engineering:
DEVELOPMENT AND EVALUATION OF
COLLAGEN-BASED BIOMATERIALS**

Paul Geutjes

**Novel tools for tissue engineering:
DEVELOPMENT AND EVALUATION OF COLLAGEN-BASED BIOMATERIALS**

Geutjes, Petrus Johannes

Thesis Radboud University Nijmegen Medical Centre, Nijmegen, The Netherlands

ISBN 978-90-9025720-4

©2010, by Paul Geutjes

All rights reserved

No parts of this publication may be reproduced in any form without permission of the author.

Cover design: Paul Geutjes

Printing: Drukkerij Ravenstein & UP Reclame Ravenstein

Novel tools for tissue engineering: DEVELOPMENT AND EVALUATION OF COLLAGEN-BASED BIOMATERIALS

Een wetenschappelijke proeve op het gebied van de
Medische Wetenschappen

Proefschrift

ter verkrijging van de graad van doctor
aan de Radboud Universiteit Nijmegen
op gezag van de rector magnificus prof. mr. S.C.J.J. Kortmann,
volgens besluit van het college van decanen
in het openbaar te verdedigen op donderdag 11 november 2010
om 13.30 uur precies

door

Petrus Johannes Geutjes

geboren op 27 juni 1977
te Wijchen

PROMOTOR:

Prof. dr. R.E. Brock

COPROMOTORES:

Dr. T.H. van Kuppevelt
Dr. ir. W.F. Daamen
Dr. J.A. van der Vliet

MANUSCRIPTCOMMISSIE:

Prof. dr. J.A. Jansen
Prof. dr. R.A. Bank (UMC Groningen)
Prof. dr. P. Buma

PARANIMFEN:

Dr. Dennis Link
Frank Geutjes

The studies presented in this thesis were performed at the Department of Biochemistry, Nijmegen Centre for Molecular Life Sciences (NCMLS), Radboud University Nijmegen Medical Centre, Nijmegen, The Netherlands, and were financially supported by Aap bio implants - EMCM BV, Nijmegen, The Netherlands.

The publication of this thesis was financially supported by:
Radboud University Nijmegen Medical Centre, Aap bio implants – EMCM BV, Symatase Biomatériaux, Urogyn BV, Dutch Society for Biomaterials and Tissue Engineering (NBTE), Nijmegen Centre for Molecular Life Sciences (NCMLS), Drukkerij Ravenstein, UP Reclame Ravenstein, Zirbus Technology Benelux BV



TABLE OF CONTENTS

7	Chapter 1 General introduction & Aim of the study. From molecules to matrix: construction and evaluation of molecularly-defined bioscaffolds. <i>Advances in Experimental Medicine and Biology</i> 2006;585:279-95.
25	Chapter 2 Expression, production and biological activity analyses of recombinant rat-VEGF-164. <i>Protein Expression and Purification</i> 2010;69(1):76-82.
39	Chapter 3 Increased angiogenesis and blood vessel maturation in acellular collagen-heparin scaffolds containing both FGF2 and VEGF. <i>Biomaterials</i> 2007;28(6):1123-31.
53	Chapter 4 An animal model for femoral artery pseudoaneurysms. <i>Journal of Vascular and Interventional Radiology</i> 2010;21(7):1078-83.
65	Chapter 5 Preparation and characterisation of injectable fibrillar type I collagen and evaluation for pseudoaneurysm treatment in a pig model. <i>Journal of Vascular Surgery</i> 2010. <i>In press</i> .
81	Chapter 6 Preparation of differently sized injectable collagen micro-scaffolds. <i>Journal of Tissue Engineering and Regenerative Medicine</i> 2010. <i>In press</i> .
87	Chapter 7 “Lyophilisomes”: a new type of (bio)capsule. <i>Advanced Materials</i> 2007;19(5):673-77.
97	Chapter 8 Summary and future directions Samenvatting en toekomstvisie
105	Chapter 9 Author information: Curriculum Vitae, List of publications and Dankwoord
112	Colour figures

ABBREVIATIONS USED IN THIS THESIS

AMP	ampicillin resistance gene
AOX-1	alcohol oxidase
AU	arbitrary unit
FGF-2	basic fibroblast growth factor
BMGY	buffered glycerol-complex medium
BMMY	buffered methanol-complex medium
BSA	bovine serum albumin
COL	collagen
CLSM	confocal laser scanning microscopy
CS	chondroitin sulfate
DEAE	diethylaminoethyl
DNA	deoxyribonucleic acid
dNTP	deoxynucleoside triphosphate
DO	dissolved oxygen
DS	dermatan sulfate
EC	ethics committee
ECGF	endothelial cell growth factor
ECM	extracellular matrix
EDC	1-ethyl-3-(3-dimethyl aminopropyl) carbodiimide
EGF	epidermal growth factor
EL	elastin
EvG	elastin von Gieson
EtO	ethylene oxide gas
FA	femoral artery
FCS	foetal calf serum
FGF	fibroblast growth factor
FPLC	fast protein liquid chromatography
GAG	glycosaminoglycan
HA	hyaluronic acid
HE	haematoxylin eosin
His	histidine
HS	heparan sulfate
HUVEC	human umbilical vein endothelial cell
KS	keratan sulfate
LM	light microscopy
LMW	low molecular weight
MMP	matrix metalloproteinase
MES	2-morpholinoethane sulfonic acid
NHS	N-hydroxysuccinimide
NIH	National Institutes of Health
NSAID	non-steroidal anti-inflammatory drug
PB	phosphate buffer
PBS	phosphate buffered saline
PCR	polymerase chain reaction
PSA	pseudoaneurysm
rr	recombinant rat
RNA	ribonucleic acid
SDS-PAGE	sodium dodecyl sulphate polyacrylamide gel electrophoresis
SEM	scanning electron microscopy
SIS	small intestinal submucosa
TEM	transmission electron microscopy
VEGF	vascular endothelial growth factor
VEGFR	vascular endothelial growth factor receptor
YNB	yeast nitrogen base

Chapter 1

GENERAL INTRODUCTION & AIM OF THE STUDY

FROM MOLECULES TO MATRIX: CONSTRUCTION AND EVALUATION OF MOLECULARLY-DEFINED BIOSCAFFOLDS

Paul J. Geutjes¹
Willeke F. Daamen¹
Pieter Buma²
Wout F. Feitz¹
Kaeuis A. Faray^{1,4}
Toin H. van Kuppevelt¹

^{1,2,3}Radboud University Nijmegen Medical Centre, Departments of ¹Biochemistry (280), ²Orthopaedics (800) and ³Urology (659), P.O. Box 9101, 6525 GA Nijmegen, The Netherlands and ⁴Aap bio implants - EMCM BV, Middenkampweg 17, 6645 CH Nijmegen, The Netherlands P.O. Box 9101, 6525 GA Nijmegen, The Netherlands

Advances in Experimental Medicine and Biology 2006;585:279-95

Abstract

In this chapter, we describe the fundamental aspects of the preparation of molecularly-defined scaffolds for soft tissue engineering, including the tissue response to the scaffolds after implantation. In particular, scaffolds prepared from insoluble type I collagen fibres, soluble type II collagen fibres, insoluble elastin fibres, glycosaminoglycans (GAGs) and growth factors are discussed. The general strategy is to prepare tailor-made “smart” biomaterials which will create a specific microenvironment thus enabling cells to generate new tissues. As an initial step, all biomolecules used were purified to homogeneity. Next, porous scaffolds were prepared using freezing and lyophilisation, and these scaffolds were crosslinked using carbodiimides. Crosslinking resulted in mechanically stronger scaffolds and allowed the covalent incorporation of GAGs. Scaffold characteristics were controlled to prepare tailor-made scaffolds by varying e.g. collagen to elastin ratio, freezing rate, degree of crosslinking, and GAGs attachment. The tissue response to scaffolds was evaluated following subcutaneous implantations in rats. Crosslinked scaffolds maintained their integrity and supported the formation on new extracellular matrix. Collagen-GAG scaffolds loaded with basic fibroblast growth factor significantly enhanced neovascularisation and tissue remodelling. Animal studies of two potential applications of these scaffolds were discussed in more detail, i.e. for bladder and cartilage regeneration.

INTRODUCION

Tissue engineering is a rapidly growing area that aims to create, repair and/or replace tissues and organs by using combinations of biomaterials and cells. All tissues are composed of cells embedded in extracellular matrix. Tissue engineered constructs should have the capacity to become structurally integrated with the surrounding tissue, and to initiate restoration of essential functions of the lost or damaged tissue (1, 2). Most techniques of tissue engineering rely either on biocompatible scaffolds alone or a combination of scaffolds with cells to achieve new tissue formation. The scaffolds need to be compatible and designed to meet the nutritional and biological needs of the cell populations involved in the formation of new tissue (3). Ideally, scaffolds should be able to guide cells, which may be achieved by signals that sustain cellular growth, migration and differentiation (4). Engineered molecularly-defined smart scaffolds that resemble tissue-specific micro-environments may provide a means to accomplish this goal.

Major extracellular matrix (ECM) components in tissue and organs are collagens, elastin, proteoglycans, laminin, fibronectin and glycosaminoglycans (GAGs). Each tissue has its own unique set and content of scaffold biomolecules (5). By selectively incorporating biologically active molecules into tissue-engineering constructs, cellular behaviour may be fine-tuned (6). Since scaffolds are to be used inside the human body, special demands are put upon preparations used for this purpose. These include: purity (to avoid immunological response due to contaminants), porosity (for cellular ingrowth), biocompatibility and biodegradability. In this study, scaffolds were constructed on basis of collagen and/or elastin, and combined with GAGs and growth factors. We will first focus on the properties of the individual components, next on the purification/production of these components, then on the preparation, characterisation and evaluation of porous matrices. Finally, we will discuss some potential applications for clinical use.

Collagen

Collagen provides strength and structural integrity to almost all organs in the body, especially skin, ligaments, cartilage, bone, tendon and dental elements (7-9). Fibrillar collagen is a 'triple helical' molecule (1.5 x 300 nm) with a molecular mass of about 300 kDa. It is composed of three left-handed polypeptides (α -chains) which are wrapped together to form a right-handed helical structure. The tight wrapping into a triple helix provides great tensile strength with virtually no capacity to stretch. Collagen molecules are grouped into fibrils in a head to tail alignment, and are covalently crosslinked to each other. At least 26 genetically distinct types of collagen are known. Type I collagen is the main fibrillar collagen of bone, tendon, and skin and provides tissues with tensile strength. Insoluble type I collagen has found ample usage in the biomedical field (1, 4, 9-12). Type II collagen is the principal collagenous component of cartilage, intervertebral discs and the vitreous body. Its mechanical function is to provide tensile strength and resists shearing forces (13).

Elastin

Elastin provides elasticity to organs, especially skin, lung, arteries and ligaments (14). Elastin can stretch to several times its normal length. Despite its remarkable mechanical properties, elastin has found little use as a biomaterial (5, 15, 16). Elastin is a desirable protein for tissue engineering (15, 17). Due to its remarkable mechanical properties, elasticity and long term stability, elastin fibres maybe important in a wide variety of applications, including skin substitutes, vascular grafts, heart valves, and elastic cartilage.

The high content of hydrophobic amino acids and intermolecular crosslinks (desmosine and isodesmosine) makes elastin one of the most chemically resistant proteins in the body. The precursor, tropoelastin, is composed of a 72 kDa single polypeptide chain. Individual molecules are secreted into the extracellular space, in association with microfibrillar components and crosslinked to each other to form elastic fibres (18).

Glycosaminoglycans (GAGs)

GAGs mediate many biological functions, e.g. hydration of tissue and the binding and modulation of effector molecules such as growth factors and cytokines (19, 20). These characteristics are essential for basic cellular phenomena like cell adhesion, growth differentiation and activation, and implicate a role for GAGs in wound healing, inflammation, tissue morphogenesis and homeostasis. GAGs are linear polysaccharides comprised of alternating hexuronic acid and hexosamine residues (21). Due to the high degree of carboxylation and sulfation, GAGs are highly negatively charged molecules. Based on their backbone structure, GAGs can be grouped in four major classes; these are heparan sulphate (HS)/heparin, chondroitin sulfate (CS)/dermatan sulfate (DS), keratan sulfate (KS), and hyaluronic acid (HA). With the exception of HA, GAG chains are covalently attached to a core protein, forming proteoglycans. GAGs absorb water, causing osmotic swelling which provides the tissue with stiffness, strength and shock absorption (13). Characteristics like growth factor binding and biocompatibility can be exploited in biomaterials.

Growth factors

Growth factors are polypeptides that modulate cellular activities. Growth factors can either stimulate or inhibit cellular adhesion, migration, proliferation, and differentiation (22, 23). Growth factors initiate their action by binding to specific receptors on target cells. Hundreds of growth factors have been identified, characterised and, based on structural homologies, grouped into at least twenty families and superfamilies (24). The ECM serves as a reservoir for growth factors, and promotes their long term bioavailability. Growth factors are stabilised and protected from proteolytic degradation by their interactions with e.g. GAGs. A sustained release of growth factors may be established by GAGs of ECM. HS for example, is a natural polysaccharide which stores and protects bFGF (25).

Specific control of tissue regeneration is achieved by controlled growth factor release from devices. Vascularisation of bioscaffolds is commonly a prerequisite for achieving appropriate tissue regeneration and function. Angiogenic factors like basic fibroblastic growth factors (bFGF) and vascular endothelial growth factor (VEGF) have a great potential for biomedical applications (26). bFGF stimulates the growth of smooth muscle cells and fibroblasts as well as endothelial cells, whereas VEGF primarily stimulates endothelial cells. Interestingly, combining VEGF and bFGF produces a greater and more rapid improvement in angiogenesis than administration of either VEGF or bFGF alone (27). bFGF is an 18 kDa protein with a length of 155 amino acids which does not contain disulfide bonds and is not glycosylated (28). VEGF is a 34- to 42-kDa heparin-binding dimeric ligand which appears in different isoforms (29). Since both growth factors have heparin binding sites, they can be specifically attached to GAG-containing scaffolds to improve neovascularisation and tissue generation.

The biocharacteristics of collagen, elastin, GAGs and growth factors make them valuable molecules to be incorporated into biomaterials. In the following, we will discuss the construction of tailor-made and biocompatible collagen-GAG and collagen-elastin-GAG scaffolds combined with growth factors, with defined physical, chemical, and biological

characteristics, for use as a biomaterial for tissue engineering. Porous collagen or collagen-elastin scaffolds were fabricated by freezing and subsequently lyophilisation of a suspension of highly purified collagen and elastin. GAGs were covalently attached by using carbodiimide crosslinking, thus offering the opportunities to exploit GAG-mediated phenomena such as binding, modulation, and release of growth factors, and allowing the construction of bioactive smart scaffolds (Fig. 1).

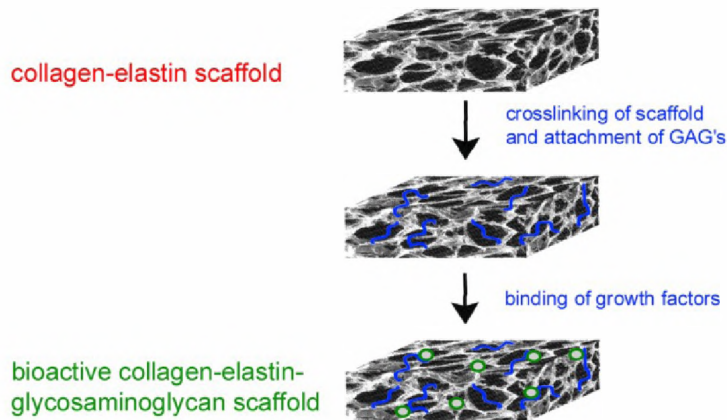


Fig 1 Overview of the preparation of a bioactive scaffold: GAGs in blue and growth factors in green.

PREPARATION OF BIOACTIVE SCAFFOLDS

Isolation/production of components and purity assessment

Insoluble type I collagen was purified from bovine achilles tendon. Briefly, tendons were cleared from surrounding tissue, pulverised under liquid nitrogen conditions and extensively rinsed using diluted acetic acid, NaCl, urea, acetone and demineralised water as described (30). The purity and fibril structure of the type I collagen preparation was analysed by sodium dodecyl sulphate polyacrylamide gel electrophoresis (SDS-PAGE), amino acid analysis, transmission electron microscope (TEM) and scanning electron microscope (SEM). SDS-PAGE indicated that the isolated collagen was essentially free of other proteins, and CNBr digestion of collagen revealed a specific type I collagen profile. TEM and SEM showed intact thin collagen fibrils with its characteristic striated pattern (Fig. 2A).

Soluble type II collagen was isolated from bovine tracheal cartilage. Trachea were defatted, stripped from surrounding conjunctiva, cut into small pieces (0.5 cm³) and washed/treated with Tris-HCl, guanidinium chloride, acetic acid, pepsin, and specific salt precipitation followed by dialysis against phosphate buffer (31). The purity of the type II collagen preparation was analysed by SDS-PAGE, amino acid analysis, and immunohistochemistry. No contaminating proteins could be detected by SDS-PAGE, and after CNBr digestion a profile typical for type II collagen was obtained. Amino acid composition revealed an increase in glycine, hydroxyproline and hydroxylysine residues, relative to tracheal cartilage. No chondroitin sulfate, a major component of cartilage, could be detected by immunohistochemistry.

Insoluble elastin fibres were isolated from equine ligamentum nuchae. Non-elastinous tissue was removed and ligaments were pulverised and washed/treated with NaCl, organic solvents, CNBr in formic acid, urea with diluted 2-mercaptoethanol, and trypsin (32). The purity of the elastin preparation was analysed by SDS-PAGE, TEM and SEM. Only soluble contaminations and/or elastin breakdown products will enter an SDS-PAGE gel, whereas insoluble elastin will not. SDS-PAGE of the purified elastin indicated no contaminations. SEM and TEM indicated that the purified elastin fibres were intact and free of microfibrils and no other elements could be detected in contrast to traditionally prepared elastin (Fig. 2B) (33, 34).

The GAGs chondroitin sulphate (CS) from bovine trachea and heparan sulphate (HS) from bovine kidney were isolated using extensive papain digestion, mild alkaline borohydride treatment, diethylaminoethyl (DEAE) ion exchange chromatography, and glycosidase digestion (35). Isolated GAGs were characterised by agarose gel electrophoresis (Fig. 2C) (36), and quantified using a modified Farndale-assay (37). To study whether protein contaminations were present, the GAG preparations were evaluated using SDS-PAGE under reducing conditions. According to these methods, no contaminations with other GAGs or proteins could be detected in CS and HS preparations.

The growth factors VEGF and bFGF (38) were produced in mg quantities using recombinant DNA technology and purified using immobilised heparin affinity chromatography. The purity and structure of these components are essential for the reproducible preparation of bioactive scaffolds. The purity and bioactivity of the growth factors were assessed using SDS-PAGE. The expressed and purified recombinant rat growth factors (VEGF and bFGF) had their apparent molecular weight and no contaminated proteins could be detected (Fig. 2D). Under non-reducing conditions, VEGF was present as a dimer, its active form. The biological activity of growth factors was evaluated *in vitro* using human umbilical vein endothelial cells for rrVEGF-164 and human dermal fibroblasts for rrbFGF (38). The addition of a growth factor stimulated cell proliferation threefold relative to cell cultures without growth factor.

Preparation of scaffolds

Scaffold morphology is another important aspect since it influences cellular migration and tissue remodelling. Cellular migration and supply of nutrients and oxygen is more straightforward when the scaffold has a higher porosity. To prepare a porous scaffold, collagen or collagen-elastin suspensions were made by incubation in diluted acetic acid at 4°C for 16 h. The suspension was homogenised using a Potter-Elvehjem homogeniser, deaerated, poured into a mould, frozen and lyophilised, resulting in porous scaffolds. By using different freezing temperatures, the porosity of the collagen scaffold can be varied to some extent (39). With higher freezing rates, smaller ice crystals were formed, leading to a scaffold with a smaller average pore diameter.

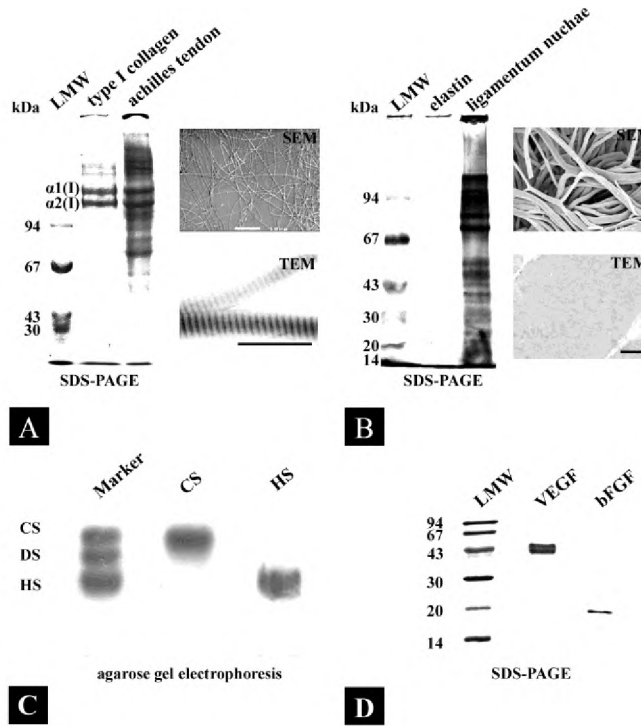


Fig 2 Purity of scaffold components. Shown are: A) Type I collagen. SDS-PAGE of low molecular weight marker (LMW), purified type I collagen α_1 , α_2 and β chains, and bovine achilles tendon. Scanning and transmission electron microscopy showed intact collagen fibrils. B) Elastin. SDS-PAGE of low molecular weight marker (LMW), purified insoluble elastin, and equine ligamentum nuchae. After purification, no contaminants could be detected using SDS-PAGE, scanning and transmission electron microscopy. C) Chondroitin sulfate (CS) and heparan sulfate (HS). Agarose gel electrophoresis of GAG marker (CS, dermatan sulfate (DS) and HS) and isolated CS and HS. No other GAGs could be found. D) Vascular endothelial growth factor 164 (VEGF-164) and basic fibroblast growth factor (bFGF). No contaminants could be detected in VEGF-164 and bFGF with SDS-PAGE under non-reducing conditions. Bar is 10 μ m in SEM micrographs and 0.5 μ m in TEM micrographs.

To strengthen the porous structure and to covalently attach GAGs to the scaffold, 1-ethyl-3-(3-dimethyl aminopropyl) carbodiimide (EDC) crosslinking was used. EDC crosslinking is generally applied to prevent rapid degradation, to suppress antigenicity, and to improve mechanical properties. EDC is a zero length crosslinker which couples biomolecules to each other by virtue of an amide (peptide) linkage, which is non-toxic and biocompatible (40). The strength of the scaffold and the rate of biodegradation can be varied depending on the degree of crosslinking. The crosslinking of the scaffolds in the presence or absence of GAGs was performed using EDC and N-hydroxysuccinimide (NHS) in 2-morpholinoethane sulfonic acid (MES) in the presence of 40% ethanol for 4 h with or without HS or CS (5, 30). The presence of ethanol in the EDC solution preserves the porosity of the scaffold. Scaffolds were loaded with growth factors, by incubation in phosphate buffered saline (PBS) at 20°C, followed by incubation in PBS containing 7 μ g growth factor/ml for 1 h at 20°C, and washing with PBS to remove unbound growth factor.

Characterisation of scaffolds

The morphology of the scaffold was characterised using SEM. The air-and pan-side of the scaffold consisted of porous structures with pore diameter ranging from 20 to 200 μm (Fig. 3A). The inner site generally consisted of lattice like structures when scaffolds were frozen at -80°C . Collagen fibrils and elastin fibres physically interacted with each other in the collagen-elastin scaffold. Collagen and elastin were randomly distributed in the scaffold, although elastin tended to be present in small clusters (Fig. 3B). EDC crosslinking and GAG coupling to the scaffolds did not alter the porosity (35).

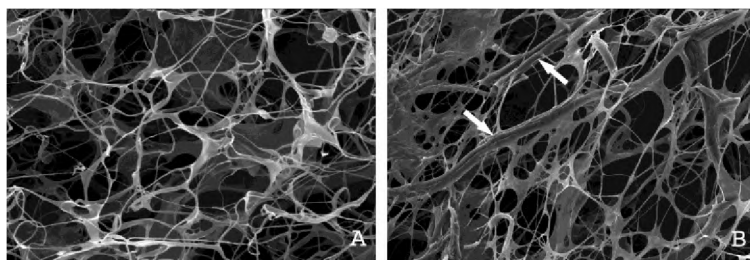


Fig 3 Scanning electron micrographs of a porous scaffold made of A) 100% collagen and B) 50% collagen and 50% elastin. The small fibrils consist of collagen, and the large fibres are elastin (arrows). Bar is 10 μm .

Physicochemical characteristics of various non-crosslinked and crosslinked collagen (elastin)scaffolds, with and without GAGs, are shown in Table 1. The degree of scaffold crosslinking was assessed by determination of the amine group content of the scaffolds spectrophotometrically after using 2,4,6-trinitrobenzene sulfonic acid (40). The rate of crosslinking depended on the amine group content of the non-crosslinked scaffold and the crosslinking conditions. The amine group content of collagen is higher than elastin, thus more crosslinks could be induced in collagen scaffolds than collagen-elastin scaffolds (5). Up to 60% of the available amine groups were used in the crosslinking reaction (5, 30, 35). For collagenous scaffolds, the denaturation time T_d is also indicative for the degree of crosslinking. The T_d of collagen scaffolds was determined by differential scanning calorimetry and could be increased from 62 to almost 80°C by crosslinking (30).

The amount of GAGs was determined by hexosamine analyses using p-dimethyl-aminobenzaldehyde (41). The GAG amount bound to the scaffold depended on the rate of crosslinking and the type of GAG. Up to 10% of HS and 6% of CS could be incorporated in the scaffolds. Specific phage display-generated antibodies (42) were used to localise these GAGs in the scaffold (43). Immunostaining indicated that the covalently bound GAGs were distributed throughout the whole scaffold (Fig. 4) (5).

The total amount of bFGF bound to the scaffold and its release were determined using radioactive labelling with ^{125}I . Crosslinked scaffolds, with and without HS, revealed a biphasic release profile, i.e. an initial burst of bFGF followed by a gradual and sustained release. More bFGF could be bound to a HS-containing scaffold (1.26% vs. 0.37%) compared to a scaffold without GAG (38). Immunohistochemistry was also used to localise growth factors in the scaffold, and bFGF was mainly localised at the margins of the scaffold (38).

Table 1. Biochemical, biophysical and biomechanical characteristics of various scaffolds.

Scaffold	Crosslinked with EDC/NHS	Denaturation Temperature T_d [°C]	Amine group content [nmol/g]	Amount of GAG per g scaffold [mg]	Amount of bFGF per g scaffold [μ g]	Water-binding capacity [#times dry weight]	Tensile strength [kPa]	E-modulus [MPa]
COL	-	62 \pm 1	281 \pm 7	0	0	20 \pm 1	103 \pm 15	0.39 \pm 0.07
COL	+	79 \pm 1	185 \pm 3	0	0	20 \pm 1	677 \pm 191	1.03 \pm 0.08
COL-CS	+	77 \pm 1	186 \pm 8	100 \pm 4	0	33 \pm 3	520 \pm 105	0.97 \pm 0.07
COL-EL 1:1	-	N.D.	147 \pm 12	0	0	16 \pm 1	63 \pm 23	0.24 \pm 0.06
COL-EL 1:1	+	N.D.	87 \pm 5	0	0	16 \pm 3	142 \pm 8	0.42 \pm 0.04
COL-EL-CS 1:1	+	N.D.	83 \pm 2	58 \pm 5	0	21 \pm 3	128 \pm 10	0.54 \pm 0.11
COL	+	72 \pm 1	236 \pm 9	0	0	N.D.	N.D.	N.D.
COL-bFGF	+	72 \pm 1	236 \pm 9	0	372 \pm 75	N.D.	N.D.	N.D.
COL-HS	+	69 \pm 1	227 \pm 17	80 \pm 5	0	N.D.	N.D.	N.D.
COL-HS-bFGF	+	69 \pm 1	227 \pm 17	60 \pm 5	1260 \pm 207	N.D.	N.D.	N.D.

COL= collagen; EL= elastin; CS= chondroitin sulfate; HS= heparan sulfate; bFGF= basic fibroblast growth factor. Scaffolds above the dashed line were crosslinked with 33 mM EDC and 6 mM NHS; scaffolds below with 14 mM EDC and 8 mM NHS. Results are mean \pm SD of at least 3 individual experiments. Values from (5, 38).

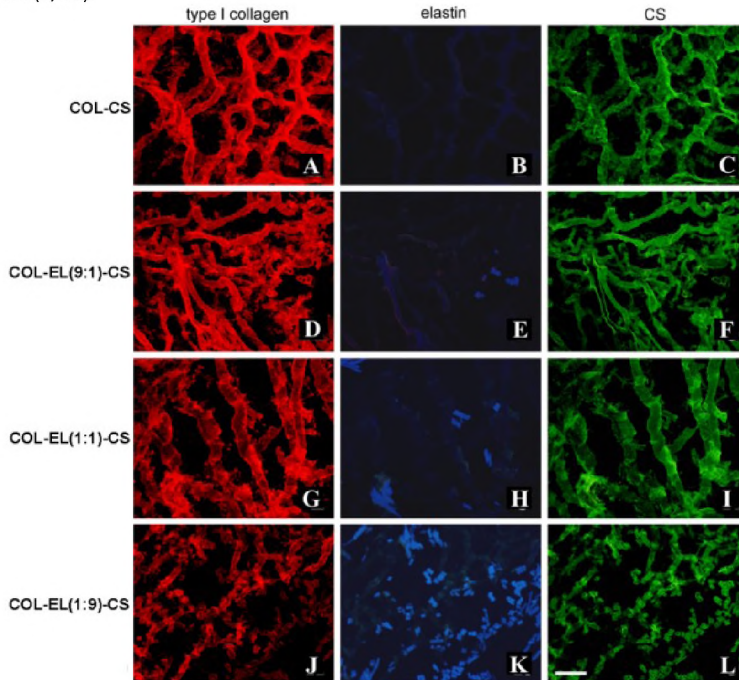


Fig 4 Immunostaining of scaffolds containing variable amounts of collagen and elastin with covalently attached chondroitin sulfate using immunostaining for type I collagen (red) and CS (green), whereas elastin was analysed by UV optics (blue). Bar is 50 μ m. COL=collagen, EL=elastin, CS=chondroitin sulphate. Figure modified with permission from Daamen *et al.* (5).

TISSUE RESPONSE TO COLLAGENOUS SCAFFOLDS (38, 43)

Before a bioactive scaffold can be applied for tissue engineering, the tissue response and biocompatibility have to be studied in animal models. To evaluate the tissue response, collagenous scaffolds were implanted subcutaneously in 3 months old male Albino Oxford rats for periods up to 10 weeks. On the back of the anaesthetised rats, subcutaneous pockets were made and scaffolds (\varnothing 8 mm) were implanted at a distance of about 1 cm from the incisions. The implants with surrounded tissue were harvested at day 2, and at 1, 2, 4, and 10 weeks after implantation. The tissue response was evaluated by using (immuno)histological methods. Results were analysed for non-crosslinked and crosslinked scaffolds with and without GAGs and with and without growth factors.

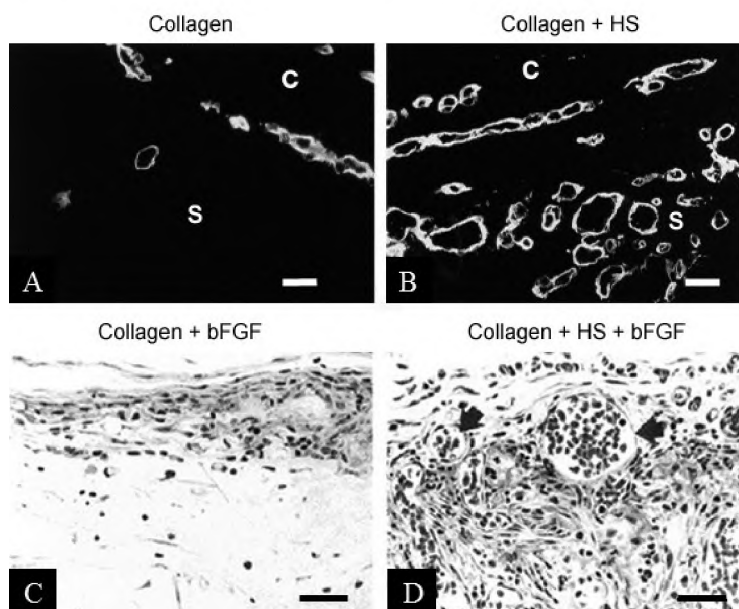


Fig 5 Light-microscopy of subcutaneously implanted crosslinked collagen scaffolds. Shown are: A) collagen and B) collagen-HS scaffold immunostained for type IV collagen as a marker for blood vessels 2 weeks after implantation. Note that HS induces angiogenesis. c= capsule surrounding the implants; s= implanted scaffold. C) collagen-bFGF and D) collagen-HS-bFGF scaffold 10 weeks after implantation (HE staining). Arrows indicate blood vessels. Bar indicates 25 μ m in (A, B) and 50 μ m in (C, D). Figure A and B reproduced from Pieper *et al.* with permission (43).

Non-crosslinked collagen scaffolds were gradually resorbed and completely replaced by collagenous connective tissue 10 weeks after implantation. Crosslinked collagen scaffolds, however, maintained their integrity for at least 3 months and supported the formation of new ECM, i.e. deposition of type I and III collagen.

To study the effect of GAGs (e.g. HS and CS), crosslinked collagen scaffolds with and without GAGs were implanted. Even after 10 weeks, the GAGs remained immobilised on the collagen scaffold as analysed by immunohistochemistry. An increased angiogenesis was found in collagen-HS relative to collagen scaffolds (Fig. 5A and B), indicating the angiogenesis

promoting activity of HS. The presence of GAGs preserved the porous scaffold structures and delayed scaffold degradation. After 10 weeks of implantation, a minor infiltration of macrophages and giant cells was observed in both collagen-HS and collagen-CS scaffolds. It was therefore concluded that attachment of GAGs to collagenous scaffolds modulated tissue response.

The presence of GAGs promoted angiogenesis into the scaffold periphery. Angiogenesis could be further enhanced by loading the collagen-HS scaffold with bFGF. A number of growth factors, including bFGF, have a high affinity for HS and display angiogenic and mitogenic properties. Binding bFGF to collagen-HS scaffolds resulted in a major influx of cells. Collagen-HS-bFGF scaffolds became highly vascularised and remained their structural integrity throughout the implantation period (Fig. 5C and D). Although bFGF distribution was not homogenous, vascularisation was increased throughout the scaffold after subcutaneous implantation. bFGF loading of crosslinked collagen-GAG scaffolds is thus of additional value for tissue engineering applications that require angiogenesis.

SOME APPLICATIONS

Collagen scaffolds for bladder augmentation (rabbit) (44)

Approximately 1.2 million people worldwide suffer from bladder disease. Individuals with end-stage bladder disease often require bladder replacement or repair (45). Currently, most common techniques of bladder reconstruction with intestinal tissues are associated with various complications like mucus productions, chronic bacteria, stone formation, leakage and ruptures, electrolyte imbalance and possible development of malignancies (46-48). Different biodegradable scaffolds have been used for pre-clinical studies. Among these, SIS is a xenogenic membrane that is harvested from porcine small intestine, which is mainly composed of a submucosal layer (49). Complications occur when using grafts for bladder reconstruction, i.e. graft shrinkage, graft incrustation, or infection (45, 50-54). A collagen-based biocompatible and biodegradable scaffold may solve these problems.

The operation procedure was as follows: the bladder of a New Zealand white rabbit (2.5-3.5 kg) was exposed and part of the ventral surface of the detrusor (1.5 x 1.5 cm) resected (Fig. 6A). Collagen scaffolds were sewed into place with a running resolvable suture (6 x 0 Monocryl, Ethicon, USA) and four non-resolvable marker sutures (Fig. 6B). The bladder was then filled with saline solution to examine leakages (Fig. 6C). None of the scaffolds showed any leakage. After 1 month, the urothelium on the scaffold was multilayered and some ingrowth of smooth muscle cells was observed (Fig. 6E). After three months, the scaffold was fully incorporated in the bladder tissue (Fig. 6D) and after 9 months, the central smooth muscle cells and the periphery of the graft were further organised and the muscle layers were in a similar direction as the native bladder muscle layer (Fig. 6F). The collagen scaffold showed good epithelialisation and ingrowth of smooth muscle cells. However, a few rabbits developed bladder stones. A considerable amount of rabbits showed encrustation (adhesion of urate/CaO_x microcrystals) after 2 weeks, but these remarkably disappeared in time (3-9 months). Future research focuses on the introduction of HS and epidermal growth factor (EGF) on to the scaffolds in order to improve the regeneration of the bladder wall.

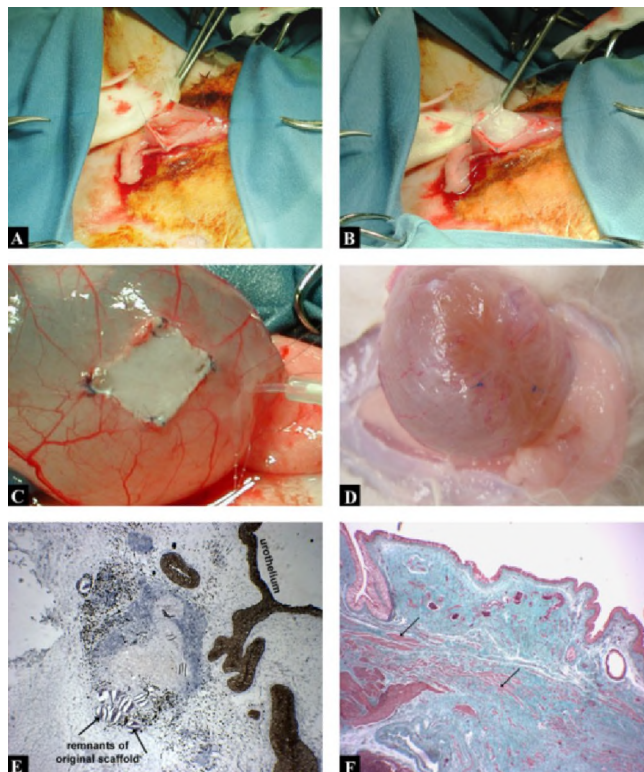


Fig 6 Surgery and immunohistochemistry of an augmentation cystoplasty using a crosslinked type I collagen scaffold. Shown are: A) exposed bladder; B) collagen scaffold being sewed into the resected bladder; C) bladder with collagen scaffold filled with saline solution to examine leakage; D) collagen scaffold 3 months after implantation incorporated in the bladder wall; E) immunostaining of urothelium with cytokeratin 5 and 8 one month post-operatively; F) Masson trichrome staining of bladder wall with collagen scaffold three months post-operatively (arrows indicate muscle cells). Figure reproduced with permission from Elsevier (44).

Tissue engineering of cartilage (55)

The extracellular matrix of articular cartilage consists mainly of type II collagen and glycosaminoglycans (GAGs). The collagen of articular cartilage is organised in a highly specific way. Most collagen bundles run from the deep mineralised layer of the cartilage to the superficial zone of the cartilage where they bent to run parallel to the surface. The cells of articular cartilage, the chondrocytes, lie more or less scattered in this matrix. In the superficial region, they are parallel to the surface, in the deeper regions they are located in columns perpendicular to the surface in-between the collagen bundles. The tissue is not innervated by nerves and is avascular, making spontaneous repair after injury or disease slow. With the increase in frequency of osteoarthritis and cartilage trauma in the population, makes cartilage a particular target for tissue engineering (56). Various scaffolds have been reported for tissue engineering of cartilage (31, 57-61).

An initial *in vivo* experiment was performed to evaluate the effect of collagenous scaffolds for cartilage regeneration. Scaffolds, made from isolated and crosslinked type I and

II collagen with and without attached chondroitin sulphate (CS), were tested on their cartilage inductive properties in knees of young rabbits. Scaffolds were implanted into full-thickness articular cartilage defects. After luxation of the patella, two full-thickness defects (\varnothing 4 mm; 3 mm high) were made in the trochlea (Fig. 7A). Type I and II collagen scaffolds (Fig. 7B), with or without CS, were implanted and empty defects were used as controls (Fig. 7C). The follow-up period was 4 and 12 weeks. Empty control defects showed a considerable healing response consisting of the restoration of the original cartilage contours with cartilaginous-like tissue, and in the 12-week group, remodelling of the deeper area of the defect into bone. This unexpected good repair of the empty defects was probably related to the relatively young rabbits, which are known for their larger repair potency compared to older animals. Although differences between different scaffold types was not very large, type I and II collagen scaffolds in combination with CS showed a trend for a better defect repair as compared to the same scaffolds without CS. Scaffolds were almost completely degraded after 12 weeks and integration with the subchondral bone and adjacent cartilage was observed. In some cases, a direct connection between the graft and host cartilage was found (Fig. 7D). Scaffolds based on both type I and II collagen appeared to be biocompatible and biodegradable and these scaffolds favoured the maintenance of the chondrocytic phenotype in the reconstructed defect area.

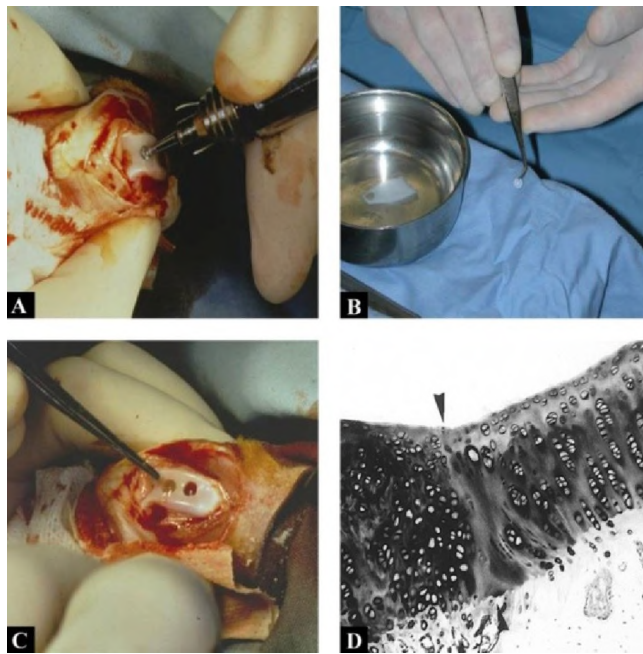


Fig 7 Surgery and histology of full-thickness/subchondrial defects in the rabbit knee joint. A) Two full thickness defects were created in the trochlea using a dental high speed drill into the subchondral bone. B) Wetted collagen scaffold to be placed in the defect. C) A type II collagen-CS scaffold is applied to one defect (left); an empty defect is used as a control (right). D) Light microscopy of a defect with implanted crosslinked type II collagen-CS scaffold 12 weeks after implantation showed that the cartilage-like tissue of the implant site (right of arrowhead) is in some cases directly connected to the adjacent host tissue (left of arrowhead). Figure D reproduced from Buma *et al.* with permission from Elsevier (55).

AIM OF THIS THESIS

The primary aim of this study was to develop novel tissue engineering tools for clinical applications. Tissue engineering and regenerative medicine are fairly new disciplines which aim on the regeneration of damaged or lost tissues. One of the basic principles of tissue engineering is the use of biocompatible materials which restore local processes. Within regenerative medicine, various approaches are known, e.g. the use of scaffolds, injectables, coatings and/or delivery devices. The development and applicability of novel tissue engineering tools is the main aim of this thesis.

A review about the fundamental aspects of the preparation of molecularly-defined scaffolds for soft tissue engineering is presented in chapter 1. Particularly the preparation of scaffolds composed of type I collagen, elastin, glycosaminoglycans and growth factors, and the possible applications are discussed. In chapter 2, the large production and purification of a vascular endothelial growth factor (VEGF) using the *Pichia pastoris* expression system is demonstrated. This growth factor plays a key role in the enhancement of local angiogenesis, which will be further addressed in chapter 3. In this chapter, the preparation and subcutaneous implantation of collagen-glycosaminoglycan scaffolds with VEGF and/or FGF-2 is presented, highlighting the neovascularisation and tissue response.

Collagen is well known for its adjunct for hemostasis. When collagen comes in contact with blood, the primary hemostasis is initiated. This makes collagen a good candidate for local hemostasis, e.g. pseudoaneurysms treatment. In chapter 4, a new pig model for femoral pseudoaneurysm is described. This model is used in Chapter 5 which addresses the preparation and characterisation of injectable collagen, and its use for femoral arterial pseudoaneurysm treatment.

Chapter 6 and 7 describe straightforward methods to prepare micro-capsules (lyophilisomes) and injectable micro-scaffolds, and discuss the possibilities and further strategies for their use in both drug delivery and tissue engineering.

Finally, summary and future directions are given in chapter 8.

REFERENCES

1. R.Langer and J.P.Vacanti. "Tissue engineering." *Science* 260, no. 5110(1993):920-6.
2. R.S.Langer and J.P.Vacanti. "Tissue engineering: the challenges ahead." *Sci Am* 280, no. 4(1999):86-9.
3. L.G.Griffith and G.Naughton. "Tissue engineering--current challenges and expanding opportunities." *Science* 295, no. 5557(2002):1009-14.
4. M.P.Lutolf and J.A.Hubbell. "Synthetic biomaterials as instructive extracellular microenvironments for morphogenesis in tissue engineering." *Nat Biotechnol* 23, no. 1(2005):47-55.
5. W.F.Daamen, H.T.van Moerkerk, T.Hafmans, L.Buttafoco, A.A.Poot, J.H.Veerkamp, and T.H.van Kuppevelt. "Preparation and evaluation of molecularly-defined collagen-elastin-glycosaminoglycan scaffolds for tissue engineering." *Biomaterials* 24, no. 22(2003):4001-9.
6. J.A.Hubbell. "Materials as morphogenetic guides in tissue engineering." *Curr Opin Biotechnol* 14, no. 5(2003):551-8.
7. P.H.Byers. "Inherited disorders of collagen gene structure and expression." *Am J Med Genet* 34, no. 1(1989):72-80.
8. G.J.Laurent. "Dynamic state of collagen: pathways of collagen degradation in vivo and their possible role in regulation of collagen mass." *Am J Physiol* 252, no. 1 Pt 1(1987):1-9.
9. D.J.Prockop and K.I.Kivirikko. "Collagens: molecular biology, diseases, and potentials for therapy." *Annu Rev Biochem* 64,(1995):403-34.
10. G.Marmieri, M.Pettenati, C.Cassinelli, and M.Morra. "Evaluation of slipperiness of catheter surfaces." *J Biomed Mater Res* 33, no. 1(1996):29-33.
11. F.J.O'Brien, B.A.Harley, I.V.Yannas, and L.J.Gibson. "The effect of pore size on cell adhesion in collagen-GAG scaffolds." *Biomaterials* 26, no. 4(2005):433-41.
12. Y.S.Pek, M.Spector, I.V.Yannas, and L.J.Gibson. "Degradation of a collagen-chondroitin-6-sulfate matrix by collagenase and by chondroitinase." *Biomaterials* 25, no. 3(2004):473-82.
13. J.A.Buckwalter and H.J.Mankin. "Articular cartilage: tissue design and chondrocyte-matrix interactions." *Instr Course Lect* 47,(1998):477-86.
14. C.M.Kielty, M.J.Sherratt, and C.A.Shuttleworth. "Elastic fibres." *J Cell Sci* 115, no. Pt 14(2002):2817-28.
15. J.D.Berglund, R.M.Nerem, and A.Sambanis. "Incorporation of intact elastin scaffolds in tissue-engineered collagen-based vascular grafts." *Tissue Eng* 10, no. 9-10(2004):1526-35.
16. T.Chandy, G.H.Rao, R.F.Wilson, and G.S.Das. "The development of porous alginate/elastin/PEG composite matrix for cardiovascular engineering." *J Biomater Appl* 17, no. 4(2003):287-301.
17. M.Li, M.J.Mondrinos, M.R.Gandhi, F.K.Ko, A.S.Weiss, and P.I.Lelkes. "Electrospun protein fibers as matrices for tissue engineering." *Biomaterials* 26, no. 30(2005):5999-6008.
18. C.M.Kielty, T.J.Wess, L.Haston, J.L.Ashworth, M.J.Sherratt, and C.A.Shuttleworth. "Fibrillin-rich microfibrils: elastic biopolymers of the extracellular matrix." *J Muscle Res.Cell Motil.* 23, no. 5-6(2002):581-96.
19. D.R.Coombe and W.C.Kett. "Heparan sulfate-protein interactions: therapeutic potential through structure-function insights." *Cell Mol Life Sci* 62, no. 4(2005):410-24.
20. R.Raman, V.Sasisekharan, and R.Sasisekharan. "Structural insights into biological roles of protein-glycosaminoglycan interactions." *Chem Biol* 12, no. 3(2005):267-77.
21. S.Valla, J.Li, H.Ertsevag, T.Barbeyron, and U.Lindahl. "Hexuronyl C5-epimerases in alginate and glycosaminoglycan biosynthesis." *Biochimie* 83, no. 8(2001):819-30.
22. D.G.Fernig and J.T.Gallagher. "Fibroblast growth factors and their receptors: an information network controlling tissue growth, morphogenesis and repair." *Prog Growth Factor Res* 5, no. 4(1994):353-77.
23. M.E.Nimni. "Polypeptide growth factors: targeted delivery systems." *Biomaterials* 18, no. 18(1997):1201-25.
24. J.E.Babensee, L.V.McIntire, and A.G.Mikos. "Growth factor delivery for tissue engineering." *Pharm Res* 17, no. 5(2000):497-504.

25. M.Salmivirta, K.Lidholt, and U.Lindahl. "Heparan sulfate: a piece of information." *Faseb J* 10, no. 11(1996):1270-9.
26. A.Perets, Y.Baruch, F.Weisbuch, G.Shoshany, G.Neufeld, and S.Cohen. "Enhancing the vascularization of three-dimensional porous alginate scaffolds by incorporating controlled release basic fibroblast growth factor microspheres." *J Biomed Mater Res A* 65, no. 4(2003):489-97.
27. T.Asahara, C.Bauters, L.P.Zheng, S.Takeshita, S.Bunting, N.Ferrara, J.F.Symes, and J.M.Isner. "Synergistic effect of vascular endothelial growth factor and basic fibroblast growth factor on angiogenesis in vivo." *Circulation* 92, no. 9(1995):365-71.
28. J.D.Zhang, L.S.Cousens, P.J.Barr, and S.R.Sprang. "Three-dimensional structure of human basic fibroblast growth factor, a structural homolog of interleukin 1 beta." *Proc.Natl.Acad.Sci.U.S.A* 88, no. 8(April 1991):3446-50.
29. N.Ferrara. "Role of vascular endothelial growth factor in regulation of physiological angiogenesis." *Am J Physiol Cell Physiol* 280, no. 6(June 2001):C1358-C1366.
30. J.S.Pieper, A.Oosterhof, P.J.Dijkstra, J.H.Veerkamp, and T.H.van Kuppevelt. "Preparation and characterization of porous crosslinked collagenous matrices containing bioavailable chondroitin sulphate." *Biomaterials* 20, no. 9(1999):847-58.
31. J.S.Pieper, P.M.van der Kraan, T.Hafmans, J.Kamp, P.Buma, J.L.van Susante, W.B.van den Berg, J.H.Veerkamp, and T.H.van Kuppevelt. "Crosslinked type II collagen matrices: preparation, characterization, and potential for cartilage engineering." *Biomaterials* 23, no. 15(2002):3183-92.
32. W.F.Daamen. "Isolation of intact elastin fibres devoid of microfibrils." *Tissue Eng* 11, no. 7/8(2005):1168-76.
33. W.F.Daamen, T.Hafmans, J.H.Veerkamp, and T.H.van Kuppevelt. "Comparison of five procedures for the purification of insoluble elastin." *Biomaterials* 22, no. 14(2001):1997-2005.
34. W.F.Daamen, S.T.Nillesen, T.Hafmans, J.H.Veerkamp, M.J.van Luyn, and T.H.van Kuppevelt. "Tissue response of defined collagen-elastin scaffolds in young and adult rats with special attention to calcification." *Biomaterials* 26, no. 1(2005):81-92.
35. J.S.Pieper, T.Hafmans, J.H.Veerkamp, and T.H.van Kuppevelt. "Development of tailor-made collagen-glycosaminoglycan matrices: EDC/NHS crosslinking, and ultrastructural aspects." *Biomaterials* 21, no. 6(2000):581-93.
36. C.H.van de Lest, E.M.Versteeg, J.H.Veerkamp, and T.H.van Kuppevelt. "Quantification and characterization of glycosaminoglycans at the nanogram level by a combined azure A-silver staining in agarose gels." *Anal Biochem* 221, no. 2(1994):356-61.
37. C.H.van de Lest, E.M.Versteeg, J.H.Veerkamp, and T.H.van Kuppevelt. "A spectrophotometric method for the determination of heparan sulfate." *Biochim Biophys Acta* 1201, no. 2(1994):305-11.
38. J.S.Pieper, T.Hafmans, P.B.van Wachem, M.J.van Luyn, L.A.Brouwer, J.H.Veerkamp, and T.H.van Kuppevelt. "Loading of collagen-heparan sulfate matrices with bFGF promotes angiogenesis and tissue generation in rats." *J Biomed Mater Res* 62, no. 2(2002):185-94.
39. F.J.O'Brien, B.A.Harley, I.V.Yannas, and L.Gibson. "Influence of freezing rate on pore structure in freeze-dried collagen-GAG scaffolds." *Biomaterials* 25, no. 6(2004):1077-86.
40. L.H.H.Olde Damink, P.J.Dijkstra, M.J.A.van Luyn, P.B.van Wachem, P.Nieuwenhuis, and J.Feijen. "Cross-linking of dermal sheep collagen using a water-soluble carbodiimide." *Biomaterials* 17, no. 8(1996):765-73.
41. I.V.Yannas and J.F.Burke. "Design of an artificial skin. I. Basic design principles." *J Biomed Mater Res* 14, no. 1(1980):65-81.
42. T.H.van Kuppevelt, M.A.Dennissen, W.J.van Venrooij, R.M.Hoet, and J.H.Veerkamp. "Generation and application of type-specific anti-heparan sulfate antibodies using phage display technology. Further evidence for heparan sulfate heterogeneity in the kidney." *J Biol Chem* 273, no. 21(1998):12960-6.
43. J.S.Pieper, P.B.van Wachem, M.J.A.van Luyn, L.A.Brouwer, T.Hafmans, J.H.Veerkamp, and T.H.van Kuppevelt. "Attachment of glycosaminoglycans to collagenous matrices modulates the tissue response in rats." *Biomaterials* 21, no. 16(2000):1689-99.

44. J.E.Nuininga, H.T.van Moerkerk, A.Hanssen, C.A.Hulsbergen, J.Oosterwijk-Wakka, E.Oosterwijk, R.P.de Gier, J.A.Schalken, T.H.van Kuppevelt, and W.F.Feitz. "A rabbit model to tissue engineer the bladder." *Biomaterials* 25, no. 9(2004):1657-61.
45. F.Oberpenning, J.Meng, J.J.Yoo, and A.Atala. "De novo reconstitution of a functional mammalian urinary bladder by tissue engineering." *Nat Biotechnol* 17, no. 2(1999):149-55.
46. N.Arikan, K.Turkolmez, M.Budak, and O.Gogus. "Outcome of augmentation sigmoidocystoplasty in children with neurogenic bladder." *Urol.Int.* 64, no. 2(2000):82-85.
47. S.Herschorn and R.J.Hewitt. "Patient perspective of long-term outcome of augmentation cystoplasty for neurogenic bladder." *Urology* 52, no. 4(October 1998):672-78.
48. S.V.Lima, L.A.Araujo, F.O.Vilar, C.L.Kummer, and E.C.Lima. "Nonsecretory sigmoid cystoplasty: experimental and clinical results." *J Urol.* 153, no. 5(May 1995):1651-54.
49. A.Atala. "Regenerative medicine and urology." *BJU.Int.* 92 Suppl 1,(October 2003):58-67.
50. B.P.Kropp, B.L.Eppley, C.D.Prevel, M.K.Rippy, R.C.Harruff, S.F.Badylak, M.C.Adams, R.C.Rink, and M.A.Keating. "Experimental assessment of small intestinal submucosa as a bladder wall substitute." *Urology* 46, no. 3(1995):396-400.
51. B.P.Kropp. "Small-intestinal submucosa for bladder augmentation: a review of preclinical studies." *World J Urol* 16, no. 4(1998):262-7.
52. P.A.Merguerian, P.P.Reddy, D.J.Barrieras, G.J.Wilson, K.Woodhouse, D.J.Bagli, G.A.McLorie, and A.E.Khoury. "Acellular bladder matrix allografts in the regeneration of functional bladders: evaluation of large-segment (> 24 cm) substitution in a porcine model." *BJU Int* 85, no. 7(2000):894-8.
53. M.Probst, R.Dahiya, S.Carrier, and E.A.Tanagho. "Reproduction of functional smooth muscle tissue and partial bladder replacement." *Br J Urol* 79, no. 4(1997):505-15.
54. P.P.Reddy, D.J.Barrieras, G.Wilson, D.J.Bagli, G.A.McLorie, A.E.Khoury, and P.A.Merguerian. "Regeneration of functional bladder substitutes using large segment acellular matrix allografts in a porcine model." *J Urol* 164, no. 3 Pt 2(2000):936-41.
55. P.Buma, J.S.Pieper, T.van Tienen, J.L.van Susante, P.M.van der Kraan, J.H.Veerkamp, W.B.van den Berg, R.P.Veth, and T.H.van Kuppevelt. "Cross-linked type I and type II collagenous matrices for the repair of full-thickness articular cartilage defects--a study in rabbits." *Biomaterials* 24, no. 19(2003):3255-63.
56. P.M.D.Nastaran Mahmoudifar. "Tissue engineering of human cartilage in bioreactors using single and composite cell-seeded scaffolds." *Biotechnology and Bioengineering* 91, no. 3(2005):338-55.
57. H.A.Breinan, S.D.Martin, H.P.Hsu, and M.Spector. "Healing of canine articular cartilage defects treated with microfracture, a type-II collagen matrix, or cultured autologous chondrocytes." *J Orthop Res* 18, no. 5(2000):781-9.
58. S.B.Cohen, C.M.Meirisch, H.A.Wilson, and D.R.Diduch. "The use of absorbable co-polymer pads with alginate and cells for articular cartilage repair in rabbits." *Biomaterials* 24, no. 15(2003):2653-60.
59. J.S.Douchis, W.C.Bae, A.C.Chen, R.L.Sah, R.D.Coutts, and D.Amiel. "Cartilage repair with autogenic perichondrium cell and polylactic acid grafts." *Clin Orthop Relat Res* no. 377(2000):248-64.
60. S.W.Kang, O.Jeon, and B.S.Kim. "Poly(lactic-co-glycolic acid) microspheres as an injectable scaffold for cartilage tissue engineering." *Tissue Eng* 11, no. 3-4(2005):438-47.
61. R.Westreich, M.Kaufman, P.Gannon, and W.Lawson. "Validating the subcutaneous model of injectable autologous cartilage using a fibrin glue scaffold." *Laryngoscope* 114, no. 12(2004):2154-60.

Chapter 2

EXPRESSION, PRODUCTION AND BIOLOGICAL ACTIVITY ANALYSES OF RECOMBINANT RAT VEGF-164

Paul J. Geutjes¹
Suzan T. Nillesen¹
Gerwen Lammers¹
Willeke F. Daamen¹
Toin H. van Kuppevelt¹

¹Radboud University Nijmegen Medical Centre, Department of
¹Biochemistry (280), P.O. Box 9101, 6525 GA Nijmegen, The Netherlands

Protein Expression and Purification 2010;69(1):76-82

ABSTRACT

INTRODUCTION Large-scale production of recombinant rat vascular endothelial growth factor (rrVEGF-164) is desirable for angiogenic studies. **METHODS** In this study, biologically active recombinant rat vascular endothelial growth factor (rrVEGF-164) was cloned and expressed in the yeast *P. pastoris*, and large-scale production was performed by fermentation. cDNA encoding VEGF-164 was prepared from embryonic rat tissue RNA, and a recombinant pPIC9HV/rVEGF-164 plasmid, containing an AOX1 promoter, was constructed. The methylotrophic *P. pastoris* was used as the eukaryotic expression system. **RESULTS** After transformation, rrVEGF-164 was produced by fermentation (~124 mg/L) and purified by heparin affinity chromatography. SDS-PAGE indicated that rrVEGF-164 was produced as a disulphide-bridged dimer of 48 kDa which was purified to near homogeneity by heparin affinity chromatography in a large quantity. A bioassay indicated a three to five-fold increase in endothelial cell proliferation after 3 days, due to the addition of the produced rrVEGF-164. The produced rrVEGF-164 showed a higher biological activity than a commercially available, mouse cell line-based, growth factor. **CONCLUSIONS** In conclusion, using the *P. pastoris* expression system we were able to produce biologically active rat VEGF-164 in high quantities and this may provide a powerful tool for basic and applied life sciences.

INTRODUCTION

Vascular endothelial growth factor (VEGF) is one of the most celebrated mediators in the process of angiogenesis. VEGF is a hypoxia-inducible protein that promotes the proliferation and survival of vascular endothelial cells (1). At least five different rat VEGF alternatively spliced isoforms have been identified originating from a single VEGF pre-mRNA: VEGF-120, -144, -164, -188 and -205 (2-4). These isoforms resemble the human VEGF isoforms (VEGF-121, -145, -165, -189 and -206) and differ in length from them by one amino acid. VEGF is only active in its dimeric form (5, 6). All rat VEGF isoforms are mitogenic to vascular endothelial cells and induce permeabilisation of blood vessels (7). VEGF-164, VEGF-188 and VEGF-205 are able to bind heparin (7-9). VEGF-164 binds to the VEGF receptor (VEGFR) present on endothelial cells, stimulating the production of matrix metalloproteinases (MMPs). MMPs degrade the basement membrane, allowing proliferation and migration of endothelial cells towards the interstitium, so-called sprouting. Subsequently, pericytes proliferate and migrate towards the newly formed sprouts and induce maturation by forming a layer around the sprout (10, 11).

Large-scale production and purification of rat VEGF-164 is desirable for angiogenic studies *in vitro* and *in vivo*, especially in rat animal models for tissue engineering in which enhanced angiogenesis is an issue. Since the source of natural (rat) growth factors is limited, attempts have been made to produce growth factors on a large-scale by recombinant DNA technology. Growth factors have been produced in *Escherichia coli* and have played an important role in basic research of rat angiogenesis (12, 13). *E. coli* is a prokaryote and its intrinsic characteristics such as protein processing, protein folding, and post translational modifications, differ from those of eukaryotes. In *E. coli*, dimeric growth factors such as VEGF are produced as a monomer and need to be dimerised after production. The *Pichia pastoris* yeast expression system allows correct folding of dimeric proteins in addition to efficient expression, intact secretion, large-scale production, and stable genetics (14, 15). Human VEGF has been efficiently expressed in *P. pastoris* (16). Expression of biologically active rat VEGF in *P. pastoris*, however, has -to our knowledge- never been published.

In this study, rrVEGF-164 was inserted into the pPIC9HV expression vector and transfected into the *P. pastoris* yeast cells. RrVEGF-164 was secreted in large quantities, purified using heparin affinity chromatography, and its biological activity was studied *in vitro* using human umbilical vein endothelial cells (HUVECs).

MATERIALS AND METHODS

Materials

Unless stated otherwise, all materials were from Merck (Darmstadt, Germany). The VEGF upstream (5'-GTA GAA TTC GCA CCC ACG ACA GAA GG-3') and VEGF downstream (5'-TAT GCG GCC GCT CAC CGC CTT GGC TTG T-3') primer containing *EcoRI* and *NotI* restriction sites were synthesised by Isogen Biosciences BV (Maarsse, The Netherlands). The *P. pastoris* expression vector pPIC9 and *P. pastoris* host strain GS115 were purchased from Invitrogen Corp. (Carlsbad, CA, USA). The commercial rrVEGF-164, produced in a mouse myeloma cell line (R&D Systems, Minneapolis, MN, USA) was used as a positive control and for reference.

LB-medium consisted per litre of; 10 g NaCl, 10 g peptone (Gibco BRL), 5 g yeast extract (Difco Laboratories, Detroit, MI, USA), containing 10 g glucose and 0.1 g ampicillin (Sigma).

Buffered Glycerol-complex Medium (BMGY) containing glycerol as the carbon source, consisted per litre of; 10 g yeast extract, 20 g peptone, 21.2 g potassium sulphate (pH 6.0), 13.4 g yeast nitrogen base (YNB) (Sigma Chemical Co., St Louis, MO, USA), 0.4 mg biotin and 10 ml glycerol.

Buffered Methanol-complex Medium (BMMY) is similar to BMGY, but with 5 ml methanol instead of glycerol.

Basal salts medium (BSM) consisted per litre of; 26.7 ml phosphoric acid, 1.18 g calcium sulphate·2H₂O, 18.2 g potassium sulphate, 14.9 g magnesium sulphate·7H₂O, 4.1 g potassium hydroxide and 40 ml glycerol.

PTM1 trace salts (Invitrogen) consisted per litre of; 5 ml sulphuric acid, 6 g cupric sulphate·5H₂O, 0.08 g sodium iodide, 3 g manganese sulphate·H₂O, 0.2 g sodium molybdate·2H₂O, 0.02 g boric acid, 0.5 g cobalt chloride, 20 g zinc chloride, 65 g ferrous sulphate·7H₂O, and 0.2 g biotin.

YPD-medium consisted per litre of; 10 g yeast extract, 20 g peptone, 20 g D-glucose, with 100000 U penicillin and 0.1 g streptomycin (Gibco BRL).

YNB dropout plates consisted per litre of; 6.7 g YNB, 1.92 g yeast synthetic dropout medium supplement (Sigma), 20 g glucose and 20 g agar (Gibco BRL).

TYE agar plates consisted per litre of; 8 g NaCl, 10 g peptone, 5 g yeast extract, 15 g agar (Gibco BRL), 10 g glucose and 100 g ampicillin (Sigma).

Preparation of rat VEGF-164 cDNA

Total RNA was isolated from *Rattus norvegicus* embryonic tissue (17 days post-conception) using the SV Total RNA Isolation System (Promega, Madison, WI, USA). After denaturation (10 min at 65°C) of the total RNA (~0.5 µg), cDNA (~0.4 µg) was synthesised using hexanucleotide primers. A reverse transcriptase reaction was performed for 90 min at 37°C using the following reaction mixture; 200 units reverse transcriptase (Promega) in 50 mM Tris-HCl (pH 8.3) containing 75 mM KCl, 3 mM MgCl₂ [M-MLV Reversed Transcriptase buffer (Gibco BRL, Gaithersburg, MD, USA)], 1 mM deoxynucleoside triphosphates (dNTPs) and 10 mM DTT (Gibco BRL) in a total volume of 20 µl. PCR fragments of the full-length cDNA were prepared with 10 mM Tris-HCl (pH 8.3) containing 50 mM KCl, 1.5 mM MgCl₂, 100 µM dNTPs, 20 µM rrVEGF-164 primers and 1 unit Taq polymerase (Promega) in a total volume of 50 µL. The PCR was performed on a Peltier Thermal Cycler (PTC-200; MJ Research and Biozym, Landgraaf, The Netherlands), with a 30 cycles program (95°C for 60s, 65°C for 60s, 72°C for 90s and extension at 72°C for 5 min). The rrVEGF-164 cDNA was isolated from a 2% (w/v) agarose gel and purified with a QIAEX II gel extraction system (QIAGEN, Hilden, Germany). The SMART-ladder marker (Eurogentec) was used to estimate the sizes of the PCR products.

Construction of expression vector

The purified cDNA was subcloned into the vector pPIC9HV (J.M.H. Raats, Dept. of Biochemical Chemistry, Radboud University Nijmegen Medical Centre, Nijmegen, The Netherlands, unpublished data (pPIC9 expression plasmid was obtained from Invitrogen)) after digestion with *EcoRI* and *NotI* (Invitrogen) in the presence of 1x React® 3 buffer (GibcoBRL) for 1 h at 37°C. The pPIC9HV is similar to the original pPIC9 vector (17, 18), but contains a polyhistidine and VSV-tag for detection and purification. The rrVEGF-164 insert was ligated into pPIC9HV vector DNA using T4 ligase (Gibco BRL) in T4 ligase buffer (Gibco BRL) for 24 h at 16°C.

The host strain *Escherichia coli* (supE44ΔlacU169 (φ80lacΔM15) hsdR17 recA1 endA1 gyrA96 thi-1 relA1) was transformed with the expression vector by heat-shock (45 s at 42°C).

The *E. coli* cells were incubated for 1 h at 37°C in LB-medium. After 1 min of centrifugation at 14000g, the transformed *E. coli* cells were applied to a TYE agar plates and incubated for 24 h at 37°C. The rrVEGF-164 positive transformants were selected by means of ampicillin antibiotic resistance due to the presence of ampicillin resistance gene (AMP) in the *Pichia* expression vector. Ampicillin resistant *E. coli* transformants were selected and suspended in LB-medium. After 24 h incubation at 37°C at 200 rpm in an orbital shaker, the suspension was centrifuged for 1 min at 14000g. Plasmid DNA was isolated using the QIAprep spin mini-prep kit (QIAGEN) according to the manufacturer's instructions, and positive transformants were identified by automated sequencing using an α -factor primer (5'-ACTACTATTGCCAGCATTGCTGCT-3') at the DNA Sequencing Facility, Dept. of Human Genetics, Radboud University Nijmegen Medical Centre, The Netherlands.

Transformation into P. pastoris yeast cells

P. pastoris GS115 cells were grown in 100 ml YPD-medium overnight at 30°C at 200 rpm in an orbital shaker, until an OD600 of 1.5 was reached, which corresponds to a cell density of approximately 109 cells/ml. Competent GS115 cells were freshly prepared before transformation by consecutive washings with ice-cold sterile MilliQ water and 1 M sorbitol according to the Invitrogen manual. The DNA was linearised by digesting 10 µg of plasmid DNA with *Sall*. Subsequently, the linearised DNA was purified using the QIAGEN PCR cleanup kit. To clone the expression vector into the *P. pastoris* yeast cells, cells were resuspended in 1 M sorbitol on ice, and 80 µl of competent cells were electroporated by means of pulse discharges (1.5 kV, 25 µF, 400 Ohm, Bio-Rad Gene Pulser, CA, USA) for 9 ms in the presence of 10 µg linearised plasmid DNA (20 µl). After electroporation, cells were put on ice for 5 min, 10x diluted in 1 M sorbitol and incubated for 1 h at 30°C (without shaking). Cells were spread on YNB dropout plates and incubated at 30°C. The plasmid contains the *His4* gene (encoding histidinol dehydrogenase) which initiates the yeast cell to synthesise histidine (His⁺). Therefore, only positive transformants can grow on the histidine deficient plates (YNB dropout plates), which can be used for positive clone selection (19). After 2 days of culturing, the positive transformants were counted, picked, and streaked on new dropout plates. After a 45 h incubation at 30°C, single colonies were picked and cultured in a baffled flask containing 25 ml BMGY-medium for an overnight period at 30°C at 200 rpm in an orbital shaker. To store the cultures, frozen stocks were prepared by adding 60% (v/v) glycerol (0.5 ml) to the *P. pastoris* recombinants in YPD-medium (0.5 ml) and freezing at -80°C.

Expression screening of rrVEGF-164

To analyse the expression levels of the constructed transformants, a small-scale expression screening was performed using a fast induction method with methanol. His⁺ transformants were picked and added to 15 ml BMGY-medium, and cultured in 200 ml baffled flasks overnight at 30°C, 200 rpm in an orbital shaker. To induce production of rrVEGF-164, cells were centrifuged (1500g, 4°C, for 10 min) and resuspended in BMMY-medium containing 25% (v/v) methanol as the major carbon source. Cells were incubated for 2 days at 30°C, 200 rpm in an orbital shaker. After centrifugation (1500g, 4°C, 10 min), the secreted rrVEGF-164 was concentrated from the supernatant by adding 50 µl heparin-acryl beads (Sigma Chemical Co.) to 1 ml supernatant, and incubation for 1 h at 21°C under rotating conditions. Heparin beads were concentrated by centrifugation (1500g, 4°C, 10 min) and analysed using SDS-PAGE and Western blotting analysis as described below.

Large-scale production of rrVEGF-164

For large-scale rrVEGF-164 production, a 1 L baffled flask with 200 ml YNB-medium was inoculated with 1 ml thawed *P. pastoris* host strain GS115 containing the rrVEGF-164 expression vector. An overnight culture was incubated at 30°C at 200 rpm in an orbital shaker until an OD₆₀₀ of approximately 6 was reached. The Bioflo® 3000 fermentor (New Brunswick Scientific, Edison, NJ, USA), containing 2 L of basal salts medium, was sterilised by autoclaving for 45 min at 121°C. After autoclaving, 4.35 ml/L PTM1 trace salts (Sigma) were added aseptically to the initial fermentation volume. Ammonium hydroxide (28% (w/v), Sigma) was used as a nitrogen source and to increase the pH during the fermentation process. The 200 ml inoculum was transferred into the fermentor after setting the dissolved oxygen (DO) at 100%, the pH at 6.0 and the temperature at 30°C. Anti-foam solution 289 (Sigma) diluted 1:500 in MilliQ water was used to reduce foam production during fermentation. Yeast cells use oxygen for oxidative metabolism of glycerol. When glycerol is consumed the need for oxygen declines and as a consequence the DO rises. After approximately 24 h of batch culture, the glycerol was completely consumed which was indicated by a sharp rise in DO (up to 70%, see Fig. 4). The 5 h glycerol fed-batch was started by feeding 50% (v/v) glycerol containing 12 ml/L PTM1 trace salts with feed rate of 18.15 ml/L/h. After the glycerol was used (DO of ~100%), the methanol feed (100% (v/v) methanol (Labscan) with 12 ml/L PTM1 trace salts) was started to fully induce the AOX1 promoter of the expression system. During the methanol feed, DO decreased rapidly from ~100% to 30% and was continued at 30% for another 30 h. The culture was then harvested and centrifuged (20 min at 5000 g). The supernatant was filtered using a 0.45 µm cellulose acetate membrane filter (Schleicher and Schuell, Dassel, Germany) and dialysed against 10 mM phosphate buffered saline (pH 7.4).

Purification and identification of rrVEGF-164

For purification of rrVEGF-164, the dialysed supernatant (300 ml) was 1:1 diluted with 10 mM phosphate buffer (PB) containing 0.2 M NaCl and adjusted to pH 7.0 with 1 M Na₂HPO₄. The solution was subjected to fast protein liquid chromatography (FPLC), using a 5 ml heparin-sepharose HiTrap™ column (Amersham Biosciences, Stockholm, Sweden). The rrVEGF-164 was eluted with 1 M NaCl in 10 mM PB (pH 7.0) for 20 min, followed by 2 M NaCl in 10 mM PB (pH 7.0) for 20 min at 2.5 ml/min for both solutions (see Fig. 5). Five fractions (2.5 ml/fraction) with highest A₂₈₀ absorbance were collected, pooled and directly frozen at -80°C. Purity and dimer formation were evaluated by sodium dodecyl sulphate polyacrylamide gel electrophoresis (SDS-PAGE; 15% (w/v); Serva GmbH, Frankfurt, Germany) (20). Briefly, the supernatant was diluted 1:1 with sample buffer with and without 5% (v/v) β-mercaptoethanol (with and without reducing conditions) and denatured for 5 min at 95°C. Then 10 µl (~0.6 µg) of denatured rrVEGF-164 was loaded on the gel and was visualised by Coomassie Brilliant Blue (0.1% (w/v)) staining or further identified by Western blotting using goat anti-rat VEGF antibody (1:1000) (R&D Systems) (21). The amount of purified rrVEGF-164 was determined by a Lowry analysis using bovine serum albumin (BSA) as a standard (22).

Biological activity of produced rrVEGF-164

Human umbilical vein endothelial cells (HUVECs, ATCC, CRL-1730, Rockville, MD, USA) were grown in F12K medium (Gibco BRL, Carlsbad, CA, USA) with 20% (v/v) foetal calf serum (FCS), 1.5 % (w/v) calf brain extract (as a source for endothelial cell growth factor (ECGF)), 0.14 mg/ml heparin, 200 mM L-glutamine, 100 U/ml penicillin and 100 µg/ml streptomycin (Gibco BRL). After coating the 96-wells plate with 1% (v/v) gelatine, 4000 cells were seeded per well and these were left to attach overnight in the above medium without ECGF. Next,

medium was replaced by F12K medium without ECGF and 0-100 ng/ml rrVEGF-164 was added. A cell proliferation assay (WST-1, Roche, Mannheim Germany), based on the reduction of a tetrazolium salt to formazan by mitochondrial dehydrogenases in viable cells, was used to determine the relative number of cells at day 1 and 3 (23). Proliferation of cells in medium without VEGF was set to 100%. A student's t-test was used for statistical analyses and $p < 0.05$ was considered statistically significant.

RESULTS AND DISCUSSION

Preparation of rat VEGF-164 cDNA

Total RNA was isolated from embryonic *Rattus norvegicus* tissue and transcribed into cDNA using random hexanucleotide primers. After amplification with VEGF specific primers, PCR products were separated on agarose gel, and three VEGF splice variants (VEGF-188 (564bp), VEGF-164 (492bp) and VEGF-120 (360bp)) could be identified on the basis of their molecular mass (Fig. 1A). The 492bp fragment was extracted from the gel, and reamplified. This fragment and the pPIC9HV vector were cut with *EcoRI* and *NotI* and put on an agarose gel for isolation and for further ligation (Fig. 1B).

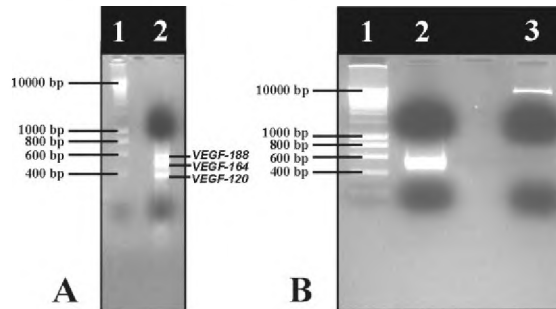


Fig 1 Agarose gel electrophoresis of PCR products. A) ethidium bromide-stained agarose gel shows in lane 1: DNA marker, lane 2: PCR products after amplification using VEGF specific primers, indicating three VEGF splice variants, VEGF-188 (564bp), VEGF-164 (492bp) and VEGF-120 (360bp). B) lane 1: DNA marker, lane 2: the rrVEGF-164 insert (492 bp) and in lane 3 the pPIC9HV vector (8580 bp).

Construction of expression vector

After *EcoRI* and *NotI* digestion, purification and ligation, the resulting pPIC9HV-rrVEGF-164 expression vector (Fig. 2) was transformed into *E. coli*. Positive clones were selected by means of ampicillin resistance. Eight of 64 colonies able to grow on ampicillin plates were sequenced. After verifying the nucleotide sequence of the insert using DNA sequencing (Fig. 3) and a subsequent BLAST search, one colony was found identical with seven rrVEGF-164 sequences published. The nucleotide sequence encoding the rrVEGF-164 (Genbank reference GQ423618) showed a 100% homology with the nucleotide sequence of rrVEGF-164 published by Conn *et al.* 1990 (24) (Genbank reference AAA41211) and Strausberg *et al.* 2002 (25) (Genbank reference AAI68708).

Cloning and production of rat VEGF-164

After isolation and linearisation of the plasmid DNA of the positive clone with *Sall*, the competent *P. pastoris* GS115 cells were transformed with plasmid DNA by means of electroporation. The transformants were cultured in the absence of histidine and 6 colonies were

picked and examined for rrVEGF-164 production. Western blot analyses indicated that 4 of the 6 clones produced rrVEGF-164 (data not shown).

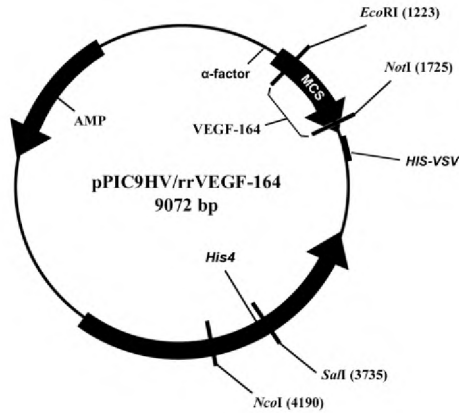


Fig 2 Map of the rrVEGF-164 expression vector based on the pPIC9HV vector. MCS: multiple cloning site. The α -factor directs VEGF to the secretory pathway. *EcoRI* and *NotI* restriction sites were used to insert rVEGF-164 into the multiple cloning site. The ampicillin resistance gene (AMP) was used for *E. coli* transformant selection. The histidine independent gene (*His4*) allows growth in the absence of histidine, and was used for *P. pastoris* transformant selection. The *SalI* restriction site was used to inactivate the *His4* gene and only a successful ligation results in an intact *His4* gene.

Met Arg Phe Pro Ser Ile Phe Thr Ala Val Leu Phe Ala Ala Ser Ser Ala Leu Ala Ala Pro Val									
ATG AGA TTT CGT TCA ATT TTT ACT GCA GTT TTA TTC GCA GCA TCC GCC TTA GCT GCT CGA GTC									
<i>α-factor Signal Sequence</i>									
Asn Thr Thr Thr Glu Asp Glu Thr Ala Gln Ile Pro Ala Glu Ala Val Ile Gly Tyr Ser Asp Leu									
AAC ACT ACA ACA GAA GAT GAA ACG GCA CAA ATT CCG GCT GAA GCT GTC ATC GGT TAC TCA GAT TTA									
<i>α-factor primer</i>									
Glu Gly Asp Phe Asp Val Ala Val Leu Pro Phe Ser Asn Ser Thr Asn Asn Gly Leu Leu Phe Ile Asn									
GAA GGG GAT TTC GAT GTT GCT TTT TGC CCA TTT TCC AAC AGC ACA AAT AAC GGG TTA TTG TTT ATA AAT									
<i>EcoRI</i>									
Thr Thr Ile Ala Ser Ile Ala Ala Lys Glu Glu Gly Val Ser Leu Glu Lys Arg Glu Ala Glu Ala									
ACT ACT ATT GCC AGC ATT GCT GCT AAA GAA GAA GGG GTA TCT CTC GAG AAA AGA GAG GCT GAA GCT									
<i>EcoRI</i>									
Tyr Val Glu Phe Ala Pro Thr Thr Glu Gly Glu Gln Lys Ala His Glu Val Val Lys Phe Met Asp									
TAC GTA GAA TTC GCA CCC ACG ACA GAA GGG GAG CAG AAA GCC CAT GAA GTG GTG AAG TTC ATG GAC									
<i>EcoRI</i>									
Val Tyr Gln Arg Ser Tyr Cys Arg Pro Ile Glu Thr Leu Val Asp Ile Phe Gln Glu Tyr Pro Asp									
GTC TAC CAG CGC AGC TAT TGC CGT CCA ATT GAG ACC CTG GTG GAC ATC TTC CAG GAG TAC CCC GAT									
<i>EcoRI</i>									
Glu Ile Glu Tyr Ile Phe Lys Pro Ser Cys Val Pro Leu Met Arg Cys Ala Gly Cys Cys Asn Asp									
GAG ATA GAG TAT ATC TTC AAG CCG TCC TGT GTG CCC CTA ATG CGG TGT GCG GGC TGC TGC AAT GAT									
<i>EcoRI</i>									
Glu Ala Leu Glu Cys Val Pro Thr Ser Glu Ser Asn Val Thr Met Gln Ile Met Arg Ile Lys Pro									
GAA GCC CTG GAG TGC GTG CCC ACG TCG GAG AGC AAC GTC ACT ATG CAG ATC ATC CGG ATC AAA CCT									
<i>rVEGF-164</i>									
His Gln Ser Gln His Ile Gly Glu Met Ser Phe Leu Gln His Ser Arg Cys Glu Cys Arg Pro Lys									
CAC CAA AGC CAG CAC ATA GGA GAG ATG AGC TTC CTG CAG CAT AGC AGA TGT GAA TGC AGA CCA AAG									
<i>EcoRI</i>									
Lys Asp Arg Thr Lys Pro Glu Asn His Cys Glu Pro Cys Ser Glu Arg Arg Lys His Leu Phe Val									
AAA GAT AGA ACA AAG CCA GAA AAT CAC TGT GAG CCT TGT TCA GAG CCG AGA AAG CAT TTG TTT GTC									
<i>EcoRI</i>									
Gln Asp Pro Gln Thr Cys Lys Cys Ser Cys Lys Asn Thr Asp Ser Arg Cys Lys Ala Arg Gln Leu									
CAA GAT CCG CAG ACG TGT AAA TGT TCC TGC AAA AAC ACA GAC TCG CGT TGC AAG GCG AGG CAG CTT									
<i>EcoRI</i>									
Glu Leu Asn Glu Arg Thr Cys Arg Cys Asp Lys Pro Arg Arg Stop Ala Ala Ala His His His His									
GAG TTA AAC GAA CGT ACT TGC AGA TGT GAC AAG CCA AGG CCG TGA GCG GCC GCA CAT CAT CAC CAT									
<i>NotI</i>									
His His His His Tyr Thr Asp Ile Glu Met Asn Arg Leu Gly Lys									
CAT CAC CAT CAT TAT TAC ACA GAC ATA GAG ATG AAC CGA CTT GGA AAG									

Fig 3 Nucleotide sequence and the deduced amino acid sequence of the relevant part of *P. pastoris* rrVEGF-164 expression vector, indicating α -Factor Signal Sequence, the *EcoRI* restriction site, the rVEGF-164 insert, the *NotI* restriction site and the polyhistidine-VSV tag. A stop codon was positioned between rVEGF-164 and *NotI* in order to produce VEGF without tags. The α -factor signal, the rVEGF-164, and the His/VSV tag are indicated by boxes. The α -factor primer is also indicated.

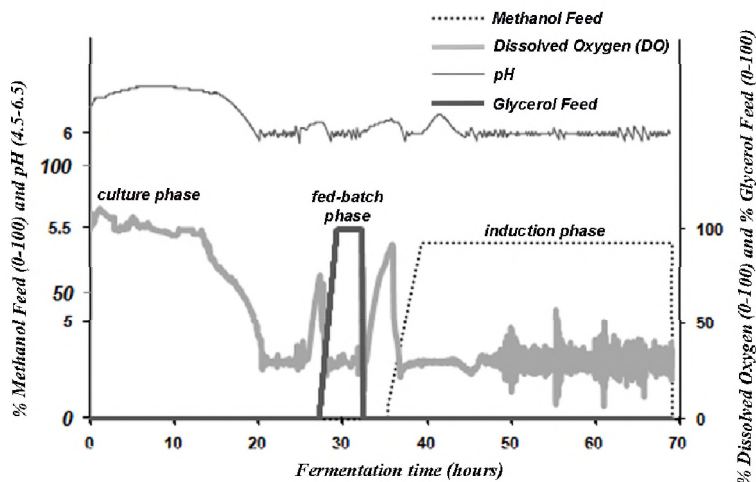


Fig 4 Profile of fermentation process describing the % methanol feed, pH, % dissolved oxygen level and % glycerol feed in time (hours). In the *culture phase* a biomass of yeast cells was formed. In the *fed-batch phase* glycerol was accumulated in the yeast cells as a major carbon source. In the *induction phase* the VEGF-164 production was induced with methanol.

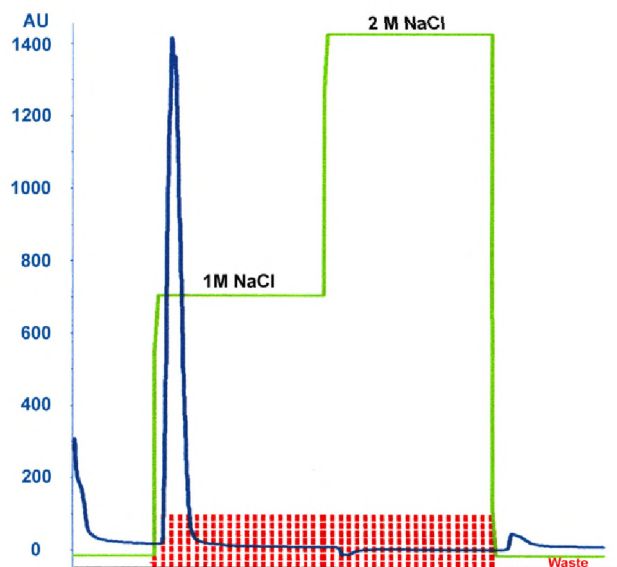


Fig. 5 FPLC flow chart of the purification of rrVEGF-164 by heparin affinity chromatography. In green the elution buffers are indicated; viz. 10 mM phosphate buffer (pH 7.0) containing 1M NaCl or 2 M NaCl. The Y-axis indicates absorbance at $\lambda = 280$ nm expressed in arbitrary units (AU). On the X-axis, the collected fractions (each containing 2 ml) are represented by the vertical dashed lines.

Purification and identification of rrVEGF-164

From the small production screening one clone with a strong band on Western blot was selected and used for large scale production. After the fermentor run, the bulk cell mass was separated from the supernatant and the expressed rrVEGF-164 was purified from the supernatant. Because rrVEGF-164 is a heparin-binding protein, the expressed product was purified with a heparin column. The rrVEGF-164 was present in the 1 M NaCl elution peak (Fig. 5). The rrVEGF-164 content in the pooled peak fractions was ~124 mg/L as determined by Lowry protein assay (22). Using non-reducing conditions, SDS-PAGE showed one broad band of about 48 kDa (dimer), whereas under reducing conditions a main band of about 24 kDa band (monomer) was observed (Fig. 6A). It was to be expected that on an SDS-PAGE gel dimeric and monomeric rrVEGF-164 migrate at 45 kDa and 23 kDa, respectively (26). Western blot analysis using an anti rat VEGF-164 antibody further indicated that the protein was rat VEGF-164 (Fig. 6B). Under non-reducing conditions, the expressed rrVEGF-164 existed in the biologically active form of a homodimer. Dimers of VEGF are disulphide-bridged, which is essential for the biological activity of VEGF-164 (5). These data indicate that rrVEGF-164 is produced as a disulphide-bridged dimer which can be purified to near homogeneity by heparin affinity chromatography.

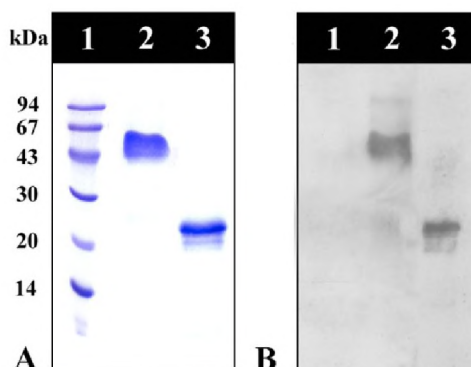


Fig 6 Analysis of produced rrVEGF-164 by SDS-PAGE and Western blot analysis. A) Coomassie Brilliant Blue staining; lane 1: markers; lane 2: rrVEGF-164 under non-reducing conditions (about 48 kDa); lane 3: rrVEGF-164 under reducing conditions (about 24 kDa). B) Western blot analysis of the produced rrVEGF-164; lane 1: markers; lane 2: rrVEGF-164 under non-reducing conditions (about 48 kDa); lane 3: rrVEGF-164 under reducing conditions (about 24 kDa). Figure A and B are both composite images of VEGF-164 monomer and dimer products, taken from separate reducing and non-reducing gels respectively.

Biological activity of produced rrVEGF-164

The biological activity of the purified rrVEGF-164 was determined by a WST-1 proliferation assay using human endothelial cells (HUVECs). HUVECs are generally used to evaluate the activity of VEGF from various species (16, 27). Already after 1 day, the 25 ng/ml content resulted in a three-fold increase in proliferation compared to medium without added VEGF (Fig 7A). After 3 days, the amount of proliferation at content of 12.5-25 ng/ml showed a three to five-fold increase (Fig 7B). We also compared our produced *Pichia* VEGF with commercial rrVEGF-164 which is produced in a mouse myeloma cell line. At amounts of 12.5-100 ng/ml, the produced rrVEGF-164 showed a significantly higher proliferation than the commercial batch of rrVEGF-164 ($p < 0.05$; Fig. 7A and B).

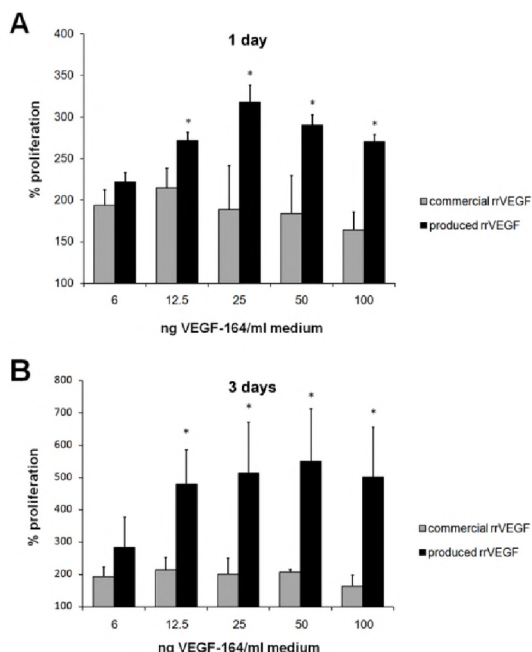


Fig 7 Biological activity of the produced rrVEGF-164 and commercially available rrVEGF-164 analysed using a WST-1 assay. A) Proliferation after 1 day of culture. B) Proliferation after 3 days of culture. The proliferation without added VEGF was set to 100%. Results are mean \pm SD for 3 separate experiments. All values were significantly increased compared to the control values. * Indicates $p < 0.05$ when comparing produced and commercial rrVEGF-164.

The difference in activity for the commercial VEGF and our Pichia-derived VEGF might be due to the presence of inactive forms as influenced by the production method. Until now, both mouse myeloma cell lines and *E. coli* have been used to produce rrVEGF-164 commercially. The myeloma and *E. coli* production methods can result in heterogeneity of molecules with variable biological activities (28). Additionally, for *E. coli* the expressed product is present in inclusion bodies and in order to be active the protein must be refolded (dimerised) after purification. For rrVEGF-164 produced in *P. pastoris*, the protein has already been processed, including disulfide-linked dimers, before secretion into the cell medium. This pre-processing can result in a potentially more homogeneous, more highly active population of the product.

CONCLUSIONS

In this study, we have cloned and expressed biologically active recombinant rat vascular endothelial growth factor (rrVEGF-164) in the yeast *P. pastoris*. Recombinant rat VEGF-164 was successfully produced as an active dimer in a large quantity. The produced rrVEGF-164 had a higher biological activity than commercially available growth factor (produced in a mouse myeloma cell line). The high level expression of biologically active recombinant rat VEGF-164 provides a useful tool for basic and applied research.

REFERENCES

1. N.Ferrara. "Role of vascular endothelial growth factor in regulation of physiological angiogenesis." *AJP - Cell Physiology* 280, no. 6(June 2001):C1358-C1366.
2. T.Burchardt, M.Burchardt, M.W.Chen, R.Buttyan, T.A.de la, A.Shabsigh, and R.Shabsigh. "Expression of VEGF splice variants 144/145 and 205/206 in adult male tissues." *IUBMB Life* 48, no. 4(October 1999):405-08.
3. A.Hara, C.J.Chapin, R.Ertsey, and J.A.Kitterman. "Changes in fetal lung distension alter expression of vascular endothelial growth factor and its isoforms in developing rat lung." *Pediatr.Res.* 58, no. 1(July 2005):30-37.
4. I.Zachary. "Vascular endothelial growth factor." *The International Journal of Biochemistry & Cell Biology* 30, no. 11(November 1998):1169-74.
5. N.Ferrara. "Molecular and biological properties of vascular endothelial growth factor." *Journal of Molecular Medicine* 77, no. 7(September 1999):527-43.
6. A.Hoeben, B.Landuyt, M.S.Highley, H.Wildiers, A.T.Van Oosterom, and E.A.De Bruijn. "Vascular endothelial growth factor and angiogenesis." *Pharmacological Reviews* 56, no. 4(December 2004):549-80.
7. K.A.Houck, D.W.Leung, A.M.Rowland, J.Winer, and N.Ferrara. "Dual regulation of vascular endothelial growth factor bioavailability by genetic and proteolytic mechanisms." *Journal of Biological Chemistry* 267, no. 36(December 1992):26031-37.
8. J.E.Park, G.A.Keller, and N.Ferrara. "The vascular endothelial growth factor (VEGF) isoforms: differential deposition into the subepithelial extracellular matrix and bioactivity of extracellular matrix-bound VEGF." *Mol.Biol Cell* 4, no. 12(December 1993):1317-26.
9. H.Gitay-Goren, T.Cohen, S.Tessler, S.Soker, S.Gengrinovitch, P.Rockwell, M.Klagsbrun, B.Z.Levi, and G.Neufeld. "Selective binding of VEGF121 to one of the three vascular endothelial growth factor receptors of vascular endothelial cells." *J Biol Chem.* 271, no. 10(March 1996):5519-23.
10. H.Gerhardt and C.Betsholtz. "Endothelial-pericyte interactions in angiogenesis." *Cell and Tissue Research* 314, no. 1(October 2003):15-23.
11. V.Nehls, E.Schuchardt, and D.Drenckhahn. "The Effect of Fibroblasts, Vascular smooth muscle cells, and pericytes on sprout formation of endothelial cells in a fibrin gel angiogenesis system." *Microvascular Research* 48, no. 3(November 1994):349-63.
12. J.S.Pieper, T.Hafmans, P.B.van Wachem, M.J.van Luyn, L.A.Brouwer, J.H.Veerkamp, and T.H.van Kuppevelt. "Loading of collagen-heparan sulfate matrices with bFGF promotes angiogenesis and tissue generation in rats." *J Biomed.Mater.Res.* 62, no. 2(November 2002):185-94.
13. B.M.Shi, X.Y.Wang, Q.L.Mu, T.H.Wu, H.J.Liu, and Z.Yang. "Angiogenesis effect on rat liver after administration of expression vector encoding vascular endothelial growth factor D." *World J Gastroenterol.* 9, no. 2(February 2003):312-15.
14. J.M.Cregg, J.L.Cereghino, J.Shi, and D.R.Higgins. "Recombinant protein expression in *Pichia pastoris*." *Mol.Biotechnol.* 16, no. 1(September 2000):23-52.
15. G.P.L.Cereghino, J.L.Cereghino, C.Ilggen, and J.M.Cregg. "Production of recombinant proteins in fermenter cultures of the yeast *Pichia pastoris*." *Current Opinion in Biotechnology* 13, no. 4(August 2002):329-32.
16. L.Ma, X.N.Wang, Z.Q.Zhang, X.M.Zhou, G.F.Zeng, and A.J.Chen. "Expression, purification and biological activity analysis of human vascular endothelial growth factor (VEGF(165)) in *Pichia pastoris*." *Sheng Wu Hua Xue.Yu Sheng Wu Wu Li Xue.Bao.(Shanghai)* 33, no. 3(2001):325-30.
17. X.Yu, Z.Li, X.Xia, H.Fang, C.Zhou, and H.Chen. "Expression and purification of ancrod, an anticoagulant drug, in *Pichia pastoris*." *Protein Expression and Purification* 55, no. 2(October 2007):257-61.
18. Y.Yan, J.Chen, and J.Li. "Overexpression of a small medicinal peptide from ginseng in the yeast *Pichia pastoris*." *Protein Expression and Purification* 29, no. 2(June 2003):161-66.
19. J.M.Cregg, K.J.Barringer, A.Y.Hessler, and K.R.Madden. "*Pichia pastoris* as a host system for transformations." *Mol.Cell Biol* 5, no. 12(December 1985):3376-85.
20. U.K.Laemmli. "Cleavage of structural proteins during the assembly of the head of bacteriophage T4." *Nature* 227, no. 5259(August 1970):680-85.

21. W.N.Burnette. "Western Blotting": Electrophoretic transfer of proteins from sodium dodecyl sulfate-polyacrylamide gels to unmodified nitrocellulose and radiographic detection with antibody and radioiodinated protein A." *Analytical Biochemistry* 112, no. 2(April 1981):195-203.
22. O.H.Lowry, N.J.Rosebrough, A.L.Farr, and R.J.Randall. "Protein measurement with the folin phenol reagent." *Journal of Biological Chemistry* 193, no. 1(November 1951):265-75.
23. K.Hamasaki, K.Kogure, and K.Ohwada. "A biological method for the quantitative measurement of tetrodotoxin (TTX): Tissue culture bioassay in combination with a water-soluble tetrazolium salt." *Toxicon* 34, no. 4(April 1996):490-95.
24. G.Conn, M.L.Bayne, D.D.Soderman, P.W.Kwok, K.A.Sullivan, T.M.Plisi, D.A.Hope, and K.A.Thomas. "Amino Acid and cDNA Sequences of a vascular endothelial cell mitogen that is homologous to platelet-derived growth factor." *Proceedings of the National Academy of Sciences* 87, no. 7(April 1990):2628-32.
25. R.L.Strausberg, E.A.Feingold, L.H.Grouse, J.G.Derge, R.D.Klausner, F.S.Collins, L.Wagner, C.M.Shenmen, G.D.Schuler, S.F.Altschul, B.Zeeberg, K.H.Buetow, C.F.Schaefer, N.K.Bhat, R.F.Hopkins, H.Jordan, T.Moore, S.I.Max, J.Wang, F.Hsieh, L.Diatchenko, K.Marusina, A.A.Farmer, G.M.Rubin, L.Hong, M.Stapleton, M.B.Souares, M.F.Bonaldo, T.L.Casavant, T.E.Scheetz, M.J.Brownstein, T.B.Ustin, S.Toshiyuki, P.Carninci, C.Prange, S.S.Raha, N.A.Loquellano, G.J.Peters, R.D.Abramson, S.J.Mullahy, S.A.Bosak, P.J.McEwan, K.J.McKernan, J.A.Malek, P.H.Gunaratne, S.Richards, K.C.Worley, S.Hale, A.M.Garcia, L.J.Gay, S.W.Hulyk, D.K.Villalon, D.M.Muzny, E.J.Sodergren, X.Lu, R.A.Gibbs, J.Fahey, E.Helton, M.Ketteman, A.Madan, S.Rodrigues, A.Sanchez, M.Whiting, A.Madan, A.C.Young, Y.Shevchenko, G.G.Bouffard, R.W.Blakesley, J.W.Touchman, E.D.Green, M.C.Dickson, A.C.Rodriguez, J.Grimwood, J.Schmutz, R.M.Myers, Y.S.Butterfield, M.I.Krzywinski, U.Skalska, D.E.Smailus, A.Schnerch, J.E.Schein, S.J.Jones, and M.A.Marra. "Generation and initial analysis of more than 15,000 full-length human and mouse cDNA sequences." *Proc.Natl.Acad.Sci.U.S.A* 99, no. 26(December 2002):16899-903.
26. W.Petersen, D.Varoga, T.Zantop, J.Hassenpflug, R.Mentlein, and T.Pufe. "Cyclic strain influences the expression of the vascular endothelial growth factor (VEGF) and the hypoxia inducible factor 1
27. K.Ono, H.Hattori, S.Takeshita, A.Kurita, and M.Ishihara. "Structural features in heparin that interact with VEGF165 and modulate its biological activity." *Glycobiology* 9, no. 7(July 1999):705-11.
28. G.Siemeister, B.Schnurr, K.Mohrs, C.Schachtele, D.Marme, and G.Martiny-Baron. "Expression of biologically active isoforms of the tumor angiogenesis factor VEGF in *Escherichia coli*." *Biochem.Biophys.Res.Comm.* 222, no. 2(May 1996):249-55.

Chapter 3

INCREASED ANGIOGENESIS AND BLOOD VESSEL MATURATION IN ACELLULAR COLLAGEN-HEPARIN SCAFFOLDS CONTAINING BOTH FGF-2 AND VEGF

Suzan T. Nillesen¹
Paul J. Geutjes¹
Ronnie G. Wismans¹
Joost Schalkwijk²
Willeke F. Daamen¹
Toin H. van Kuppevelt¹

^{1,2}Radboud University Nijmegen Medical Centre, Departments of
¹Biochemistry (280), and ²Dermatology (370), P.O. Box 9101, 6525 GA Nijmegen,
The Netherlands

Biomaterials 2007;28(6):1123-31

ABSTRACT

INTRODUCTION An important issue in tissue engineering is the vascularisation of the implanted construct, which often takes several weeks. *In vivo*, the growth factors VEGF and FGF2 show a combined effect on both angiogenesis and maturation of blood vessels. Therefore, we hypothesise that the addition of these growth factors to an acellular construct increases blood vessel formation and maturation. **METHODS** To systematically evaluate the contribution of each scaffold component with respect to tissue response and in particular to blood vessel formation, five porous scaffolds were prepared and characterised viz.: collagen, collagen with heparin, and collagen with heparin plus one or two growth factors (rrFGF2 and rrVEGF). Scaffolds were subcutaneously implanted in 3 months old Wistar rats. **RESULTS** Of all scaffolds tested, the one with a combination of growth factors displayed the highest density of blood vessels (type IV collagen) and most mature blood vessels (smooth muscle actin). In addition, no hypoxic cells were found in this scaffold at day 7 and 21 (hypoxia inducible factor 1- α). **CONCLUSIONS** These results indicate that the addition of both FGF2 and VEGF to an acellular construct enhances an early mature vasculature. This opens prospects for (a-cellular) tissue-engineered constructs in conditions as ischemic heart disease or diabetic ulcers.

INTRODUCTION

A major problem in tissue engineered devices is the vascularisation of the construct. It usually takes several weeks for a construct to become fully vascularised (1). Vascularisation is important in several pathological conditions including ischemic heart disease (2) and diabetic ulcers (3). Impaired wound healing in case of diabetic ulcers occurs due to a lack of oxygen and nutrition to the cells and inadequate removal of waste products from the cells (4). Introduction of angiogenesis results in better healing of affected tissues (5).

In order to increase the vascularisation of tissue engineered constructs, several approaches have been employed. For instance, the pore size of the scaffold has been varied resulting in an optimum diameter for cellular adhesion and migration (~100 µm) (6). Furthermore, endothelial cells and fibroblasts have been included in gelatine-coated polystyrene scaffolds in order to initiate angiogenesis *in vitro*, resulting in sprouts prior to transplantation (7). The addition of glycosaminoglycans and growth factors also proved to increase angiogenesis *in vivo* (1). However, it still takes about four weeks to develop sufficient vasculature.

Angiogenesis is a multifactor process, which is regulated by an interplay of a large number of factors. Angiogenesis can be set on by e.g. hypoxia (8). An important stimulating factor in angiogenesis is vascular endothelial growth factor (VEGF) which acts on the VEGF receptors (VEGFR). VEGF stimulates cells to produce matrix metalloproteinases (MMPs) that degrade the basement membrane and surrounding extracellular matrix. As a result, endothelial cells proliferate and migrate towards the interstitium, where they start sprouting. Subsequently, pericytes proliferate and migrate towards the newly formed sprouts and induce maturation by forming a single cell layer around the sprout (9,10). The administration or overexpression of single VEGF isoforms in animal models results in angiogenesis, but the newly formed blood vessels may be leaky and phenomena such as oedema, inflammation and hemorrhagic ulcers have been reported (9).

Another growth factor known for its angiogenic potential is fibroblast growth factor 2 (FGF2). This growth factor stimulates endothelial cells to produce both MMPs and VEGF and increases VEGFR expression. FGF2 also stimulates endothelial cell migration, pericyte attraction and matrix deposition (11). Local administration of this growth factor in a rabbit ear chamber model induced angiogenesis, although some animals showed bleeding vessels and full vascularisation required at least three weeks. Clearly, the administration of one growth factor is not sufficient to create well-developed mature blood vessels. Few authors have studied the combined administration of growth factors. Tumour cells, transfected with VEGF and/or FGF2, need both VEGF and FGF2 to form blood vessels. Similar synergistic effects were found by local administration of VEGF and FGF2 in a rabbit ischemic hind limb resulting in a higher capillary density and capillary vs. muscle fibre ratio than either VEGF or FGF2 alone (14).

In this study, we tested the hypothesis that the combined application of recombinant rat VEGF-164 (rrVEGF) and recombinant rat FGF2 (rrFGF2) increases angiogenesis in acellular collagen-heparin scaffolds for tissue engineering. For that purpose, scaffolds consisting of combinations of type I collagen, heparin, FGF2 and VEGF were constructed, characterised and evaluated for *in vivo* tissue response after subcutaneous implantation in adult Wistar rats.

MATERIALS AND METHODS

Materials

Unless stated otherwise all chemicals were purchased from Merck Chemicals (Darmstadt, Germany). Type I collagen was purified from bovine achilles tendon using diluted acetic acid, NaCl, urea and acetone extractions (15). Heparin was purchased from Sigma Chemical Co. (St Louis, MO, USA). Recombinant rat FGF2 was produced in *E. coli* M15 PQE16 and recombinant rat VEGF-164 in *P. pastoris* GS115 (1).

Preparation of scaffolds

Five different scaffolds were prepared:

- COL: type I collagen only,
- COLH: type I collagen with heparin,
- COLHF: type I collagen with heparin and FGF2,
- COLHV: type I collagen with heparin and VEGF,
- COLHFV: type I collagen with heparin, FGF2 and VEGF.

The scaffolds were prepared by freezing a 0.8% collagen suspension in diluted acetic acid at -20°C (1,16) and subsequently lyophilising in a Zirbus lyophiliser (Bad Grund, Germany). All scaffolds were chemically crosslinked with and without 2.75% heparin for 4 h with 33 mM 1-ethyl-3-dimethyl aminopropyl carbodiimide (EDC) and 6 mM N-hydroxysuccinimide (NHS) in 50 mM 2-morpholinoethane sulphonic acid (pH 5.0) in the presence of 40% ethanol. After reaction, the scaffolds were washed in 0.1 M Na₂HPO₄, 1 M NaCl, 2 M NaCl and demineralised water. Scaffolds (2 punches per ml, \pm 1,5 mg each) were incubated for 60 min in 7 μ g growth factor (FGF2 or VEGF) per ml phosphate buffered saline (PBS) (pH 7.2) and washed in PBS (1). For the combination of both growth factors, 3.5 μ g/ml of FGF2 and 3.5 μ g/ml VEGF were used.

Characterisation of scaffolds

Scanning electron microscopy (SEM) was used to analyse the ultrastructure of the scaffolds. Scaffolds were mounted on stubs and sputtered with an ultrathin layer of gold in a Polaron E5100 SEM coating system, and analysed with a JEOL JSM-6310 scanning electron microscope at 15 kV.

The amine group content of the scaffolds was analysed using 2,4,6-trinitrobenzene sulphonic acid to determine the extent of crosslinking (17).

The heparin content of the scaffolds was determined by a hexosamine assay using p-dimethyl-aminobenzoaldehyde (15).

The amount of growth factor bound to the scaffold was determined by western blotting (18) with antibodies against FGF2 (1:2000) and rat VEGF (1:1000) and peroxidase-conjugated secondary antibodies visualised with a chemiluminescent detection kit (ECL) (Amersham Biosciences). Gene Tools (Syngene, Cambridge, UK) was used to analyse the intensity of the bands. 0-100 ng growth factor was used as a standard curve. Scaffolds without growth factors were taken as controls.

Immunofluorescence microscopy was used to determine the distribution of type I collagen, heparin, FGF2 and VEGF in the scaffolds, as described (20) (for dilutions see Table 1). Omission of the primary antibody was taken as a negative control.

Implantation of scaffolds

NIH guidelines for the care and use of laboratory animals (NIH publication 85-23 Rev. 1985) were observed. The study was approved by the Ethics Committee of the Radboud University Nijmegen. Wistar rats (male, 3 months) were purchased from Harlan (Horst, The Netherlands). The rats were housed per 2, fed pelleted diet (RMH-B 10 mm) and water *ad libitum*. The rats were anaesthetized with isoflurane. After disinfection, 4 subcutaneous pockets were made on both sides of two midline incisions on the back. Scaffolds (\varnothing 6 mm) were washed in 70% ethanol (4x 30 min) and sterile PBS (8x 30 min) and placed in the pockets at about 1 cm of the incision. Each rat received 4 implants (2 different scaffolds). At day 3, 7 and 21, the implants with surrounding tissue were removed. The explants were divided in halves; one half was processed for conventional histology and the other for immune-histochemistry.

Processing of explants

Conventional histology: to study the cellular reaction, paraffin sections were cut and haematoxylin-eosin stained (21). Histology of the scaffolds was evaluated independently by at least two experienced investigators.

Immunostaining: To study formation, maturation and functionality of blood vessels, sections were stained with specific antibodies. Type IV collagen (COL IV) was used to manually determine the total area of blood vessels (22). The total area of blood vessels was expressed as a percentage of the total implant size. Smooth muscle actin (SMA) was used to study the level of maturation of the newly formed blood vessels (23). The total area of SMA-positive blood vessels was expressed as a percentage of the total area of blood vessels. Hypoxia inducible factor 1- α (HIF1- α) was used to determine the number of hypoxic cells in the scaffold (24). The amount of HIF1- α -positive cells was expressed as a percentage of the total number of cells (on average, 500 cells were counted). Values were compared using the Student's t-test and $p < 0.05$ was considered to be statistically significant.

Immunofluorescence assay, Frozen sections were cut and incubated with antibodies for collagen type IV and smooth muscle actin as described (20) (for dilutions see Table 1).

Peroxidase-antiperoxidase method, the peroxidase-antiperoxidase method was used to immunolocalise molecules (hypoxia inducible factor 1- α and smooth muscle actin) in paraffin sections. 5 μ m sections were deparaffinised and incubated as described (21) (for dilutions see Table 1).

Table 1. Antibodies used for Immunohistochemistry

Primary antibody	dilution	Secondary antibody	dilution	Tertiary antibody	dilution
Mouse anti bovine type I collagen ^A	1:2000	Alexa 488 labelled goat anti mouse ^F	1:200	Alexa 594 labelled goat anti mouse ^F	1:200
Anti heparin (HS4C3) [*]	1:5	Mouse anti VSV-tag (P5D4) ^{**}	1:10		
Goat anti rat FGF2 ^A	1:500	Alexa 488 labelled donkey anti goat ^F	1:200		
Goat anti rat VEGF ^B	1:50	Alexa 488 labelled donkey anti goat ^F	1:200		
Goat anti human type IV collagen ^C	1:50	Alexa 488 labelled donkey anti goat ^F	1:200	Mouse peroxidase-antiperoxidase ^E	1:500
Mouse anti- α smooth muscle actin ^A	1:400	Alexa 488 labelled goat anti mouse ^F	1:200		
Mouse anti- α smooth muscle actin ^A	1:400	Goat anti mouse IgG ^E	1:50		
Mouse anti human HIF1- α ^D	1:1000	Goat anti mouse IgG ^E	1:50		

* Single chain variable fragment (ScFv) antibody against heparin (19)

** Antibody against the VSV-tag of the ScFv (19)

A: Sigma Chemical Co (St. Louis, Mo, USA), B: R&D systems (Minneapolis, MN, USA), C: Southern Biotechnologies (Birmingham, AL, USA), D: Abcam (Glostrup, Denmark), F: Molecular probes (Leiden, The Netherlands)

RESULTS

Scaffold characteristics

The morphology of the scaffolds was analysed by SEM (Fig. 1A, B). Rounded pores were in the range of 75 to 125 μm . The scaffold was chemically crosslinked with EDC and NHS to covalently bind heparin. During crosslinking, an amine group reacts with a carboxylic group and hence the extent of crosslinking was evaluated by analysing the remaining free amine groups. About 50- 60% of the amine groups were used for crosslinking (Table 2). The amount of heparin covalently bound to the scaffold was $\sim 68 \mu\text{g}/\text{mg}$ scaffold, as determined by hexosamine assay.

The amount of FGF2 that bound, analysed by western blotting and Gene Tools, was $1.6 \pm 0.2 \mu\text{g}/\text{mg}$ scaffold. For VEGF, it was $1.0 \pm 0.3 \mu\text{g}/\text{mg}$ scaffold. When both growth factors were present in the dipping solution, $1.0 \pm 0.2 \mu\text{g}$ FGF2 and $0.7 \pm 0.3 \mu\text{g}$ VEGF bound per mg scaffold (Fig. 2 and Table 2).

The distribution of the different components in the scaffolds was visualised using immunofluorescence and revealed that heparin, FGF2 and VEGF were equally distributed throughout the scaffold (Fig. 1C-G).

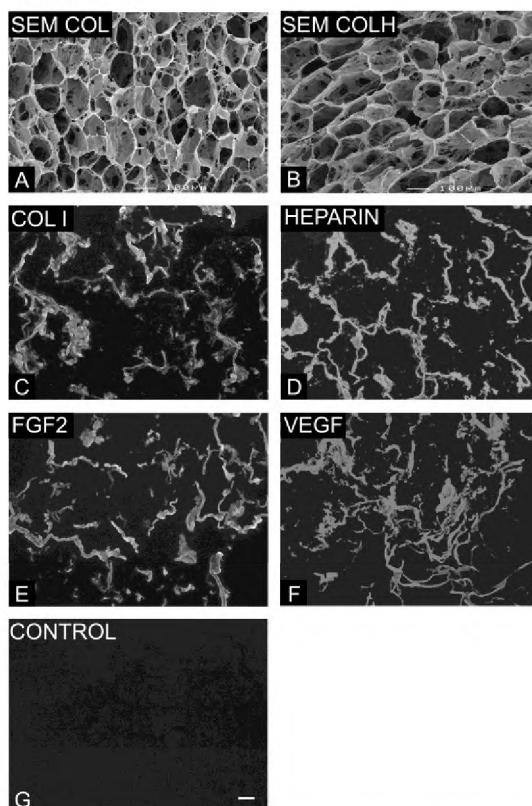


Fig. 1 Microscopical evaluation of the different scaffolds. Scanning electron micrograph of a cross-section of COL (A) and COLH scaffold (B). Immunolocalisation of type I collagen (C), heparin (D), FGF2 (E) and VEGF (F) in a COLHVF scaffold. Bar (A, B) is 100 μm ; bar (C-G) is 50 μm .

Table 2. Biochemical properties of the prepared scaffolds.

Scaffold	Crosslinked with EDC/NHS	Amine group content [nmol/mg scaffold]	Heparin content [ug/mg scaffold]	FGF2 content [ug/mg scaffold]	VEGF content [ug/mg scaffold]
COL	-	337 ± 24			
COL	+	166 ± 16			
COLH	+	180 ± 9	68 ± 3		
COLHF	+	188 ± 7	70 ± 4	1.6 ± 0.2	
COLHV	+	193 ± 24	65 ± 4		1.0 ± 0.3
COLHFV	+	186 ± 13	63 ± 5	1.0 ± 0.2	0.7 ± 0.3

Biochemical analysis of the prepared scaffolds consisting of type I collagen (COL), type I collagen and heparin (COLH), type I collagen, heparin and FGF2 (COLHF), type I collagen, heparin and VEGF (COLHV) and type I collagen, heparin, FGF2 and VEGF (COLHFV). The amine group content was determined using 2,4,6-trinitrobenzene sulfonic acid (17); the heparin content using p-dimethyl-aminobenzoaldehyde (15), and the amount of FGF2 and VEGF by western blotting (18), quantitatively analysed with Gene Tools. The results are the mean ± SD of 3 independent experiments.

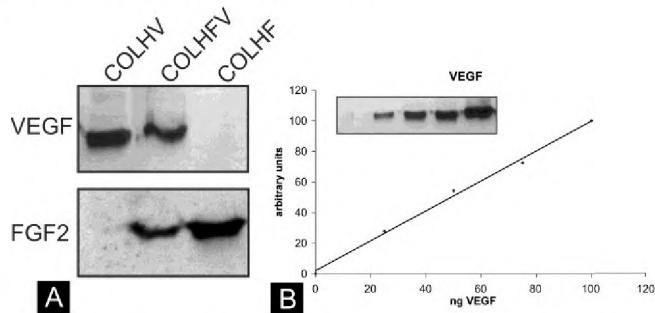


Fig 2 The amount of FGF-2 and VEGF bound to collagen-heparin scaffolds measured by western blotting and band analysis. A) Western blot of the results of the scaffolds; lane COLHV: scaffold incubated in 7 µg/ml VEGF, lane COLHFV: scaffold incubated in 3.5 µg/ml FGF2 and 3.5 µg/ml VEGF, lane COLHF: scaffold incubated in 7 µg/ml FGF2. B: The standard curve (0-100 ng) (B) of VEGF. Similar results were found for the standard curve of FGF2.

Cellular response to scaffolds

A systematic survey using five different types of scaffolds allowed us to evaluate the contribution of the different components. Cellular events are summarised in Table 3. At day 3, COL and COLH scaffolds showed minor infiltration of granulocytes and macrophages at the outer part of the scaffold, whereas COLHF and COLHV showed a moderate amount of macrophages, fibroblasts and some granulocytes further in the scaffold. COLHFV showed a moderate amount of granulocytes, macrophages and some fibroblasts throughout the scaffold (Fig. 3). A thin layer of capsule surrounded all implants. At day 7, no granulocytes were present in the scaffolds anymore. Few giant cells were found at this time point. The cellular response to COL and COLH included a moderate amount of macrophages and some fibroblasts further in the scaffold. COLHF and COLHV showed a moderate amount of macrophages and fibroblasts throughout the scaffold and some non-phagocytic cells were present. A larger amount of macrophages and fibroblasts accompanied by some non-phagocytic cells were found throughout the COLHFV scaffold. All scaffolds contained a thin layer of capsule around the implants. At day 21, macrophages and non-phagocytic cells were present throughout COL and COLH scaffolds. A larger amount of macrophages, giant cells, fibroblasts and non-phagocytic cells was found throughout the COLHF, COLHV and COLHFV scaffolds. All scaffolds contained a capsule layer around the implants.

Table 3. Tissue response to the implanted scaffolds.

Scaffold	Days after implantation	PMNs *	Phagocytic cells**	Non-phagocytic cells ***	Fibroblasts
COL	3	+	+	-	-
	7	-	++	-	+
	21	-	++	+	+
COLH	3	+	+	-	-
	7	-	++	-	+
	21	-	++	+	+
COLHF	3	+	++	-	+
	7	-	++	+	++
	21	-	+++	++	++
COLHV	3	+	+	-	+
	7	-	++	+	++
	21	-	++	++	++
COLHFV	3	++	++	-	+
	7	-	+++	+	+++
	21	-	+++	++	++

Cells were scored from not present (-) to abundantly present (+++).

The absolute numbers of PMNs and non-phagocytic cells are lower than for phagocytic cells.

* PMNs = polymorphic nuclear cells, i.e. granulocytes.

** Phagocytic cells include macrophages and monocyte-derived giant cells.

*** Non-phagocytic cells include lymphocytes, plasma cells and mast cells.

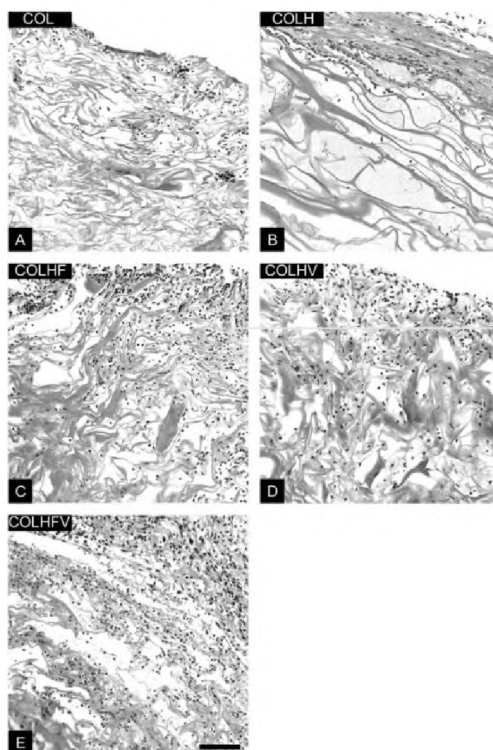


Fig 3 Histological evaluation of scaffolds explanted at day 3. Haematoxylin-eosin staining of COL (A), COLH (B), COLHF (C), COLHV (D) and COLHFV (E). COL and COLH only showed some cells in the outer part of the scaffold, whereas the scaffolds with growth factors (COLHF, COLHV and COLHFV) also revealed cells in the centre of the scaffold. Bar is 100 μ m.

Blood vessels

At day 3, no blood vessels were observed in the scaffolds, but blood vessels were found in the surrounding tissue. More blood vessels were found near COLHF, COLHV and COLHFV scaffolds compared to COL and COLH. This observation could also be made macroscopically from the red colour of the scaffolds at explantation. At day 7, no blood vessels were present in COL, whereas all other scaffolds contained blood vessels as shown by COL IV staining (Fig. 4 and 5). COLHFV showed the largest blood vessel area ($5.9\% \pm 1.6$), COLHF ($2.6\% \pm 1.9$) and COLHV ($2.3\% \pm 0.7$) somewhat lower and COLH the least ($0.9\% \pm 0.2$). No significant differences were found between COLHV-COLHF and COLHF-COLH. SMA-staining was used as a marker for matured blood vessels. The total area of SMA-positive blood vessels was expressed as a percentage of the total area of blood vessels (determined by COL IV staining) (Fig. 4 and 5). COLHFV showed most SMA-positive blood vessels ($35\% \pm 4$), more than COLHF ($18.3\% \pm 7.4$), COLH ($17.2\% \pm 0.9$) and COLHV ($16.9\% \pm 2.2$). No significant differences were found between COLHV-COLHF, COLHV-COLH and COLHF-COLH. At day 21, blood vessels were found in all scaffolds (Fig. 5). COLH ($3.2\% \pm 0.9$), COLHV ($4.8\% \pm 1.8$) and COLHFV ($6.1\% \pm 1.2$) had a significantly larger blood vessel area than COL ($1.7\% \pm 0.8$). COLHFV more than COLH and COLHF ($3.2\% \pm 0.9$), but no significant differences were found between COLHFV-COLHV, COLHV-COLHF, COLHV-COLH, COLHF-COLH and COLHF-COL. COLHFV ($83.4\% \pm 4.9$) showed a significant higher percentage of SMA-positive blood vessels than all other scaffolds (Fig. 6): COL ($34.7\% \pm 10.5$), COLH ($32.3\% \pm 5.9$), COLHF ($34.2\% \pm 3.5$) and COLHV ($58.2\% \pm 12$). No significant differences were found between COLHF-COLH, COLHF-COL and COLH-COL.

Hypoxia

At day 3, all scaffolds contained 97-98% HIF1- α -positive cells (hypoxic cells). The cells in the most outer region of the scaffolds, especially the scaffolds with one or two growth factors, stained less intense for HIF1- α , probably due to a partial supply of oxygen and nutrients from the surrounding tissue. At day 7, all scaffolds showed both HIF1- α positive and negative cells in the scaffold centre (Fig. 6). COLHFV ($2.2\% \pm 0.9$) had significantly less hypoxic cells than COL ($36.6\% \pm 9.9$), COLH ($35\% \pm 13.5$), COLHF ($16\% \pm 9.2$) and COLHV ($10.4\% \pm 2.2$). COLHF and COLHV had significantly less hypoxic cells than COL and COLH. At day 21, COLHFV ($0.2\% \pm 0.04$) had significantly less HIF1- α positive cells than COL ($21.2\% \pm 3.6$), COLH ($14.7\% \pm 2.6$), COLHF ($4.9\% \pm 1.4$) and COLHV ($4.0\% \pm 1.8$) (Fig. 6). COLHF and COLHV had significantly less hypoxic cells than COL and COLH.

DISCUSSION

In tissue engineering, vascularisation of the transplanted constructs is often limited at early time points and this seriously hampers the survival of cells. Cells die due to lack of oxygen, nutrients and inadequate removal of waste products. This confines the size of tissue-engineered constructs to a maximum of a few cm² (4). Generally, it takes several weeks for a construct to become fully vascularised. This slow development of blood vessels hampers wound healing or tissue regeneration in certain pathological conditions (3,5). A means to increase angiogenesis is to administer growth factors either by injection or preferably in a slow-release system such as a bioscaffold. Scaffolds can be built up from several components and in this study, we used highly purified type I collagen, heparin, recombinant rat FGF2 and recombinant rat VEGF.

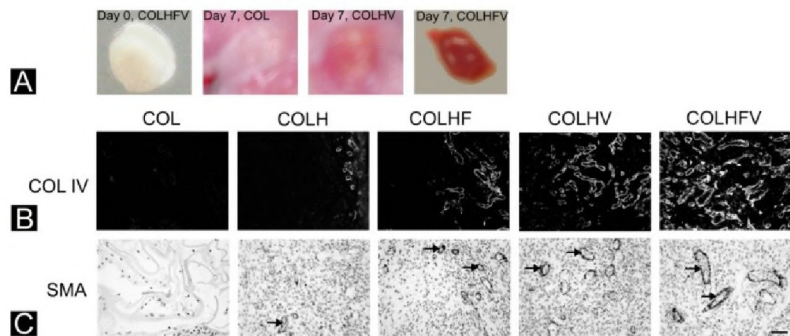


Fig 4 Macroscopical (A) and immunohistochemical evaluation of the scaffolds explanted at day 7 (B, C). A) Macroscopical evaluation of a non-implanted scaffold at day 0 and explants at day 7 (COL, COLHV and COLHFV). Note the red appearance of the COLHFV scaffold. B) Immunohistochemical evaluation using type IV collagen staining of the scaffolds explanted at day 7. COLHFV showed the most and largest area of blood vessels compared to COLHV, COLHF and COLH. No blood vessels were found in COL at this time point. C) Immunohistochemical evaluation using smooth muscle actin staining of scaffolds explanted at day 7. COLHFV displayed the largest percentage of mature blood vessels compared to COLHV, COLHF and COLH. Arrows indicate SMA-positive blood vessels. Bar is 50 μ m.

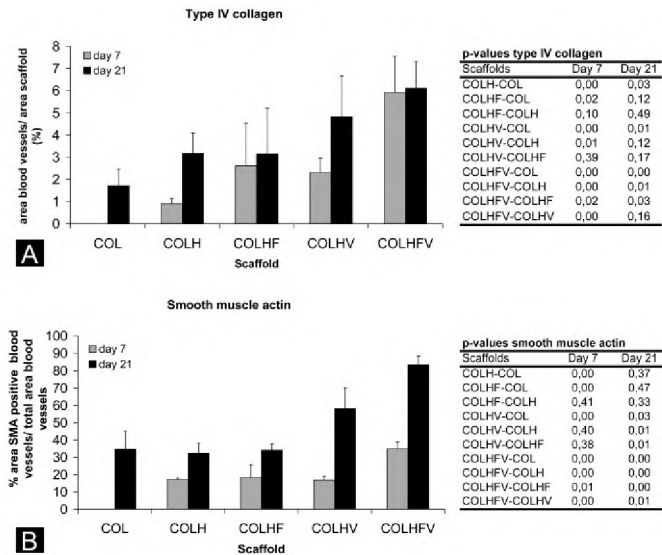


Fig 5: Analysis of the blood vessels present in the scaffolds using COL IV and SMA staining. Scaffolds containing two growth factors showed both a larger total area of blood vessels and more mature blood vessels. A) The total area of blood vessels per scaffold was calculated from COL IV staining. At day 7, COLHFV had significantly more blood vessel area than all the other scaffolds. At day 21, COLHV had a significantly larger blood vessel area than all the other scaffolds with the exception of COLHV. * $p < 0.05$. B) The total area of mature blood vessels (staining positive for SMA) was expressed as a percentage of the total area of blood vessels. At day 7 and at day 21, COLHFV had a significantly higher percentage of SMA positive blood vessels than all the other scaffolds. * $p < 0.05$.

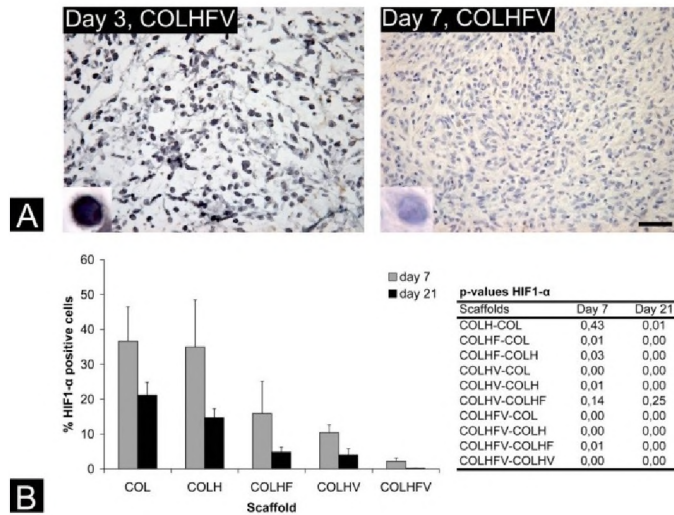


Fig 6 Immunohistochemical analysis of HIF1- α staining of cells in the scaffolds at day 3, 7 and 21. A) Photographs of COLHVF scaffold at day 3 and 7. COLHVF showed many hypoxic cells at day 3 and few at day 7. Inserts show that HIF1- α predominantly stains the nuclei of cells. Positive cells stain black and neg-atve cells stain blue. Bar is 10 μ m. B) Statistical analysis of the percentages of HIF1- α positive cells. At day 7 and 21, COLHVF had significantly less hypoxic cells than all other scaffolds. * $p < 0.05$.

We have previously shown that collagen-heparin scaffolds can give sustained release of FGF2 (1). Therefore, five different, molecularly-defined, scaffolds were made, including collagen-heparin with and without one or two growth factors. Porous collagen scaffolds (containing pores of about 100 μ m) were prepared by lyophilisation and heparin was covalently attached to allow coupling of one or two heparin-binding growth factors (FGF2 and VEGF). The amount of bound FGF2 resembled the amount found by Pieper et al., who used 125 I-FGF2 to analyse the amount of bound growth factor (1). More FGF2 than VEGF was able to bind to collagen-heparin scaffolds, perhaps due to minor differences in their affinity for heparin (25,26). Less FGF2 and VEGF bound to the scaffold after incubation in a solution containing both growth factors, which is likely due to the lower concentration of each growth factor, 3.5 μ g instead of 7 μ g/ml, in the dipping solution. The total amount of both growth factors present per mg scaffold was similar to the amount of bound FGF2 alone. This systematic approach allowed us to study the influence of single components on tissue response including blood vessel formation and maturation.

Many different factors, stimulators as well as inhibitors, are involved in angiogenesis, and they all have their own mechanism (9). VEGF is found to be one of the most important factors in angiogenesis. It stimulates endothelial cells by binding to VEGFR-2, thus inducing MMP production, proliferation and migration of the endothelial cells. FGF2 upregulates the expression of VEGF (25) and attracts pericytes, which form a single cell layer around the newly formed capillary, necessary to mature the blood vessel and to protect it from degradation (11). A HIF1- α /FGF2 amplification pathway in which FGF2 upregulates HIF1- α , leading to an angiogenic response has been reported (27). The complete mechanism behind the angiogenic response of FGF2, however, is still not fully understood (11).

COL and COLH scaffolds showed a mild cellular response, whereas the scaffold with growth factors showed a higher influx of cells, mainly macrophages and fibroblasts and, at day 3, granulocytes. COLHFV attracted the largest amount of cells as expected. VEGF attracts macrophages, which on their turn produce VEGF as well as MMPs which release additional VEGF from the surrounding tissue (28). FGF2 stimulates proliferation and differentiation of granulocytes, endothelial cells, fibroblasts and many other cells. Granulocytes also produce MMPs that degrade the extracellular matrix and release VEGF and FGF2. Pieper *et al.* (1) also found that FGF2 addition to a scaffold attracted more cells. An increased cellular reaction may be necessary to trigger angiogenesis (29).

We found that the presence of VEGF or FGF2 alone gave blood vessel formation. The administration of a single growth factor (VEGF or FGF2) seems not sufficient to develop a normal vasculature (9,12). Indeed we show that a combination of VEGF and FGF2 is superior with respect to blood vessel formation and reduction of hypoxic conditions at early time points.

Our results emphasise that the combination of two growth factors enhances angiogenesis resulting in a higher area of blood vessels, similar to the findings of Ashara *et al.* (14) after injection of VEGF and FG2 in a hind limb ischemia model. The need for multiple growth factors was further investigated by Lascke *et al.* (30), who found that angiogenesis and blood vessel maturation could only be suppressed by complete inhibition of VEGF, FGF2 and platelet derived growth factor (PDGF). We do not need PDGF to develop mature blood vessels, perhaps because VEGF and FGF2 are capable to upregulate the production of PDGF; a combined administration of VEGF and FGF2 has been reported to be sufficient to develop mature blood vessels in the absence of PDGF (9).

To analyse whether the formed blood vessel were functional, we used a marker for hypoxia (HIF1- α). Under hypoxic conditions HIF1- α is accumulated and transported to the nucleus where it dimerises with HIF1- β to its active form (31). The staining revealed that the formed blood vessels were capable of supplying the infiltrated cells with sufficient oxygen. The scaffold with both FGF2 and VEGF showed almost no hypoxic cells from day 7 on. It usually takes 3 to 4 weeks for a construct to become fully vascularised (1,12). We show a huge reduction in the time needed to induce angiogenesis. This benefits tissue regeneration, especially when you consider that this process requires sufficient blood vessels to be present (32).

The combination of VEGF and FGF2 is capable of providing the scaffold with enough mature blood vessels to supply the cells of oxygen and nutrients at a very early time point. Bioscaffolds containing these several factors may be of use in several pathological conditions, including ischemic heart disease or diabetic ulcers. For instance, in diabetic ulcers the most commonly used tissue engineered construct is Integra TM, a collagen based scaffold, which has the disadvantage that it takes several weeks to become vascularised which increases the risk of infections (3,33). We propose that addition of appropriate growth factors, like FGF2 and VEGF, that increase blood vessel formation, could contribute to improved healing and reduction of hospitalization.

CONCLUSION

Our results indicate that the addition of both FGF2 and VEGF to collagen-heparin scaffolds leads to an early and well-developed vasculature. This opens new opportunities for the use of acellular scaffolds for tissue engineering.

REFERENCES

1. J.S.Pieper, T.Hafmans, P.B.van Wachem, M.J.van Luyn, L.A.Brouwer, J.H.Veerkamp, and T.H.Van Kuppevelt. "Loading of collagen-heparan sulfate matrices with bFGF promotes angiogenesis and tissue generation in rats." *J.Biomed.Mater.Res.* 62, no. 2(November 2002):185-94.
2. S.Fukuda, S.Yoshii, S.Kaga, M.Matsumoto, K.Kugiyama, and N.Maulik. "Angiogenic strategy for human ischemic heart disease: brief overview." *Mol.Cell Biochem.* 264, no. 1-2(September 2004):143-49.
3. S.P.Bennett, G.D.Griffiths, A.M.Schor, G.P.Lee, and S.L.Schor. "Growth factors in the treatment of diabetic foot ulcers." *Br.J.Surg.* 90, no. 2(February 2003):133-46.
4. Z.S.Patel and A.G.Mikos. "Angiogenesis with biomaterial-based drug- and cell-delivery systems." *J.Biomater.Sci.Polym.Ed* 15, no. 6(2004):701-26.
5. G.C.Hughes, S.S.Biswas, B.Yin, R.E.Coleman, T.R.DeGrado, C.K.Landolfo, J.E.Lowe, B.H.Annex, and K.P.Landolfo. "Therapeutic angiogenesis in chronically ischemic porcine myocardium: comparative effects of bFGF and VEGF." *Ann.Thorac.Surg.* 77, no. 3(March 2004):812-18.
6. F.J.O'Brien, B.A.Harley, I.V.Yannas, and L.J.Gibson. "The effect of pore size on cell adhesion in collagen-GAG scaffolds." *Biomaterials* 26, no. 4(February 2005):433-41.
7. Rickert, M.A.Moses, A.Lendlein, S.Kelch, and R.P.Franke. "The importance of angiogenesis in the interaction between polymeric biomaterials and surrounding tissue." *Clin.Hemorheol.Microcirc.* 28, no. 3(2003):175-81.
8. R.Bicknell and A.L.Harris. "Novel angiogenic signaling pathways and vascular targets." *Annu.Rev.Pharmacol.Toxicol.* 44,(2004):219-38.
9. R.K.Bruick and S.L.McKnight. "Building better vasculature." *Genes Dev.* 15, no. 19(October 2001):2497-502.
10. A.Hoeben, B.Landuyt, M.S.Highley, H.Wildiers, A.T.Van Oosterom, and E.A.De Bruijn. "Vascular endothelial growth factor and angiogenesis." *Pharmacol.Rev.* 56, no. 4(December 2004):549-80.
11. M.Presta, P.Dell'Era, S.Mitola, E.Moroni, R.Ronca, and M.Rusnati. "Fibroblast growth factor/fibroblast growth factor receptor system in angiogenesis." *Cytokine Growth Factor Rev.* 16, no. 2(April 2005):159-78.
12. M.Komori, Y.Tomizawa, K.Takada, and M.Ozaki. "A single local application of recombinant human basic fibroblast growth factor accelerates initial angiogenesis during wound healing in rabbit ear chamber." *Anesth.Analg.* 100, no. 3(March 2005):830-4, table.
13. R.Giavazzi, B.Sennino, D.Coltrini, A.Garofalo, R.Dossi, R.Ronca, M.P.Tosatti, and M.Presta. "Distinct role of fibroblast growth factor-2 and vascular endothelial growth factor on tumor growth and angiogenesis." *Am.J.Pathol.* 162, no. 6(June 2003):1913-26.
14. T.Asahara, C.Bauters, L.P.Zheng, S.Takeshita, S.Bunting, N.Ferrara, J.F.Symes, and J.M.Isner. "Synergistic effect of vascular endothelial growth factor and basic fibroblast growth factor on angiogenesis in vivo." *Circulation* 92, no. 9 Suppl(November 1995):II365-II371.
15. J.S.Pieper, A.Oosterhof, P.J.Dijkstra, J.H.Veerkamp, and T.H.Van Kuppevelt. "Preparation and characterization of porous crosslinked collagenous matrices containing bioavailable chondroitin sulphate." *Biomaterials* 20, no. 9(May 1999):847-58.
16. M.J.Wissink, R.Beernink, J.S.Pieper, A.A.Poot, G.H.Engbers, T.Beugeling, W.G.van Aken, and J.Feijen. "Immobilization of heparin to EDC/NHS-crosslinked collagen. Characterization and in vitro evaluation." *Biomaterials* 22, no. 2(January 2001):151-63.
17. L.H.Olde Damink, P.J.Dijkstra, M.J.van Luyn, P.B.van Wachem, P.Nieuwenhuis, and J.Feijen. "Cross-linking of dermal sheep collagen using a water-soluble carbodiimide." *Biomaterials* 17, no. 8(April 1996):765-73.
18. W.N.Burnette. "Western blotting": electrophoretic transfer of proteins from sodium dodecyl sulfate-polyacrylamide gels to unmodified nitrocellulose and radiographic detection with antibody and radioiodinated protein A." *Anal.Biochem.* 112, no. 2(April 1981):195-203.
19. T.H.Van Kuppevelt, M.A.Dennissen, W.J.van Venrooij, R.M.Hoet, and J.H.Veerkamp. "Generation and application of type-specific anti-heparan sulfate antibodies using phage display tech-

- nology. Further evidence for heparan sulfate heterogeneity in the kidney." *J.Biol.Chem.* 273, no. 21(May 1998):12960-66.
20. W.F.Daamen, S.T.Nillesen, T.Hafmans, J.H.Veerkamp, M.J.van Luyn, and T.H.Van Kuppevelt. "Tissue response of defined collagen-elastin scaffolds in young and adult rats with special attention to calcification." *Biomaterials* 26, no. 1(January 2005):81-92.
21. Bancroft JD and O.Stoeltzing. *Theory and practice of histological techniques*, Edinburgh, UK: Churchill Livingstone, 1990.
22. I.Masaki, Y.Yonemitsu, A.Yamashita, S.Sata, M.Tanii, K.Komori, K.Nakagawa, X.Hou, Y.Nagai, M.Hasegawa, K.Sugimachi, and K.Sueishi. "Angiogenic gene therapy for experimental critical limb ischemia: acceleration of limb loss by overexpression of vascular endothelial growth factor 165 but not of fibroblast growth factor-2." *Circ.Res.* 90, no. 9(May 2002):966-73.
23. A.P.Taylor, M.Rodriguez, K.Adams, D.M.Goldenberg, and R.D.Blumenthal. "Altered tumor vessel maturation and proliferation in placenta growth factor-producing tumors: potential relationship to post-therapy tumor angiogenesis and recurrence." *Int.J.Cancer* 105, no. 2(June 2003):158-64.
24. L.E.Huang, J.Gu, M.Schau, and H.F.Bunn. "Regulation of hypoxia-inducible factor 1alpha is mediated by an O2-dependent degradation domain via the ubiquitin-proteasome pathway." *Proc.Natl.Acad.Sci.U.S.A* 95, no. 14(July 1998):7987-92.
25. M.Fujita, M.Ishihara, M.Simizu, K.Obara, T.Ishizuka, Y.Saito, H.Yura, Y.Morimoto, B.Takase, T.Matsui, M.Kikuchi, and T.Maehara. "Vascularization in vivo caused by the controlled release of fibroblast growth factor-2 from an injectable chitosan/non-anticoagulant heparin hydrogel." *Biomaterials* 25, no. 4(February 2004):699-706.
26. H.Gitay-Goren, S.Soker, I.Vlodavsky, and G.Neufeld. "The binding of vascular endothelial growth factor to its receptors is dependent on cell surface-associated heparin-like molecules." *J.Biol.Chem.* 267, no. 9(March 1992):6093-98.
27. M.Calvani, A.Rapisarda, B.Uranchimeg, R.H.Shoemaker, and G.Melillo. "Hypoxic induction of a HIF-1{alpha}- dependent bFGF autocrine loop drives angiogenesis in human endothelial cells." *Blood*(November 2005).
28. H.M.Blau and A.Banfi. "The well-tempered vessel." *Nat.Med.* 7, no. 5(May 2001):532-34.
29. M.J.van Amerongen, G.Molema, J.Plantinga, H.Moorlag, and M.J.van Luyn. "Neovascularization and vascular markers in a foreign body reaction to subcutaneously implanted degradable biomaterial in mice." *Angiogenesis.* 5, no. 3(2002):173-80.
30. M.W.Laschke, A.Elitzsch, B.Vollmar, P.Vajkoczy, and M.D.Menger. "Combined inhibition of vascular endothelial growth factor (VEGF), fibroblast growth factor and platelet-derived growth factor, but not inhibition of VEGF alone, effectively suppresses angiogenesis and vessel maturation in endometriotic lesions." *Hum.Reprod.* 21, no. 1(January 2006):262-68.
31. D.Trentin, H.Hall, S.Wechsler, and J.A.Hubbell. "Tissue Engineering Special Feature: Peptide-matrix-mediated gene transfer of an oxygen-insensitive hypoxia-inducible factor-1{alpha} variant for local induction of angiogenesis." *Proc.Natl.Acad.Sci.U.S.A* 103, no. 8(February 2006):2506-11.
32. M.G.Tonnesen, X.Feng, and R.A.Clark. "Angiogenesis in wound healing." *J.Investig.Dermatol.Symp.Proc.* 5, no. 1(December 2000):40-46.
33. K.H.Lee. "Tissue-engineered human living skin substitutes: development and clinical application." *Yonsei Med.J.* 41, no. 6(December 2000):774-79.

Chapter 4

AN ANIMAL MODEL FOR FEMORAL ARTERY PSEUDOANEURYSMS

Paul J. Geutjes¹
Daan J. A. van der Vliet²
Kaeuis A. Faraj^{1,3}
Noes de Vries³
Herman T. van Moerkerk¹
Ronnie G. Wismans¹
Thijs Hendriks²
Willeke F. Daamen¹
Toin H. van Kuppevelt¹

^{1,2}Radboud University Nijmegen Medical Centre, Departments of
¹Biochemistry (280), and ²Surgery (690), P.O. Box 9101, 6525 GA Nijmegen, The
Netherlands and ³Aap bio implants - EMCM BV, Middenkampweg 17, 6645 CH
Nijmegen, The Netherlands

Journal of Vascular and Interventional Radiology 2010;21(7):1078-83

ABSTRACT

INTRODUCTION The aim of this study is to prepare a porcine model for femoral artery pseudoaneurysm (PSA) using a one-step surgical procedure without the need for microsurgery. **METHODS** This PSA model involves the preparation of an arteriovenous shunt between the femoral artery and femoral vein, where ~2 cm of the vein is segmented by proximal and distal closure using ligatures. The femoral PSA models were evaluated by angiography, Doppler auscultation and histology. **RESULTS** In 7 out of 8 pigs, angiography and Doppler auscultation showed that the PSA models were open and that there was communication between the PSA model and the femoral artery. The mean length of the PSA model was 1.9 ± 0.3 cm (mean \pm SD, n=7) with a neck region of 4 mm. Histology confirmed that PSA models were open and no thrombi were observed. The principal advantages of this model are the location of the PSA model, the short period of clamping, and the controllable size. **CONCLUSIONS** The pseudoaneurysm pig model is straightforward and reproducible, and may serve as a useful tool in the evaluation of interventional strategies for treatment of PSA's.

INTRODUCTION

Pseudoaneurysms or false aneurysms are one of the most common arterial injuries. In contrast to a true aneurysm, the arterial wall is disrupted and a pulsatile hematoma is present. Pseudoaneurysms are often found in the groin where the femoral artery is accessed for diagnostic and therapeutic procedures using arterial catheterisation (1, 2). If the arterial puncture site is not well sealed, blood will flow into the perivascular tissue, forming a local pulsatile hematoma. If kept undiagnosed or untreated, pseudoaneurysms may continue to expand in size, resulting in compression of femoral veins, arteries and nerves. This may eventually result in deep venous thrombosis, ischemia and rupture, causing limb pain and/or motor defects (3). Femoral artery pseudoaneurysms (PSA's) occur in 0.2-7.7% of patients after femoral arterial interventions (4-7), and is dependent on multiple factors, e.g. compression, blood pressure, location of puncture, catheter/device size etc. Treatment by surgical intervention may cause complications such as haemorrhage, infection and scarring in addition to the risk of general anaesthesia. Other treatments aim for blood clotting within the femoral PSA, e.g. by manual compression (8), ultrasound-guided compression repair (9, 10) and thrombin injection (11, 12). The clinical outcome of these treatments and their complications (e.g. infections, emboli, thrombin-induced autoimmune response) have been well documented (2, 13-17). Nevertheless, a large animal model for femoral PSA may allow better evaluation of the cause and potential prevention of procedural complications, particularly when utilizing non-surgical techniques for PSA.

In a PSA model, pulsatile arterial flow and controllable PSA dimensions (size of sac and neck) are crucial, and spontaneous coagulation must be avoided. Several experimental aneurysm models (e.g. pseudoaneurysm, intracranial aneurysm or carotid aneurysm) models using (micro)surgical techniques have been reported for rats (18), rabbits (19, 20) dog (21, 22) and pigs (23, 24). In this study we have constructed a femoral PSA model by means of an arteriovenous shunt in the groin using procedures that were used in the cranial aneurysm models for dogs of Black *et al.* and Yapor *et al.* (25, 26). We used pigs, since these animals offer several advantages when constructing vascular models. They have a similar blood vessel morphology and coagulation characteristics compared to humans (27), and are appropriate for evaluation of human-sized therapeutic devices. Consequently, therapeutic investigations and possible side effects may be easy to extrapolate to the human situation. In addition, porcine vessels are large enough to manipulate surgically, so microsurgery is not necessary. Our aim was to develop a porcine femoral PSA model which closely resembles the morphological and hemodynamic characteristics of the human situation.

METHODS

Animals

This study was conducted under the supervision of veterinarians according to the NIH (National Institutes of Health) guidelines for the care and use of laboratory animals (NIH publication 85-23 Rev. 1985). The study was approved by the Ethics Committee (EC) of the Radboud University, Nijmegen, The Netherlands. Eight Landrace pigs of approximately 4 months old, 4 male (mean body weight of 50.6 ± 6.8 kg, range 43.8 to 57.4 kg) and 4 female (56.0 ± 5.7 kg, range 50.2 to 61.7 kg), were used to introduce a pseudoaneurysm in the groin. The pigs were housed at the Central Animal Facility and fed a standard diet and water *ad libitum*.

Surgery

One day before surgery, the animals received orally 4.4 mg/kg carbasalate calcium (Meda Pharma BV, Amstelveen, The Netherlands) and 1.5 mg/kg clopidogrel (Bristol-Myers Squibb/Sanofi Pharmaceuticals Partnership Bridgewater, NJ, USA) as interim anticoagulant and pain medication. At the day of surgery, the animals received orally 2 mg/kg carbasalate calcium and 0.75 mg/kg clopidogrel, which was repeated every 48 h for 4 days. For sedation, the animals were pre-medicated with an intramuscular injection of 10 mg/kg ketamine (Eurovet Animal Health BV, Bladel, The Netherlands), 1 mg/kg midazolam (Roche, Woerden, The Netherlands) and 50 µg/kg atropine sulfate (Pharmachemie BV, Haarlem, The Netherlands). Each pig was then covered with a blanket and placed on a heating pad with administration of intravenous fluids through an auricular vein (lactated Ringer's solution containing per litre: 50 g dextrose, 6.0 g sodium chloride, 3.1 g sodium lactate, 1.8 g potassium chloride, 0.2 g calcium chloride·2H₂O). Pigs were anaesthetised with an intravenous administration of 2.5 mg/kg propofol (B. Braun Melsungen AG, Melsungen, Germany). After endotracheal intubation, 2 L/min O₂/N₂O (2:1) containing 0.5% isoflurane (Baxter International, Deerfield, IL, USA) was combined with a bolus of 0.3 mg/kg midazolam and 7.5 µg/kg sufentanyl citrate (Janssen-Cilag BV, Tilburg, The Netherlands). The anaesthesia was maintained with 0.6 mg/kg/h midazolam, 10 µg/kg/h sufentanyl citrate and 25 µg/kg atropine sulfate. Continuous monitoring was provided by electrocardiography, pulse oximetry, and CO₂ and temperature registration.

A pseudoaneurysm was prepared in the groin using vascular surgery (Fig. 1). A bilateral oblique incision was made approximately 5 cm distal to the inguinal ligament, to isolate and expose the femoral artery and the femoral vein. Once isolated, 3-4 drops of 2% (w/v) lidocaine in isotonic solution (Holland Pharmaceutical Supply BV, Alphen a/d Rijn, The Netherlands) was applied to the surface of the femoral artery and vein to prevent vasospasm. Both artery and vein were located superficially and could be easily accessed. The artery and vein collaterals were then closed with 2.0 Vicryl (Ethicon, Norderstedt, Germany) suture knots. A segment of about 2 cm of both the femoral artery and femoral vein were temporarily closed using clamps (Fig. 2A). Vessel loops (Willy Rusch, Waiblingen, Germany) were used to position the artery and vein. In both femoral artery and femoral vein, a 4 mm longitudinal opening was made with #11 scalpel (Swann Norton, Sheffield, England). The artery was anastomosed to the femoral vein (side to side) with 6.0 Prolene running sutures (Ethicon) (Fig. 2B). Clamps were removed and after a 1 min observation, the PSA model was completed by closing the femoral vein both proximally and distally at the original site of the clamps using non-absorbable Serafil USP 3+4 ligatures (Serag-Wiessner, Naila, Germany) (Fig. 1 and Fig. 2C, D). The muscle layer and skin were closed with 2.0 Vicryl sutures. Amoxicillin (20 mg/kg/day, Centrafarm Services B.V., Etten-Leur, The Netherlands) was injected intramuscularly for 4 days to protect the animals from infections.

Evaluation

Food, water uptake and behaviour of the animals were monitored. Four days after the operation, the animals were anaesthetised and the site of operation was exposed to evaluate the femoral PSA model. An ImexDopCT+ ultrasonic Doppler auscultator (Nicolet Vascular, Madison, WI, USA) was positioned directly on the PSA model and was used to evaluate the blood flow. Doppler auscultation was analysed with Audio spectrum software (SpectraPLUS, Pioneer Hill Software, Poulsbo, WA, USA).

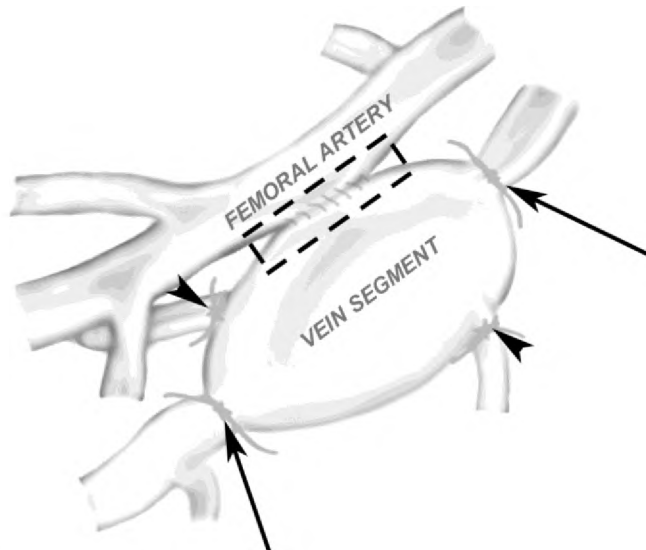


Fig. 1 Schematic overview of the pig femoral artery pseudoaneurysm (PSA) model. Collaterals were closed with ligatures (arrowheads). The femoral artery and femoral vein were anastomosed 'side to side' and a pulsatile vein segment was created by positioning ligatures proximally and distally on the femoral vein (arrows). The neck region of the PSA is indicated by the dashed rectangle

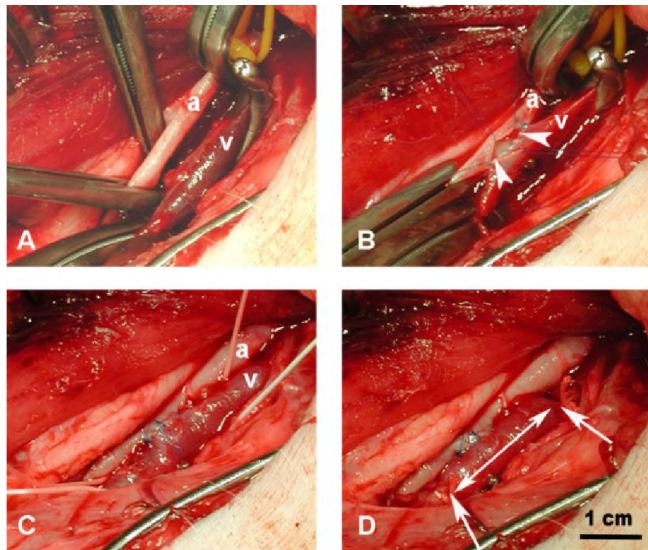


Fig. 2 Macroscopic overview of the preparation of a femoral artery pseudoaneurysm (PSA). A) Isolated and clamped femoral artery (left) and femoral vein (right). B) Anastomosing the artery and vein 'side to side'. Arrowheads point out the anastomotic site. C) View after removing the clamps from the anastomosed artery and vein. D) Final femoral PSA model after closure of the vein proximally and distally with suture knots (arrows). Double-headed arrow indicates the experimental femoral PSA model. Bar indicates 1 cm, a: femoral artery, v: femoral vein.

Angiography was performed to analyse the blood flow qualitatively and to measure the size of the PSA model. Xenetix 300 iodinated contrast fluid (Codali Guerbet, Brussels, Belgium) was used as an intravascular flow tracer. Angiograms were made by accessing the contralateral site with a 6F sheath (Cordis, Miami, FL, USA). Thereafter, a 5F angiographic catheter (Boston Scientific, Natick, MA, USA) was introduced and positioned across the aortic bifurcation in the ipsilateral common femoral artery over a guide wire. All angiograms were performed with a Philips BV-25 C-arm image intensifier (Philips, Eindhoven, The Netherlands). Then, the catheter was removed and the wound was closed. After 10 days, the animals were re-anesthetised and a second angiogram was performed as described previously. The animals were sacrificed by an overdose of intravenous barbiturate. The femoral PSA model was inspected macroscopically, removed and immediately fixed in 4 % (v/v) paraformaldehyde in 100 mM phosphate buffer (pH 7.2) for at least 24 h at 4°C, and subsequently embedded in paraffin. Consecutive 5 µm sections were mounted onto glass slides, dewaxed in xylol and rehydrated through a graded series of ethanol and stained with Hematoxylin and Eosin (H&E) and Elastin von Gieson (EvG) (28).

RESULTS

In the present study, we prepared a porcine pseudoaneurysm model using a one-stage procedure by anastomosing the femoral vein to the femoral artery side-to-side (see Fig. 1 for a schematic overview). Fig. 2 shows the macroscopic images of the surgical preparation of the PSA model. The operation did not require microsurgery. The femoral artery and vein were easily accessible and allowed standardised creation of pseudoaneurysms with a standardised length (2 cm). With arteriotomy, using microscissors, it was possible to reproducibly construct 4 mm necked pseudoaneurysms. Only a short period of clamping (~15 min) was necessary. After removing the clamps, a palpable thrill associated with the arteriovenous shunt was noticed. Generally, no severe bleeding was observed. However, in two cases bleeding occurred which was stopped with an additional suture in combination with gentle compression. This did not affect the outcome of the femoral PSA model. When the ligatures were positioned both proximally and distally on the vein, a segment filled out readily with blood and distinct pulsation was observed. No additional bleeding complications occurred.

All animals remained healthy and did not develop symptoms that are related to the surgery, e.g. swelling or mobility problems. After 4 days, a pulsatile PSA model was present in 7 out of 8 cases. In one animal the PSA model had clotted, but no mobility or health problems were observed. Macroscopic analysis of the PSA model revealed that the average length was 1.9 ± 0.3 cm (mean \pm SD, $n=7$) and width was 0.5 ± 0.1 cm (mean \pm SD, $n=7$). Macroscopic observation indicated the presence of a pulsatile mass. Doppler auscultation revealed a continuous bruit (or murmur) within the PSA model for all 7 pigs (Fig. 3). This bruit is a low and “machine-like” sound throughout systole and diastole, which is typical for pseudoaneurysm conditions (29, 30).

Four days after PSA creation, the angiogram demonstrated a flow between the femoral artery and the PSA model. The femoral PSA model remained patent during the study and resembled both dynamically and radiographically a pseudoaneurysm in the human situation, especially with regard to the morphology (Fig. 4A) (31). At day 10 (prior to sacrifice), both ultrasonic Doppler auscultation and angiography revealed that the femoral PSA model was open. After resecting the PSA, macroscopic analysis showed that both size and morphology were comparable to that observed at day 4 (Fig. 4B).

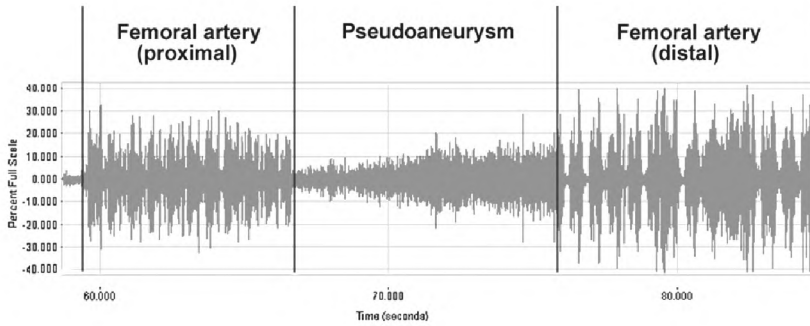


Fig. 3 Doppler waveform indicating the bruit sound of the femoral artery pseudoaneurysm (PSA) and the pulsating sound from the femoral artery both proximally (left) and distally (right) from the femoral PSA model.

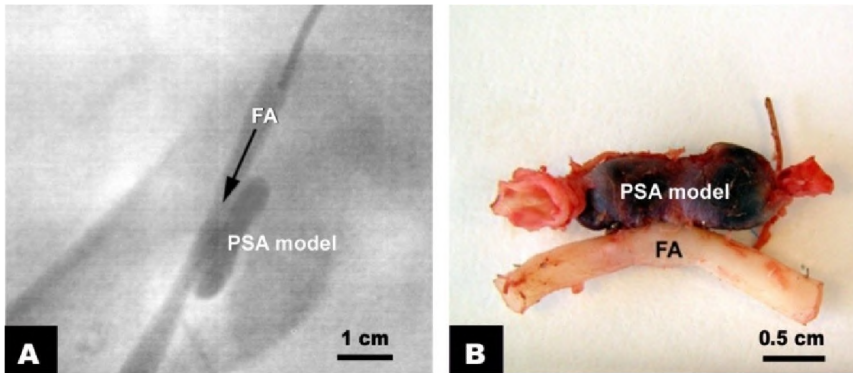


Fig. 4 Angiographic and macroscopic evaluation of femoral artery pseudoaneurysm (PSA). A) Angiogram of the right femoral artery localising the porcine femoral PSA model (arrow indicates arterial blood flow). B) Macroscopic image of resected PSA model with femoral artery at day 10. Bar indicates 1 cm in A and 0.5 cm in B. PSA: pseudoaneurysm, FA: femoral artery.

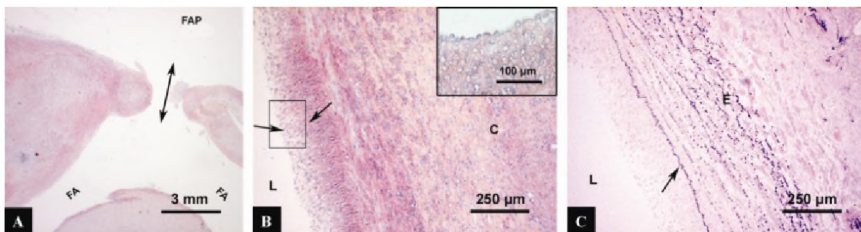


Fig. 5 Light microscopy of a femoral artery pseudoaneurysm (PSA). A) Microscopic overview (H&E staining) of the connection between the femoral artery and the femoral PSA model (arrow indicates arterial blood flow). B) Inner wall of PSA model (H&E staining); arrows indicate the endothelial area. Inset: magnification of the area indicated by the rectangle. C) Inner wall of FAB (EvG staining) showing elastic lamina (arrow) and elastic fibers (E). Bar indicates 3 mm in A, 250 µm in B and C, and 100 µm in the inset of B. C:connective tissue, E: elastic fibers, FA: femoral artery, PSA: pseudoaneurysm, L: lumen of FAB.

Histology confirmed that the femoral PSA model was open and effectively connected with the femoral artery (Fig. 5A). The femoral artery showed a normal structure. The inner layer of the wall of the PSA model consisted of the normal femoral vein structure; endothelial cells covering the elastic lamellae combined with smooth muscle cells and collagen. The outer layer of the PSA model consisted of connective tissue with blood vessels and a low number of fibroblasts (Fig. 5B and C). The EvG staining showed elastic lamina within the wall of the PSA model which were well preserved. No evidence of an inflammatory reaction was observed.

DISCUSSION

To evaluate novel and experimental femoral PSA treatments, their efficacy, safety and/or toxicological profile must be determined. In this respect, it is important to use a standardised animal model which resembles the human situation as close as possible. Different aneurysm models have been developed in a variety of animal models. Most animal models rely on the surgical creation, typically by arteriotomy and vein graft placement (22, 24). Rat, rabbit, dog and pig models have been published, involving the connection of either a vein segment or a muscle cavity to the artery (18-21, 24).

In this study we have prepared and evaluated a model for pseudoaneurysms in the groin of the pig, the femoral artery pseudoaneurysm (PSA) model. It was our aim to create an easy to handle femoral PSA model that is appropriate for evaluation of endovascular treatments, e.g. coil embolisation, balloon techniques or thrombin injection. Although many experimental aneurysm models have been published, a large animal femoral PSA model has, to our knowledge, not been described. We used an one-step intervention procedure that was comparable with the method applied for cranial aneurysm models in dogs (25, 26), and adapted it for PSA model in the groin. The location and features of our surgically created PSA model resembles the human clinical situation. We used pigs since they closely match the hemodynamic and coagulation characteristics of humans (27), making the model suitable for translational studies.

In our femoral PSA model, an arteriovenous anastomosis was made and the adjacent vein was eventually closed both proximally and distally. We were able to reproducibly prepare a pseudoaneurysm with a narrow neck (4 mm), with standardised diameter and sac dimensions, making it possible to evaluate human sized devices. It is anticipated that by changing the distance of the ligatures the size of the PSA model can be controlled, thereby creating a range of femoral PSA models representing the clinical situation. It was also possible to prepare two femoral PSA models in one pig, which makes this model even more interesting both experimentally and economically.

The angiogram of our femoral PSA model was comparable with human pseudoaneurysm angiograms (31). Both angiography and Doppler auscultation confirmed that the PSA models were open, and demonstrated communication between the PSA model and the femoral artery. Doppler interrogation indicated a bruit representing the turbulent flow in the PSA model. Although many studies use only angiography, we think that the combination with Doppler can evaluate PSA model patency more thoroughly. Colour flow Doppler imaging would be even more useful than Doppler auscultation, but was not available at our animal facility.

Two key features which we used in our model to prevent aneurysm thrombosis were: 1) pre- and postoperative treatment with NSAIDs (non-steroidal anti-inflammatory drugs; carbasalate calcium and clopidogrel) to prevent platelet deposition, and 2) minimisation of the clamping time of both femoral artery and vein (~15 min) to reduce the risks of endothelial

cell damage (32). A continuous layer of endothelial cells was present on the wall of the PSA model indicating that there was no major damage. This is of importance to prevent endogenous coagulation and is especially relevant for studies addressing the hemostatic effectiveness of treatment. When a continuous endothelial layer is absent, e.g. when anastomosing a cauterised muscular cavity with the femoral artery, spontaneous blood clotting is a regular problem (20).

Although our model offers advantages over the current models, several shortcomings may exist. In our PSA model a vein segment was used with an intact endothelium. We chose for the intact endothelial layer to make the model especially suitable for study of the effect of hemostatic agents/devices proper. It should be pointed out however, that the presence of an intact endothelial wall not truly mimics a human femoral aneurysm. In the human situation, PSA's are surrounded by interstitial tissue rather than an intact endothelium. In addition, in our PSA model, the neck region was fixed, whereas in human it may be variable. A next step in the validation of the PSA model is the evaluation of specific treatment modalities, e.g. thrombin injection or compression techniques'. Nevertheless, based on the translational characteristics of pigs, e.g. morphology and haemodynamics, we think this PSA model may be a promising pre-clinical model to study various aspects of PSA treatment both locally and systemically. Additionally, this PSA model in pig is appropriate to evaluate human sized devices. The model may also be helpful to determine the optimal dose of hemostatic agents or understand the mechanism in case of an arterial influx, and evaluate the safety and efficacy of new agents or devices. When doing so, a follow-up study with proper histology may be desirable to identify and clarify toxicological or systemic side effects.

Collectively, data indicate that the pig model for pseudoaneurysms is relatively straight forward, highly reproducible and approaches the human situation. Although we did not validate the utility of the PSA with known therapies, we anticipate that this large animal model allows the study of various aspects of PSA treatment both locally and systemically. The pseudoaneurysm model may offer new opportunities for interventional studies.

REFERENCES

1. C.Aytenkin, A.Firat, E.Yildirim, I.Kirbas, and F.Boyvat. "Ultrasound-guided glue injection as alternative treatment of femoral pseudoaneurysms." *Cardiovasc.Intervent.Radiol.* 27, no. 6(November 2004):612-15.
2. I.Kronzon. "Diagnosis and treatment of iatrogenic femoral artery pseudoaneurysm: a review." *J Am Soc.Echocardiogr.* 10, no. 3(April 1997):236-45.
3. J.W.Hallett, S.W.Wolk, K.J.Cherry, P.Gloviczki, and P.C.Pairolero. "The Femoral Neuralgia Syndrome After Arterial Catheter Trauma." *Journal of Vascular Surgery* 11, no. 5(1990):702-06.
4. T.F.Kresowik, M.D.Khoury, B.V.Miller, M.D.Winniford, A.R.Shamma, W.J.Sharp, M.B.Blecha, and J.D.Corson. "A prospective study of the incidence and natural history of femoral vascular complications after percutaneous transluminal coronary angioplasty." *J Vasc.Surg.* 13, no. 2(February 1991):328-33.
5. R.Katzenschlager, A.Ugurluoglu, A.Ahmadi, M.Hulsmann, R.Koppensteiner, E.Larch, T.Maca, E.Minar, A.Stumpflen, and H.Ehringer. "Incidence of pseudoaneurysm after diagnostic and therapeutic angiography." *Radiology* 195, no. 2(May 1995):463-66.
6. M.Ates, S.Sahin, C.Konuralp, U.Gullu, S.Cimen, M.Kizilay, R.Gunay, Y.Sensoz, and M.Akcar. "Evaluation of risk factors associated with femoral pseudoaneurysms after cardiac catheterization." *J Vasc.Surg.* 43, no. 3(March 2006):520-24.
7. R.Zahn, S.Thoma, E.Fromm, R.Lotter, M.Zander, K.Seidl, and J.Senges. "Pseudoaneurysm after cardiac catheterization: therapeutic interventions and their sequelae: experience in 86 patients." *Cathet.Cardiovasc.Diagn.* 40, no. 1(January 1997):9-15.

8. K.A.Sorrell, R.L.Feinberg, J.R.Wheeler, R.T.Gregory, S.O.Snyder, R.G.Gayle, and N.F.Parent. "Colour-flow duplex-directed manual occlusion of femoral false aneurysms." *Journal of Vascular Surgery* 17, no. 3(1993):571-77.
9. R.Feld, G.M.Patton, A.Carabasi, A.Alexander, D.Merton, L.Needleman, and J.M.Giordano. "Treatment of iatrogenic femoral-artery injuries with ultrasound-guided compression." *Journal of Vascular Surgery* 16, no. 6(1992):832-40.
10. B.D.Fellmeth, S.B.Baron, P.R.Brown, J.G.P.Ang, K.R.Clayson, S.L.Morrison, and R.I.Low. "Repair of postcatheterization femoral pseudoaneurysms by colour flow ultrasound guided compression." *American Heart Journal* 123, no. 2(1992):547-51.
11. C.S.Liau, F.M.Ho, M.F.Chen, and Y.T.Lee. "Treatment of iatrogenic femoral artery pseudoaneurysm with percutaneous thrombin injection." *Journal of Vascular Surgery* 26, no. 1(1997):18-23.
12. J.D.Ferguson and A.P.Banning. "Ultrasound guided percutaneous thrombin injection for the treatment of iatrogenic pseudoaneurysms." *Heart* 83, no. 5(2000):582.
13. T.Chatterjee, D.D.Do, U.Kaufmann, F.Mahler, and B.Meier. "Ultrasound-guided compression repair for treatment of femoral artery pseudoaneurysm: acute and follow-up results." *Cathet.Cardiovasc.Diagn.* 38, no. 4(August 1996):335-40.
14. K.Hamraoui, S.M.P.G.Ernst, P.F.H.M.van Dessel, J.C.Kelder, J.M.ten Berg, M.J.Suttorp, W.Jaarsma, and T.H.W.Plokker. "Efficacy and safety of percutaneous treatment of iatrogenic femoral artery pseudoaneurysm by biodegradable collagen injection." *Journal of the American College of Cardiology* 39, no. 8(April 2002):1297-304.
15. S.S.Kang, N.Labropoulos, M.A.Mansour, and W.H.Baker. "Percutaneous ultrasound guided thrombin injection: a new method for treating postcatheterization femoral pseudoaneurysms." *J Vasc.Surg.* 27, no. 6(June 1998):1032-38.
16. J.-M.Lemaire and R.F.Dondelinger. "Percutaneous coil embolization of iatrogenic femoral arteriovenous fistula or pseudo-aneurysm." *European Journal of Radiology* 18, no. 2(May 1994):96-100.
17. T.L.Ortel, M.C.Mercer, E.H.Thames, K.D.Moore, and J.H.Lawson. "Immunologic impact and clinical outcomes after surgical exposure to bovine thrombin." *Ann.Surg.* 233, no. 1(January 2001):88-96.
18. P.H.Young and M.G.Yasargil. "Experimental carotid artery aneurysms in rats: a new model for microsurgical practice." *J Microsurg.* 3, no. 3(1982):135-46.
19. W.E.Stehbens. "Experimental production of aneurysms by microvascular surgery in rabbits." *Vasc.Surg.* 7, no. 3(May 1973):165-75.
20. H.T.Sun, S.Z.Liao, H.Chen, W.F.Feng, Y.N.Xu, and Y.M.Zheng. "Production of animal model of traumatic pseudoaneurysm." *Microsurgery* 18, no. 2(1998):103-09.
21. W.J.German and S.P.Black. "Experimental production of carotid aneurysms." *N.Engl.J Med.* 250, no. 3(January 1954):104-06.
22. Y.S.Shin, Y.Niimi, Y.Yoshino, J.K.Song, M.Silane, and A.Berenstein. "Creation of four experimental aneurysms with different hemodynamics in one dog." *AJNR Am J Neuroradiol.* 26, no. 7(August 2005):1764-67.
23. J.V.Byrne and N.Hubbard. "A novel two-stage technique for construction of experimental aneurysms." *AJNR Am J Neuroradiol.* 25, no. 2(February 2004):319-21.
24. G.Guglielmi, C.Ji, T.F.Massoud, A.Kurata, S.P.Lowrie, F.Vinuela, and J.Robert. "Experimental saccular aneurysms. II. A new model in swine." *Neuroradiology* 36, no. 7(October 1994):547-50.
25. S.P.Black. "Experimental saccular aneurysm by an arteriovenous fistula method." *Mo.Med.* 60,(April 1963):340-43.
26. W.Yapor, J.Jafar, and R.M.Crowell. "One-stage construction of giant experimental aneurysms in dogs." *Surg.Neurol.* 36, no. 6(December 1991):426-30.
27. F.A.Osterman, W.R.Bell, R.J.Montali, G.R.Novak, and R.I.White. *Natural History of Autologous Blood Clot Embolization in Swine. Investigative Radiology* 11[4], 267-276. 1976.
28. Bancroft J.D. and Stevens A. *Theory and practice of histological techniques*, Edinburgh (UK): Churchill Livingstone, 1990.
29. M.Ma and C.P.Snook. "Ruptured femoral pseudoaneurysm presenting as a lateral abdominal wall hematoma." *Journal of Emergency Medicine* 29, no. 2(August 2005):147-50.

30. D.Gaitini, N.B.Razi, E.Ghersin, A.Ofer, and M.Soudack. "Sonographic evaluation of vascular injuries." *J Ultrasound Med.* 27, no. 1(January 2008):95-107.
31. S.Schena, C.A.Owens, H.T.Hassoun, and M.R.Kibbe. "Delayed presentation of a posttraumatic superficial femoral artery pseudoaneurysm." *Journal of the American College of Surgeons* 203, no. 2(August 2006):250-51.
32. B.Risberg, A.Bylock, and M.Romanus. "Endothelial fibrinolysis and ultrastructure following graded mechanical trauma." *Acta Chir Scand.* 154, no. 5-6(May 1988):353-58.

Chapter 5

PREPARATION AND CHARACTERISATION OF INJECTABLE FIBRILLAR TYPE I COLLAGEN AND EVALUATION FOR PSEUDOANEURYSM TREATMENT IN A PIG MODEL

Paul J. Geutjes¹
Daan J. A. van der Vliet²
Kaeuis A. Faraj^{1,3}
Noes de Vries³
Herman T. van Moerkerk¹
Ronnie G. Wismans¹
Thijs Hendriks²
Willeke F. Daamen¹
Toin H. van Kuppevelt¹

^{1,2}Radboud University Nijmegen Medical Centre, Departments of
¹Biochemistry (280), and ²Surgery (690), P.O. Box 9101, 6525 GA Nijmegen, The
Netherlands and ³Aap bio implants - EMCM BV, Middenkampweg 17, 6645 CH
Nijmegen, The Netherlands

Journal of Vascular Surgery. In press

ABSTRACT

INTRODUCTION Despite the efficacy of collagen in femoral artery pseudoaneurysm treatment, as reported in one patient study, its use has not yet gained wide acceptance in clinical practise. In the particular study, the collagen was not described in detail. To further investigate the potential of collagen preparations, we prepared and characterised highly purified injectable fibrillar type I collagen and evaluated its use for femoral artery pseudoaneurysm (PSA) treatment *in vivo*, using a pig model. **METHODS** Purified fibrillar type I collagen was characterised using electron microscopy. The effect of three different sterilisation procedures, i.e. hydrogen peroxide gas plasma (H_2O_2), ethylene oxide gas (EtO) and gamma irradiation, was studied on both SDS-PAGE and platelet aggregation. Different collagen injectables were prepared (3%, 4% and 5%) and tested using an injection force test applying a 21 gauge needle. To evaluate the network characteristics of the injectable collagen, the collagen was suspended in phosphate buffered saline (PBS) at 37°C, and studied both macroscopically and electron microscopically. To determine whether the collagen induced hemostasis *in vivo*, a pig PSA model was used applying a 4% EtO sterilised collagen injectable, and evaluation by angiography and routine histology. **RESULTS** Electron microscopy of the purified type I collagen revealed intact fibrils with a distinct striated pattern and a length < 300 µm. Both SDS-PAGE and platelet aggregation analysis of the sterilised collagen indicated no major differences between EtO and H_2O_2 sterilisation, although gamma-irradiated collagen showed degradation products. Both 3% and 4% (w/v) collagen suspensions were acceptable with respect to the force used (< 50 N). The 4% suspension was selected as the preferred injectable collagen, which formed a dense network under physiological conditions. Testing the collagen *in vivo* (n=5), the angiograms revealed that the PSA partly or completely coagulated. Histology confirmed the network formation, which was surrounded by thrombus. **CONCLUSIONS** Collagen injectables were prepared and EtO sterilised without major loss of structural integrity and platelet activity. *In vivo*, the injectable collagen formed a dense network and triggered (partial) local hemostasis. Although optimisation is needed, an injectable collagen may be used as a therapeutic agent for femoral PSA treatment.

INTRODUCTION

A femoral artery pseudoaneurysm (PSA) is a complication which may occur after arterial puncture for invasive cardiovascular procedures. When an arterial puncture site fails to seal, arterial blood jets into the surrounding tissues and forms a pulsatile hematoma. In 0.2-7.7% of the femoral arterial interventions, a femoral PSA is formed that needs treatment (1-4). When a PSA is left untreated, rupture or distal embolisation may occur. PSA enlargement may give rise to pain, neuropathy and venous obstruction. Since spontaneous repair of larger pseudoaneurysms is unlikely, a reliable and easy method to induce local hemostatic clotting is desirable. Various techniques (e.g. ultrasound-guided compression repair, percutaneous thrombin injection, balloon occlusion, stent-graft placement) have been used to stop arterial bleeding in order to replace standard compression treatment and shorten hospital stay (5-10). Thrombin treatment is highly effective. However, in some cases (especially complex pseudoaneurysms) it is not efficient and even contra-indicated. Contra-indications for the use of thrombin injection are the wide and/or short necked pseudoaneurysms (11). Several cases have reported thrombin failure in these complex pseudoaneurysms (12-14). Particularly in these cases, injectable collagen may be an attractive agent, since collagen is highly viscous and collagen fibrils aggregate and deposit at the site of injection. In one study the potentials of injectable collagen for PSA treatment in patients was described, and a very high success rate was reported (15). To follow up on this study, we prepared a well characterised injectable collagen preparation, and evaluated its use in a porcine model for PSA treatment.

Collagen is a well known structural extracellular matrix protein. It has found ample usage as a biological material for medical applications indicating its versatility as a biomaterial, including its use as a drug delivery device (16, 17) and as a matrix for the repair and regeneration of tissues (18-20). In addition it is used as an adjunct for hemostasis (21-23). Collagen-based plugs are widely used to manage the arterial puncture site and to prevent the extravasation of arterial blood (24, 25). When collagen comes in contact with blood, platelets become activated and their shape changes, resulting in the release of hemostasis-stimulating compounds, platelet adhesion and aggregation to the vessel wall. This process is also known as primary hemostasis (26, 27). Collagen is biocompatible and biodegradable which allows remodelling in the host after implantation. In addition, collagen can be fabricated in various physical forms like gels, films, and sponges. These characteristics, in combination with its hemostatic activity, make collagen a good alternative for current treatments of femoral PSA.

In 2002, Hamraoui *et al.* treated PSA patients with bovine fibrillar type I collagen aiming for a less invasive percutaneous treatment (15). According to this study, the use of collagen is a safe and effective strategy. To further elaborate on the use of collagen for PSA treatment, we prepared well characterised collagen fibrils, selected the optimal sterilisation procedure, and evaluated its use for the treatment of PSA using a recently described porcine model.

METHODS

Materials

Unless otherwise stated, chemicals were obtained from Merck (Darmstadt, Germany) and were of the highest purity available.

Preparation of injectable fibrillar type I collagen

Fibrillar type I collagen was isolated from 6 months old bovine achilles tendon (deep flexor) applying extraction procedures using neutral salt solutions, chaotropic agents, dilute acid, and acetone (28). After purification, type I collagen was lyophilised using a Sublimator 500II lyophiliser (Zirbus Technology, Bad Grund, Germany) and sterilised using either ethylene oxide gas (EtO; 24 h at 35-45°C and at 50-80% relative humidity; Sterigenics, Zoetermeer, The Netherlands), hydrogen peroxide gas plasma (H₂O₂; 6 mg/l at 35°C for 30 min) or gamma irradiation (Gamma; 20 kGy from a ⁶⁰Co source in a X-ray pallet irradiator (JS 9000; Isotron BV, 's-Hertogenbosch, The Netherlands)). Type I collagen suspensions were prepared by incubation of 3.0, 4.0 or 5.0 g type I collagen in 100 ml MilliQ water for 16 h at 4°C. The suspensions were homogenised (20 times on ice) using a Potter-Elvehjem homogeniser with an intervening space of 0.35 mm.

Characterisation of injectable fibrillar type I collagen

Scanning electron microscopy (SEM) was used to analyse the morphology and length of the purified collagen fibrils, and transmission electron microscopy (TEM) was applied to study the ultrastructure of the collagen fibrils. Collagen samples were frozen at -20°C and subsequently lyophilised. Poly-D-lysine coated glass inserts were incubated with collagen suspensions (~0.5 mg collagen/ml 0.25 M acetic acid), for 16 h at 4°C, washed 3 times with MilliQ water and air dried. Inserts were mounted on stubs and sputtered with an ultrathin layer of gold in a Polaron E5100 Coating System. The morphology of the collagen fibrils was studied in a Philips XL30 ESEM FEG apparatus at an accelerating voltage of 10 kV, and their lengths was studied with a JEOL JSM-6310 SEM (JEOL Ltd, Tokyo, Japan) at 15 kV; 100 fibrils were randomly measured at 500x magnification in 16 fields. The ultrastructure of the collagen fibrils was analysed in the diluted collagen samples using TEM. The samples were incubated on formvar-coated grids for 1 h at 21°C, washed with 0.1 M phosphate buffer (pH 7.4), washed 2 times with MilliQ water, stained with 0.1% (v/v) uranyl acetate, and examined in a JEOL 1010 TEM (Tokyo, Japan).

The purity and intactness of the type I collagen before and after sterilisation was analysed using sodium dodecyl sulphate polyacrylamide gel electrophoresis (SDS-PAGE). Samples were incubated at 95°C for 10 min under reducing conditions (5% (v/v) 2-mercaptoethanol) and analysed on a 8% (w/v) gel (29). Only potential impurities and degradation products will penetrate the gel since collagen fibrils are insoluble in sample buffer. Gels were stained with 0.1% (w/v) Coomassie Brilliant Blue R-250 solution (ICN Pharmaceuticals, CA, USA), containing 50% (v/v) methanol and 10% (v/v) acetic acid.

To evaluate the network characteristics of the type I collagen under physiological conditions, the injectable collagen suspension (4% (w/v) in MilliQ), was injected in phosphate buffered saline (PBS, pH 7.4) at 37°C. In addition, to study this on the electron microscopical level, a collagen suspension (0.5% (w/v) in MilliQ water) was 1:1 diluted with PBS at 37°C. Collagen suspension (0.5% (w/v) in MilliQ water) 1:1 diluted in MilliQ water was used as a control. The collagen were analysed using the JEOL JSM-6310 SEM apparatus as previously described.

Injection characteristics of type I collagen suspension

To determine the force that is needed to inject type I fibrillar collagen suspension, an injection force test was performed (30). Different collagen suspensions (3%, 4% and 5% (w/v) in MilliQ water) were extruded from a 1 ml syringe with a 21 gauge needle (Ø 0.7 mm). The test was performed at a crosshead speed of 1.8 mm/s. The force was recorded by a MTS

810 testing machine combined with a MTS 458.20 microconsole (MTS Systems Corporation, Eden Prairie, MN, USA).

Platelet aggregation

Platelet aggregation and thrombus formation is dependent on the structure of the collagen preparation (31). To assess the effect of sterilisation of the injectable collagen on the platelet activity, platelet aggregation was measured. The test was performed in a four-channel whole-blood aggregometer model 590 (Chrono-Log Corp, Havertown, PA, USA) measuring the impedance (%), that is increased proportional with the amount of platelet aggregation (31, 32). Briefly, whole blood was collected by vena puncture from a healthy volunteer and collected in 3.2 % (w/v) sodium citrate tubes (mean platelet count: $274 \cdot 10^3 \pm 30 \cdot 10^3 / \mu\text{l}$). Whole blood was diluted with PBS in a 1:1 ratio and incubated for 15 min at 37°C. Next, 10 μl collagen suspension (0.05 mg/ml MilliQ water) was added to 1.0 ml diluted blood. All measurements were completed within 2 h from the blood draw. The platelet aggregation of non-sterilised collagen was set on 1 arbitrary unit (AU). Single way ANOVA was used for statistical analyses and $p < 0.05$ was considered statistically significant.

Evaluation of injectable collagen in a porcine model for femoral artery pseudoaneurysm

To study the effectiveness of injectable collagen fibrils for treatment of pseudoaneurysm a pig model was used as described (33). This study was approved by the Ethics Committee (EC) of the Radboud University, Nijmegen, The Netherlands, and conducted under the supervision of veterinarians according to the NIH (National Institutes of Health) guidelines for the care and use of laboratory animals (NIH publication 85-23 Rev. 1985). The pigs were housed at the Central Animal Facility, Nijmegen, The Netherlands. The animals were fed a normal laboratory diet and water *ad libitum*. Briefly, the femoral artery and femoral vein in the groin of an adult pig were exposed and temporary clamped. A longitudinal arterio-venous anastomosis (side to side) with a 4 mm opening was prepared and about a 2 cm segment of the femoral vein was used as PSA model after closing the femoral vein both proximally and distally using non-absorbable ligatures. The muscle layer and skin were closed. Amoxicillin (20 mg/kg/day) was injected intramuscularly for 4 days to protect the animal from bacterial infections. The animals received 2 mg/kg carbasalate calcium (Meda Pharma BV, Amstelveen, The Netherlands) and 0.75 mg/kg clopidogrel (Bristol-Myers Squibb/Sanofi Pharmaceuticals Partnership Bridgewater, NJ, USA) every 48 h for 4 days, as interim anticoagulant and pain medication.

Four days after construction of the PSA model, the animals were anaesthetised and the operation site was re-opened to evaluate if the PSA model was pulsatile and to directly inject the collagen preparation. Using a 21 Gauge needle, 4% (w/v in MilliQ water) EtO sterilised 4% (w/v) collagen suspension (100-200 μl) was injected in the PSA compartment of 6 individual pigs and the blood coagulation, host response and network properties of the collagen evaluated. Intraoperative femoral artery angiography was performed to document the blood flow in the PSA model before and after collagen injection. A contrast agent (Xenetix 300, Codali Guerbet, Brussels, Belgium) was used as an intravascular flow tracer. The angiogram was performed by accessing the contralateral site with a 6F sheath (Cordis, Miami, FL, USA). A 5F angiographic catheter (Boston Scientific, Natick, MA, USA) was introduced and positioned across the aortic bifurcation in the ipsilateral proximal common femoral artery over a guide wire. All angiograms were performed with a Philips BV-25 C-arm image intensifier (Philips, Eindhoven, The Netherlands). After removal of the catheters, the wound was closed. Six days after the initial evaluation, a second angiogram was performed and the animal was subsequently sacrificed by an overdose of intravenous barbiturate. The

area of the pseudoaneurysm and the surrounding tissue was explanted and immediately fixed in 4% (v/v) formaldehyde in 10 mM phosphate buffer (pH 7.2) for 24 h at 4°C and embedded in paraffin. Consecutive 5 µm sections were mounted onto glass slides, dewaxed in xylol and rehydrated through a graded series of ethanol. Hematoxylin and Eosin (H&E) staining was employed for histological evaluation.

RESULTS

Characterisation of type I collagen

Scanning electron microscopy (SEM) and transmission electron microscopy (TEM) were used to analyse the morphology and ultrastructure of the purified type I collagen fibrils. Both SEM and TEM showed intact fibrils with distinct striated pattern, and no impurities could be detected (Fig. 1A and B). The striated pattern reflects the 3D organisation of (triple helical) collagen molecules within a collagen fibril. The measured length of collagen fibrils (Fig. 1C) indicated that fibril length was < 400 µm, 75% of the fibrils being < 150 µm.

SDS-PAGE was used to biochemically characterise the collagen before and after sterilisation (Fig. 2). For native type I collagen, SDS-PAGE showed α_1 and α_2 bands that are typical for type I collagen (Fig. 2; lane 1). No major differences were found before and after EtO sterilisation or H₂O₂ sterilisation (Fig. 2; lane 2 and 3). After gamma sterilisation however, a smear appeared on the gel, indicating collagen degradation products (Fig. 2; lane 4).

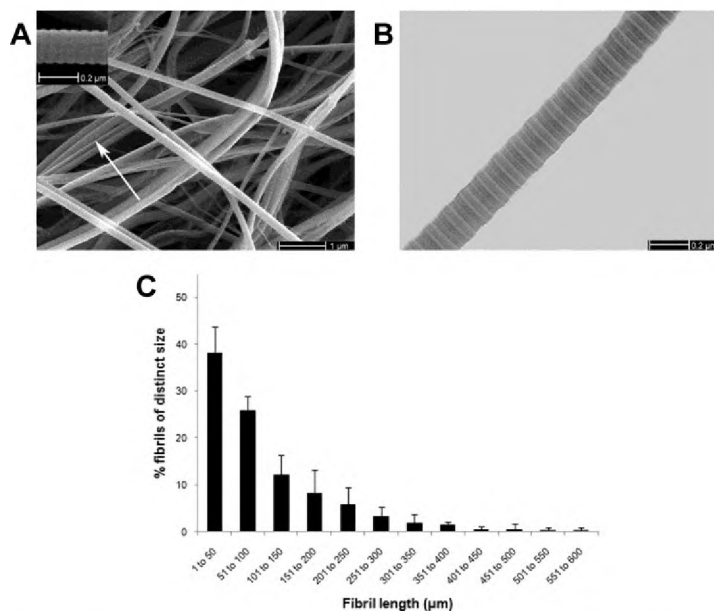


Fig. 1 Morphology and length of purified type I collagen fibrils. Scanning and transmission electron micrograph of purified type I collagen fibrils (A and B respectively), and the distribution of fibril length (µm) in the collagen preparation (C). Results are mean ± SD of 3 separate experiments. Bar in A is 1 µm and inset 0.2 µm. Bar in B is 0.2 µm.

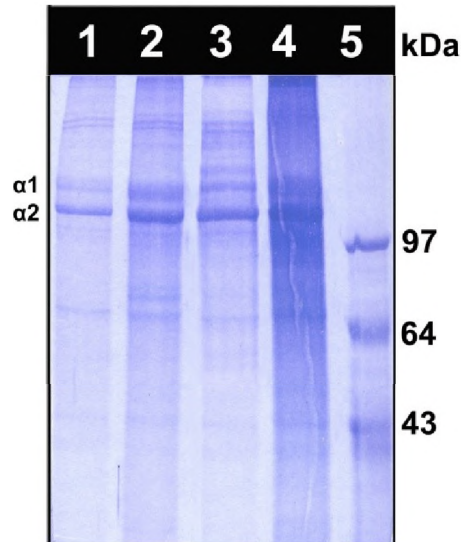


Fig. 2 Effect of sterilisation procedure on the integrity of collagen. SDS-PAGE under reducing conditions of fibrillar type I collagen before (lane 1) and after (lane 2-4) sterilisation, viz.: ethylene oxide gas sterilisation (lane 2), hydrogen peroxide (H₂O₂) gas sterilisation (lane 3) or gamma irradiation (lane 4). The low molecular weight marker is visualised in lane 5. This is a combined image taken from two separate gels (lanes 1, 2 and 4 are from one gel). Note that especially after gamma sterilisation collagen degradation products are observed.

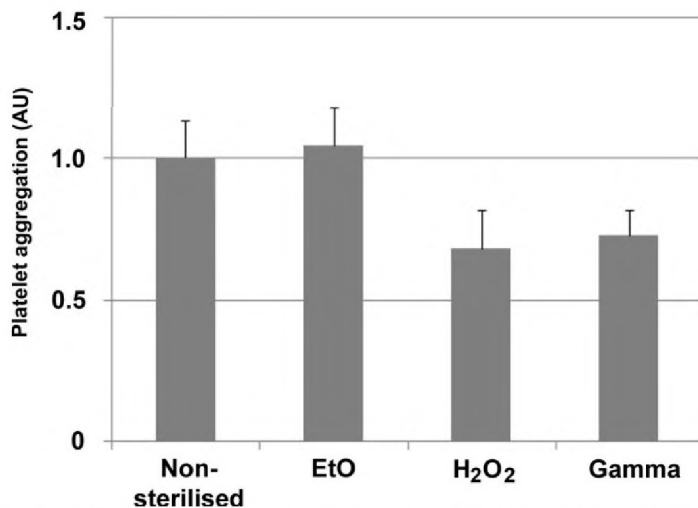


Fig. 3 Effect of sterilisation on platelet aggregation of fibrillar collagen. EtO: ethylene oxide gas sterilisation; H₂O₂: hydrogen peroxide sterilisation; Gamma: gamma irradiation. Collagen before sterilisation was set on 1 arbitrary unit (AU). Results are mean \pm SD for 3 separate experiments. Sterilised collagen showed no statistical significant differences in comparison to non-sterilised collagen ($p > 0.05$).

Platelet aggregation

A whole-blood platelet aggregation test was used to analyse the effect of sterilisation on platelet aggregation (in arbitrary units). The platelet aggregation of the native non-sterilised collagen was set to 1 arbitrary unit. The platelet aggregation of EtO, H₂O₂ and gamma were 1.05 ± 0.14 , 0.63 ± 0.14 and 0.73 ± 0.09 , respectively (Fig. 3). Although EtO sterilised collagen was most comparable to the non-sterilised collagen, other sterilisation methods did also not significantly differ. EtO sterilised collagen was used for *in vivo* studies.

Characterisation of type I collagen injectability

An injection force test was performed to analyse the effect of different concentrations of type I collagen on injectability (Fig. 4A). The force was measured while extruding a 3%, 4% or 5% (w/v) suspension from a 1 ml syringe through a 2 F (21 Gauge, 0.7 mm) needle. The suspensions required a force of 18 N, 19 N and 117 N, respectively (Fig. 4B). According to ISO regulations, both 3% and 4% (w/v) collagen suspensions are acceptable and can be used for manual injection (≤ 50 N according to ISO 7886-1:1997; 'Sterile hypodermic syringes for single use - Part 1: Syringes for manual use'). The 4% (w/v) collagen suspension was selected as the preferred injectable collagen suspension.

To analyse the network properties of the injectable type I collagen under physiological conditions, the 4% (w/v) collagen in MilliQ water (Fig. 5A) was applied to pre-heated (37°C) phosphate buffered saline (pH 7.4). Macroscopic evaluation indicated that the collagen formed a dense network immediate after extrusion in PBS (Fig. 5B). SEM analyses indicated a decrease in spacing between the collagen fibrils which is in line with aggregation of fibrils into a network (Fig. 5).

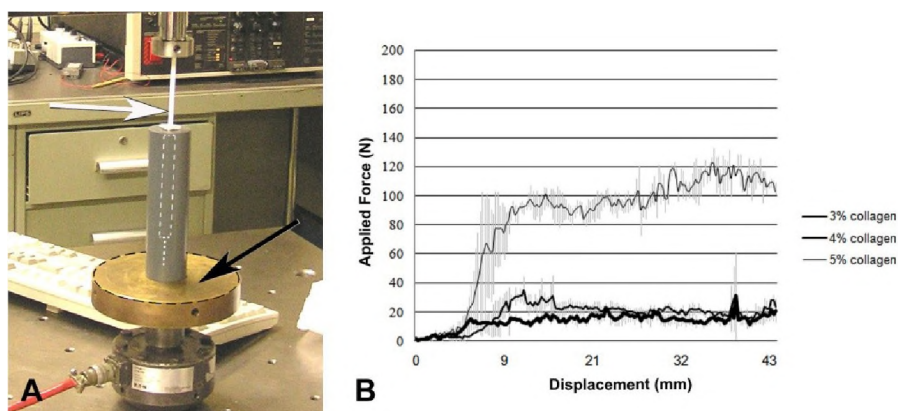


Fig. 4 Evaluation of injectability. A) Macroscopic image of the displacement test setup with type I collagen suspension in a 1 ml syringe. B) Graph of displacement test (1.8 mm/sec with maximal distance 44 mm) of 3%, 4% and 5% (w/v) type I collagen suspension in a 1 ml syringe with a 2 F (0.7 mm) needle. On the Y-axis, force is given in Newton, and on the X-axis displacement is shown in mm. Results are mean \pm SD of 3 separate experiments. The white arrow and white dashed line indicate the 1 ml syringe in the displacement set-up. The black arrow and dashed circle indicate the pressure plate.

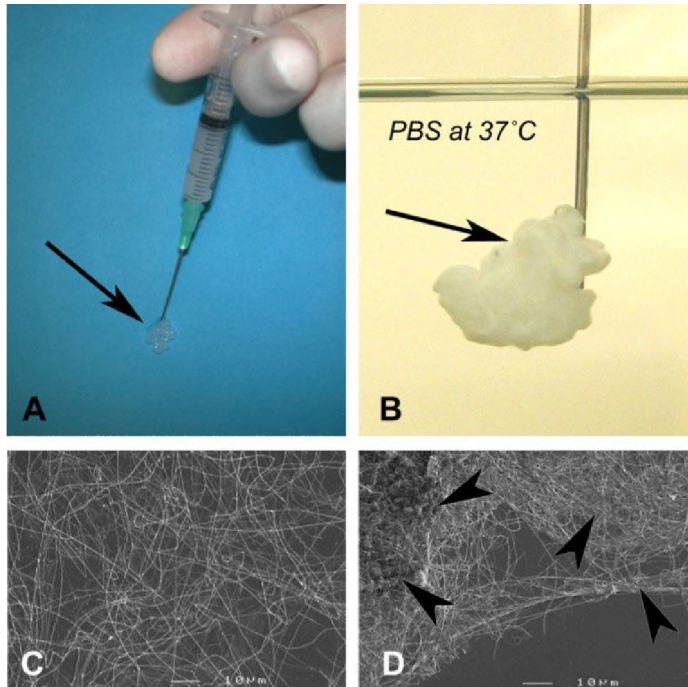


Fig. 5 Aggregation of injectable collagen under physiological conditions. Macroscopic images of 4% (w/v) type I collagen suspension in MilliQ water (A) and the network that was formed directly after injection of the type I collagen in pre-heated (37°C) phosphate buffered saline (PBS, pH 7.4) (B). Scanning electron microscopical images after applying a 0.5% (w/v) collagen suspension in MilliQ water or in PBS, resulting in an open fibril network (C) and an aggregated fibril network (D) respectively. Under physiological conditions (PBS, 37°C), the collagen fibrils formed a dense network. Arrows in A and B indicate the aggregated type I collagen suspension. Arrowheads for D indicates the aggregated collagen fibrils. Bar is 10 μ m in C and D.

Evaluation of injectable collagen in a porcine model for femoral artery pseudoaneurysm

No complications due to the surgery were observed. In 1 of 6 cases, the femoral PSA model clotted directly after the operation and this model was excluded from the experiment. No bleeding complications occurred as a result of surgery.

Four days after surgery, the PSA was evaluated with angiography before and after collagen injection. When the PSA model was open (Fig. 6A), 100 to 200 μ l 4% (w/v) type I collagen in MilliQ water was locally injected. In 4 of the 5 cases, the PSA model partly or completely coagulated within approximately 5 min after type I collagen injection, which was confirmed with angiography (Fig. 6B). In 1 case, both femoral artery and PSA coagulated. In this case, both femoral arteries were found open 6 days after injection leaving the PSA nicely closed (data not shown). After cross-sectioning the injected PSA, both the collagen and the thrombus were macroscopically visible and could be localised (Fig. 7).

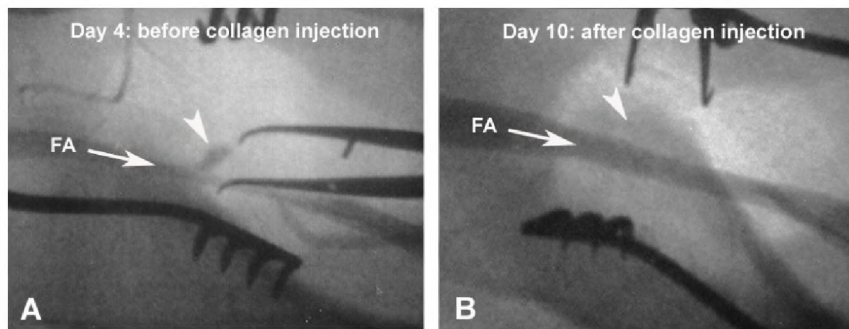


Fig. 6 Angiograms of the porcine femoral PSA (animal no. 6) at day 4 before collagen injection (A) and at day 10 (6 days after collagen injection) (B). Tweezers were positioned on the PSA segment (white arrow-heads). In A, the PSA was open. In B, it was closed after collagen injection. FA: femoral artery. White arrows indicate the direction of arterial blood flow in the femoral artery.

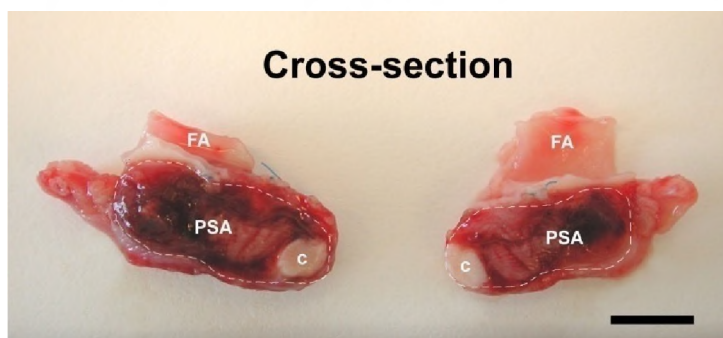


Fig. 7 Macroscopic image of cross-sectioned PSA model, 6 days after collagen injection (animal no. 1, day 10). FA: femoral artery; PSA: pseudoaneurysm model with thrombus; c: injected type I collagen suspension (4% (w/v) in MilliQ water). The white dashed lines indicate the boundary of the PSA wall. Bar indicates 5 mm.

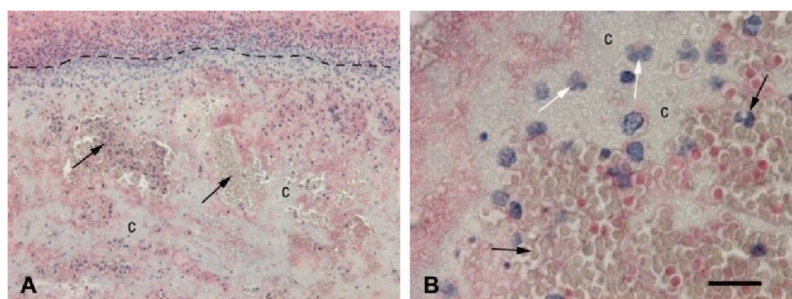


Fig. 8 Microscopic images of coagulated PSA model (luminal site) 6 days after type I collagen injection. Hematoxylin-eosin stained sections showed a clotted PSA filled with type I collagen (c) and coagulated blood cells (black arrows) (A, B). The wall of the PSA is indicated by dashed line (A). Leukocytes were found within the collagen network (white arrows) (B). c: collagen network. Bar indicates 500 μ m in A and 50 μ m in B.

Histological evaluation

Six days after injection, a minor infiltration of inflammatory cells was observed (Fig. 8A). Specimens demonstrated a prominent thrombus and partial leukocyte infiltration towards the centre of the thrombus (Fig. 8B). The PSA wall was clearly visible and the injected collagen was observed in a network which appeared to be interconnected with the thrombus.

DISCUSSION

Collagen is well-known for its hemostatic activity, and has been widely used as a biodegradable plug to prevent hemorrhagic complications after arterial puncture, i.e. catheterisation or coronary angioplasty (34, 35). To our knowledge, only one study describes the use of collagen treatment after femoral PSA occurrence (15). Despite the reported efficacy of this study (97%), its use has not currently gained wider acceptance (21). However, the promising results of this study warrant further investigations to the use of collagen for PSA treatment.

Compared with thrombin there may be several additional values for use of collagen for (complex) PSA treatment. The first advantage may lay in its physico-chemical properties. With fibrillar type I collagen as an injectable, the consistency of the material is important. Collagen swells at low pH (36), making it possible to prepare a suspension or paste which can be injected. When the pH of the collagen suspension was increased to a physiological range (pH 7.4), the collagen fibrils formed a dense network. After applying the injectable collagen in the PSA model, fibrils aggregated and concentrated at the site of injection. Leukocytes infiltrated this collagen network, which is commonly found after applying collagenous biomaterials *in vivo* (37). The consistency and the ability to form a network may be an advantage to reduce the risk of arterial influx of collagen fibrils. In addition, complex pseudoaneurysm have been described as contra-indications for thrombin treatment (11). Several cases reported thrombin failure in these complex pseudoaneurysms (12-14). The soluble thrombin may quickly diffuse through the wide neck of the pseudoaneurysm toward the lumen of the artery. In most cases these complex pseudoaneurysms need to be revised surgically. Especially in such cases, injectable collagen can be an attractive agent, since collagen is highly viscous and collagen fibrils aggregate and deposit at the site of injection, as shown in this study. The pseudoaneurysm model used in this study involves the preparation of an arteriovenous shunt between the femoral artery and femoral vein, where ~2 cm of the vein is segmented by proximal and distal closure using ligatures. This model presents a complex pseudoaneurysm (with a relative wide opening (~4 mm) (33)) and makes the experimental model highly challenging with respect to pseudoaneurysm treatment.

A second issue may be the difference in immunogenicity between thrombin and collagen. There are several reported cases of immune complex reactions to bovine thrombin resulting in antibody formation. Although less for recombinant human thrombin (38), the antibodies may cross-react with the coagulation cascade, resulting in factor inhibition and clinical coagulopathy. 40% to 66% of patients who underwent cardiac surgery and 20% of patients who underwent neurosurgery developed bovine thrombin-associated factor V anti-bodies (39). This complication may be overcome by the use of collagen, since fibrillar bovine collagen is almost non-immunogenic.

Other advantages may relate to technical issues. The injectability of collagen is critical for its clinical performance and for patient comfort, e.g. in case of the use of collagen as a dermal filler (40). Especially for percutaneous PSA treatment, it is important that the agent

can be injected through a needle with a limited diameter. In the clinical study of Hamraoui *et al.*, a 1% (w/v) collagen suspension was injected through a relatively large 9F (\varnothing 3 mm) needle which may come with discomfort for the patient. In our suspension the collagen content was higher (4% (w/v)) and could be injected through a 2F (\varnothing 0.7 mm) needle, which is comparable with the procedure using thrombin injections (\varnothing 0.6 mm) (21). In addition, one well known technical difficulty in the use of thrombin is blood clotting inside the needle tip resulting in injection problems (41). With injectable collagen we did not observe this problem. The high consistency of the collagen may prevent the entrance of blood into the needle and subsequent clot formation.

Proper sterilisation is an important issue when using injectable collagen for medical applications. The injectable collagen must be supplied as a sterile product, but the efficacy of the collagen must not be compromised by the sterilisation technique. It has been described that techniques like gamma irradiation affect the structural properties of the collagen fibrils (42, 43). This may adversely affect the platelet aggregation and thrombus formation. For this reason, we tested different sterilisation techniques, and evaluated both biochemical and primary hemostatic characteristics. Both EtO and H₂O₂ sterilised collagen did not compromise the integrity of the collagen. We selected EtO for its tendency to have less influence on collagen-induced platelet aggregation *In vivo*, the injectable collagen suspension did induce local hemostasis within an approximate 5 min clotting time, but this was often partial. However, in one case we found that both the femoral artery and the PSA coagulated after collagen injection. Although the artery was open after 6 days, it demonstrates the existing risk of injecting hemostatic agents in femoral PSA. It has been described that a percutaneous thrombin injection in a femoral PSA, may be associated with an increased risk of thrombus extension (44). For thrombin injection, various methods are known in order to decrease this risk, e.g. directing the needle away from the PSA neck (9) or placing a balloon in the PSA neck (45). In case of high risk (complex) PSAs, these methods may also prevent the risk on distal embolisation when using injectable collagen. Particularly for the complex femoral PSA treatment, it might be attractive to combine collagen fibrils with thrombin to not only initiate the primary hemostasis, but also induce the secondary hemostasis (clotting factor mediated). Although not tested in this study, such an approach has been successful in giant splenic artery pseudoaneurysm treatment (46).

In view of our results, we conclude that an EtO sterilised, injectable 4% collagen could be prepared with defined structural characteristics and platelet activity. *In vivo*, the injectable collagen formed a dense network, which was (partially) hemostatic active. Injectable collagen may be an effective therapeutic alternative for current femoral PSA treatment, but additional studies are needed to prove its efficacy.

REFERENCES

1. M.Ates, S.Sahin, C.Konuralp, U.Gullu, S.Cimen, M.Kizilay, R.Gunay, Y.Sensoz, and M.Akcar. "Evaluation of risk factors associated with femoral pseudoaneurysms after cardiac catheterization." *J Vasc.Surg.* 43, no. 3(March 2006):520-24.
2. T.F.Kresowik, M.D.Khoury, B.V.Miller, M.D.Winniford, A.R.Shamma, W.J.Sharp, M.B.Blecha, and J.D.Corson. "A prospective study of the incidence and natural history of femoral vascular complications after percutaneous transluminal coronary angioplasty." *J Vasc.Surg.* 13, no. 2(February 1991):328-33.
3. R.Zahn, S.Thoma, E.Fromm, R.Lotter, M.Zander, K.Seidl, and J.Senges. "Pseudoaneurysm after cardiac catheterization: therapeutic interventions and their sequelae: experience in 86 patients." *Cathet.Cardiovasc.Diagn.* 40, no. 1(January 1997):9-15.
4. R.Katzenschlager, A.Ugurluoglu, A.Ahmadi, M.Hulsmann, R.Koppensteiner, E.Larch, T.Maca, E.Minar, A.Stumpflen, and H.Ehringer. "Incidence of pseudoaneurysm after diagnostic and therapeutic angiography." *Radiology* 195, no. 2(May 1995):463-66.
5. B.D.Coley, A.C.Roberts, B.D.Fellmeth, K.Valji, J.J.Bookstein, and R.J.Hye. "Postangiographic femoral artery pseudoaneurysms: further experience with US-guided compression repair." *Radiology* 194, no. 2(February 1995):307-11.
6. J.D.Ferguson and A.P.Banning. "Ultrasound guided percutaneous thrombin injection for the treatment of iatrogenic pseudoaneurysms." *Heart* 83, no. 5(May 2000):582.
7. S.S.Kang, N.Labropoulos, M.A.Mansour, and W.H.Baker. "Percutaneous ultrasound guided thrombin injection: a new method for treating postcatheterization femoral pseudoaneurysms." *J Vasc.Surg.* 27, no. 6(June 1998):1032-38.
8. J.M.Lemaire and R.F.Dondelinger. "Percutaneous coil embolization of iatrogenic femoral arteriovenous fistula or pseudo-aneurysm." *Eur.J Radiol.* 18, no. 2(May 1994):96-100.
9. C.S.Liau, F.M.Ho, M.F.Chen, and Y.T.Lee. "Treatment of iatrogenic femoral artery pseudoaneurysm with percutaneous thrombin injection." *J Vasc.Surg.* 26, no. 1(July 1997):18-23.
10. E.K.Paulson, D.H.Sheafor, M.A.Kliwer, R.C.Nelson, L.B.Eisenberg, M.W.Sebastian, and M.H.Sketch, Jr. "Treatment of iatrogenic femoral arterial pseudoaneurysms: comparison of US-guided thrombin injection with compression repair." *Radiology* 215, no. 2(May 2000):403-08.
11. M.Luedde, U.Krumsdorf, J.Zehelein, B.Ivandic, T.Dengler, H.A.Katus, and C.Tiefenbacher. "Treatment of iatrogenic femoral pseudoaneurysm by ultrasound-guided compression therapy and thrombin injection." *Angiology* 58, no. 4(August 2007):435-39.
12. J.M.Hanson, M.Atri, and N.Power. "Ultrasound-guided thrombin injection of iatrogenic groin pseudoaneurysm: Doppler features and technical tips." *Br.J.Radiol.* 81, no. 962(February 2008):154-63.
13. A.Kuzuya, K.Fujimoto, S.Iyomasa, and M.Matsuda. "Transluminal coil embolization of an inferior gluteal artery aneurysm by ultrasound-guided direct puncture of the target vessel." *Eur.J.Vasc.Endovasc.Surg.* 30, no. 2(August 2005):130-32.
14. P.L.La Perna, J.W.Olin, D.Goines, M.B.Childs, and K.Ouriel. "Ultrasound-guided thrombin injection for the treatment of postcatheterization pseudoaneurysms." *Circulation* 102, no. 19(November 2000):2391-95.
15. K.Hamraoui, S.M.Ernst, P.F.van Dessel, J.C.Kelder, J.M.ten Berg, M.J.Suttorp, W.Jaarsma, and T.H.Plokker. "Efficacy and safety of percutaneous treatment of iatrogenic femoral artery pseudoaneurysm by biodegradable collagen injection." *Journal of the American College of Cardiology* 39, no. 8(April 2002):1297-304.
16. K.Takaoka, M.Kozuka, and H.Nakahara. "Telo peptide-depleted bovine skin collagen as a carrier for bone morphogenetic protein." *J Orthop.Res.* 9, no. 6(November 1991):902-07.
17. Z.Wachol-Drewek, M.Pfeiffer, and E.Scholl. "Comparative investigation of drug delivery of collagen implants saturated in antibiotic solutions and a sponge containing gentamicin." *Biomaterials* 17, no. 17(September 1996):1733-38.
18. W.F.Daamen, S.T.Nillesen, T.Hafmans, J.H.Veerkamp, M.J.van Luyn, and T.H.van Kuppevelt. "Tissue response of defined collagen-elastin scaffolds in young and adult rats with special attention to calcification." *Biomaterials* 26, no. 1(January 2005):81-92.

19. P.J.Geutjes, W.F.Daamen, P.Buma, W.F.Feitz, K.A.Faraj, and T.H.van Kuppevelt. "From molecules to matrix: construction and evaluation of molecularly-defined bioscaffolds." *Adv.Exp.Med.Biol* 585,(2006):279-95.
20. J.S.Pieper, P.B.van Wachem, M.J.A.van Luyn, L.A.Brouwer, T.Hafmans, J.H.Veerkamp, and T.H.van Kuppevelt. "Attachment of glycosaminoglycans to collagenous matrices modulates the tissue response in rats." *Biomaterials* 21, no. 16(August 2000):1689-99.
21. F.Ahmad, S.A.Turner, P.Torrie, and M.Gibson. "Iatrogenic femoral artery pseudoaneurysms--a review of current methods of diagnosis and treatment." *Clin.Radiol.* 63, no. 12(December 2008):1310-16.
22. I.W.Browder and M.S.Litwin. "Use of absorbable collagen for hemostasis in general surgical patients." *Am Surg.* 52, no. 9(September 1986):492-94.
23. B.E.Evans, S.P.Irving, and L.M.Aledort. "Use of microcrystalline collagen for hemostasis after oral surgery in a hemophilic." *J Oral Surg.* 37, no. 2(February 1979):126-28.
24. J.S.Gibbs, A.K.Slade, J.Blake, J.E.Nordrehaug, A.F.Rickards, N.P.Buller, and U.Sigwart. "Femoral arterial hemostasis using a collagen plug after coronary artery stent implantation." *J Interv.Cardiol* 5, no. 2(June 1992):85-88.
25. J.G.Webb, R.A.Carere, and A.A.Dodek. "Collagen plug hemostatic closure of femoral arterial puncture sites following implantation of intracoronary stents." *Cathet.Cardiovasc.Diagn.* 30, no. 4(December 1993):314-16.
26. L.F.Brass and H.B.Bensusan. "The role of collagen quaternary structure in the platelet: collagen interaction." *J Clin.Invest* 54, no. 6(December 1974):1480-87.
27. N.N.Tandon, U.Kralisz, and G.A.Jamieson. "Identification of glycoprotein IV (CD36) as a primary receptor for platelet-collagen adhesion." *J Biol Chem.* 264, no. 13(May 1989):7576-83.
28. J.S.Pieper, A.Oosterhof, P.J.Dijkstra, J.H.Veerkamp, and T.H.van Kuppevelt. "Preparation and characterization of porous crosslinked collagenous matrices containing bioavailable chondroitin sulphate." *Biomaterials* 20, no. 9(May 1999):847-58.
29. U.K.Laemmli. "Cleavage of structural proteins during the assembly of the head of bacteriophage T4." *Nature* 227, no. 5259(August 1970):680-85.
30. B.B.Lieber, A.K.Wakhloo, R.Siekmann, and M.J.Gounis. "Acute and chronic swine rete arteriovenous malformation models: effect of ethiodol and glacial acetic acid on penetration, dispersion, and injection force of N-butyl 2-cyanoacrylate." *AJNR Am J Neuroradiol.* 26, no. 7(August 2005):1707-14.
31. B.Savage, M.H.Ginsberg, and Z.M.Ruggeri. "Influence of fibrillar collagen structure on the mechanisms of platelet thrombus formation under flow." *Blood* 94, no. 8(October 1999):2704-15.
32. W.D.Zwierzina and F.Kunz. "A method of testing platelet aggregation in native whole blood." *Thromb.Res.* 38, no. 1(April 1985):91-100.
33. P.J.Geutjes, J.A.van der Vliet, V, K.A.Faraj, N.de Vries, H.T.van Moerkerk, R.G.Wismans, T.Hendriks, W.F.Daamen, and T.H.van Kuppevelt. "An animal model for femoral artery pseudoaneurysms." *J.Vasc.Interv.Radiol.*(April 2010).
34. J.M.Pachence. "Collagen-based devices for soft tissue repair." *J Biomed.Mater.Res.* 33, no. 1(1996):35-40.
35. M.Koreny, E.Riedmuller, M.Nikfardjam, P.Siostrzonek, and M.Mullner. "Arterial puncture closing devices compared with standard manual compression after cardiac catheterization: systematic review and meta-analysis." *JAMA* 291, no. 3(January 2004):350-57.
36. R.H.Marriott. "The swelling of single collagen fibre-bundles." *Biochem.J* 26, no. 1(1932):46-53.
37. M.Lenartova and T.Tak. "Iatrogenic pseudoaneurysm of femoral artery: case report and literature review." *Clin.Med.Res.* 1, no. 3(July 2003):243-47.
38. F.A.Weaver, W.Lew, K.Granke, L.Yonehiro, B.Delange, and W.A.Alexander. "A comparison of recombinant thrombin to bovine thrombin as a hemostatic ancillary in patients undergoing peripheral arterial bypass and arteriovenous graft procedures." *J.Vasc.Surg.* 47, no. 6(June 2008):1266-73.
39. M.B.Streiff and P.M.Ness. "Acquired FV inhibitors: a needless iatrogenic complication of bovine thrombin exposure." *Transfusion* 42, no. 1(January 2002):18-26.

40. J.Rosenblatt, B.Devereux, and D.G.Wallace. "Effect of electrostatic forces on the dynamic rheological properties of injectable collagen biomaterials." *Biomaterials* 13, no. 12(1992):878-86.
41. B.S.Taylor, R.Y.Rhee, S.Muluk, J.Trachtenberg, D.Walters, D.L.Steed, and M.S.Makaroun. "Thrombin injection versus compression of femoral artery pseudoaneurysms." *J.Vasc.Surg.* 30, no. 6(December 1999):1052-59.
42. M.Tzaphlidou, E.Kounadi, I.Leontiou, D.P.Matthopoulos, and D.Glaros. "Influence of low doses of gamma-irradiation on mouse skin collagen fibrils." *Int.J Radiat.Biol* 71, no. 1(January 1997):109-15.
43. M.Grimes, J.T.Pembroke, and T.McGloughlin. "The effect of choice of sterilisation method on the biocompatibility and biodegradability of SIS (small intestinal submucosa)." *Bio-med.Mater.Eng* 15, no. 1-2(2005):65-71.
44. M.J.Hughes, J.M.McCall, D.M.Nott, and S.P.Padley. "Treatment of iatrogenic femoral artery pseudoaneurysms using ultrasound-guided injection of thrombin." *Clin.Radiol.* 55, no. 10(October 2000):749-51.
45. H.W.Loose and P.J.Haslam. "The management of peripheral arterial aneurysms using percutaneous injection of fibrin adhesive." *Br.J Radiol.* 71, no. 852(December 1998):1255-59.
46. I.H.Huang, D.A.Zuckerman, and J.B.Matthews. "Occlusion of a giant splenic artery pseudoaneurysm with percutaneous thrombin-collagen injection." *J.Vasc.Surg.* 40, no. 3(September 2004):574-77.

Chapter 6

PREPARATION OF DIFFERENTLY SIZED INJECTABLE COLLAGEN MICRO-SCAFFOLDS

Paul J. Geutjes¹
Kaeuis A. Faraj^{1,2}
Willeke F. Daamen¹
Toin H. van Kuppevelt¹

¹Radboud University Nijmegen Medical Centre, Department of
¹Biochemistry (280), P.O. Box 9101, 6525 GA Nijmegen, The Netherlands and ²Aap
bio implants - EMCM BV, Middenkampweg 17, 6645 CH Nijmegen, The Netherlands

Journal of Tissue Engineering and Regenerative Medicine. In press

ABSTRACT

Collagen scaffolds have been widely used as biomaterials for tissue engineering. In general, application of scaffolds requires surgery. In this study, we describe a new and simple technique to prepare porous micro-scaffolds from type I collagen fibrils which can be injected, thus preventing surgery. The size of the micro-scaffolds could be easily controlled using sieves with varying cut offs. EDC/NHS crosslinking was essential to stabilise the collagen micro-scaffolds. Micro-scaffolds were highly porous and could be injected through small diameter needles (18-21 Gauge). Collagen micro-scaffolds may be used as injectables for the local delivery of effector molecules and/or cells, thus creating specific niches to enhance local tissue regeneration.

INTRODUCTION

A wide range of collagen-based biomaterials have been used for tissue engineering applications. (1-4). Collagen is often applied because of its biodegradability and biocompatibility, in addition to its good mechanical characteristics. Implantation of collagen scaffolds generally comes with surgery and introduces some risk of complications (e.g. infection, tissue damage). The availability of stable injectable scaffolds would facilitate (local) tissue regeneration without the need for surgery. Injectable porous micro-scaffolds may be attractive delivery vehicles for cells and effector molecules, which will further increase the applicability of collagen.

Injectable collagen particles have been developed for drug delivery (5, 6), or as thrombotic agents (7-9) combined with antibiotics delivery (10). However, highly porous micro-scaffolds prepared from native collagen fibrils for tissue engineering have not been reported. In this study, we introduce a straightforward technique to prepare stable collagen micro-scaffolds of different sizes, with good injectability, and discuss the possible applications within the field of tissue engineering. The outline of the procedure is given in Table 1.

Table 1 Outline of the procedure to prepare injectable type I collagen micro-scaffolds.

Step	Preparation of type I collagen micro-scaffolds
1	Swelling of purified collagen fibrils in diluted acetic acid
2	Deaeration by centrifugation
3	Homogenisation using Potter-Elvehjem with intervening space of 0.35 mm
4	Freezing at -80°C
5	Pulverisation using a cutting mill with defined sieve inserts (e.g. 0.5, 1.0 or 2.0 mm meshes)
6	Freeze drying
7	EDC/NHS crosslinking under stirring conditions
8	Freezing in liquid nitrogen and freeze drying

MATERIALS & METHODS

Fibrillar type I collagen was isolated from 6 months old bovine achilles tendon using a series of NaCl, acetic acid, urea and acetone extractions (11). After purification, type I collagen suspensions were prepared in 0.25 M acetic acid (0.8% w/v) and shaken for 16 h at 4°C. The suspension was homogenised on ice using a Potter-Elvehjem homogeniser with a intervening space of 0.35 mm (20 strokes). Air bubbles were removed by centrifugation at 525 g for 10 min at 4°C. The suspension was poured into 50 ml tubes and frozen at -80°C for 16 h. To prepare micro-scaffolds with different sizes, frozen collagen suspensions were pulverised under liquid nitrogen conditions using a Pulverisette 19 cutting mill with three different sieve inserts (0.5, 1.0 or 2.0 mm meshes) (Fritsch, Idar-Oberstein, Germany). Pulverised material was subsequently lyophilised in a Zirbus lyophiliser (Sublimator 500 II, Bad Grund, Germany). Freeze-dried collagen was crosslinked by means of N-ethyl-3-(3-dimethylaminopropyl)-carbodiimide (EDC, Fluka Chemical, AG Buchs, Switzerland) and N-hydroxysuccinimide (NHS, Fluka Chemical, AG Buchs, Switzerland). Briefly, 250 mg collagen was pre-incubated in 100 ml 50 mM 2-morpholinoethane sulfonic acid (MES) pH 5.0 containing 40% (v/v) ethanol in MilliQ water for 30 min at 4°C. Then, collagen was crosslinked for 4 h at 21°C under stirring conditions (magnetic stirrer) by adding 100 ml EDC/NHS (final concentrations 33 mM/6 mM, respectively) in MES buffer (11). Crosslinking was stopped by adding 200 ml 0.1 M Na₂HPO₄ and incubation for 1 h at 21°C under stirring conditions (2 times). The crosslinked collagen

was washed with 1 M NaCl (2 times 1 h), 2 M NaCl (5 times 30 min) and MilliQ water (6 times 30 min), using centrifugation (1750 g, 20 min, 21°C) after each step to recover the micro-scaffolds. Crosslinked collagen micro-scaffolds were frozen in liquid nitrogen and lyophilised.

The collagen micro-scaffolds were evaluated using conventional light microscopy (LM) and scanning electron microscopy (SEM). For LM analysis, the micro-scaffolds were resuspended in MilliQ water and analysed using a DM IL Leica microscope (Leica Microsystems, Wetzlar, Germany). For SEM analysis, dried micro-scaffold were mounted on stubs, sputtered with an ultrathin layer of gold in a Polaron E5100 Coating System, and studied with a JEOL JSM-6310 SEM (JEOL Ltd, Tokyo, Japan) apparatus at an accelerating voltage of 15 kV.

Injectables were prepared by resuspending 0.5% (w/v) micro-scaffolds in MilliQ water. The injectability was tested by injecting 1 ml suspension through 18-21 Gauge sized needles (BD Microlance™ 3, BD, Drogheda, Ireland).

RESULTS

Figure 1 shows the morphology of crosslinked collagen micro-scaffolds with three different sizes. Only the crosslinked samples resulted in micro-scaffolds with an intact network (Fig. 1A2). Without crosslinking, micro-scaffolds partly fell apart resulting in small collagen structures (Fig. 1A1). Both LM and SEM analysis revealed that the collagen micro-scaffolds were highly porous (Fig. 1B). The structures contained lattice-like lamellae mostly orientated parallel or perpendicular to the surface. The mean scaffold size of the 0.5 mm, 1.0 mm or 2.0 mm sieved materials was $263 \pm 78 \mu\text{m}$, $396 \pm 115 \mu\text{m}$, and $988 \pm 364 \mu\text{m}$ ($n=50$) respectively. From all micro-scaffolds, injectables (0.5% w/v) in MilliQ water could be prepared (Fig. 2). The smallest needles through which the scaffolds could be injected were 21, 19 and 18 Gauge needles (diameter 0.7, 0.9 and 1.0 mm) for 0.5, 1.0 and 2.0 mm micro-scaffolds, respectively.

DISCUSSION

Crosslinking has frequently been used to stabilise collagen network and/or to prevent rapid degradation *in vivo* (3). Using crosslinking, it is also possible to covalently attached heparin (and glycosaminoglycans in general) to the collagen, making it possible to create a niche of (heparin-binding) effector molecules (e.g. growth factors) in order to recruit (progenitor) cells from surrounding tissue, blood or bone marrow. Collagen scaffolds loaded with growth factors (i.e. FGF-2 and VEGF) have been used to create specific environments, initiating processes such as angiogenesis and tissue remodelling (12). Micro-scaffolds combined with angiogenic factors, may be helpful to induce local neovascularisation in ischemic tissues (e.g. in skeletal muscle or skin damaged by trauma or infection, or in myocardium that has been affected by infarction). The pore size of the collagen micro-scaffolds was comparable to those described for large collagen scaffolds (50-100 μm) (13). Particular the $\sim 100 \mu\text{m}$ pores favour cell attachment on collagen-glycosaminoglycan scaffolds (14). Next to this, it is likely that more cells may attach to the micro-scaffolds, since the surface area is larger. In this perspective the micro-scaffolds may function as carriers to deliver cells with a desired phenotype to the site of the defect to create specific cell niches, for example to deliver cells producing insulin in case of diabetes, or local administration of chondrocytes for topical cartilage repair in case of cartilage destruction.

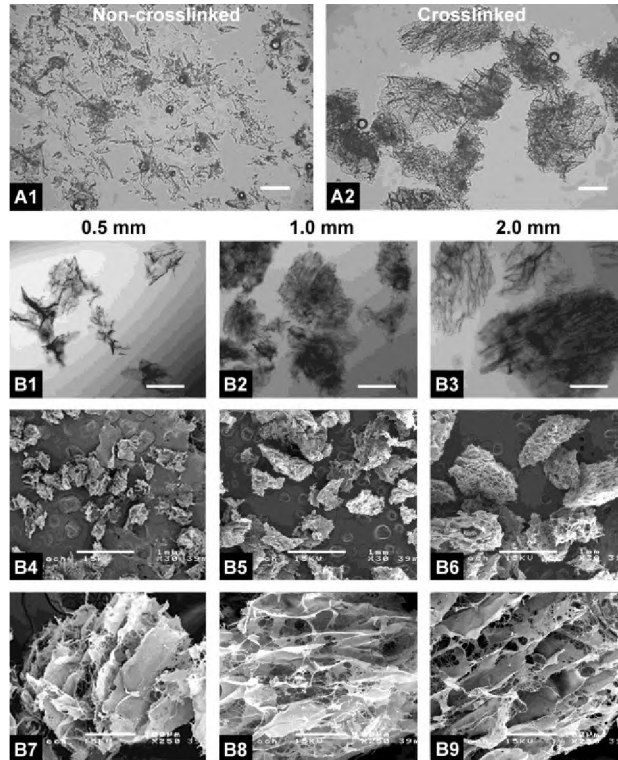


Fig. 1 Morphology of micro-scaffolds. A) Necessity of crosslinking of the micro-scaffolds (0.5 mm); A1 non-crosslinked and A2 crosslinked micro-scaffolds. B1-3) Light microscopical images of crosslinked micro-scaffolds suspended in MilliQ water. B4-9) Scanning electron microscopical images of dried collagen micro-scaffolds. Micro-scaffolds were prepared using a chopping device with different sieves with cut off values of 0.5 mm (B1, B4, B7), 1.0 mm (B2, B5, B8) or 2.0 mm (B3, B6, B9). In A1 and A2 bars represent 100 μ m. In B1-3 bars represent 250 μ m, in B4-6 1 mm, and in B7-9 100 μ m.

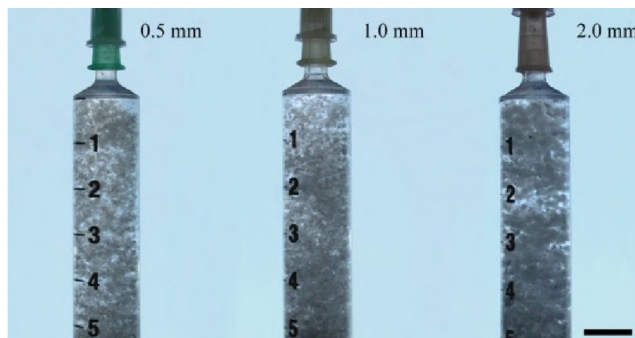


Fig. 2 Macroscopic image of 5 ml syringes filled with differently sized resuspended micro-scaffolds. Injectables were prepared by resuspending 0.5% (w/v) crosslinked type I collagen micro-scaffolds after chopping and sieving (0.5 mm, 1.0 mm or 2.0 mm fractions) in MilliQ water. Bar represents 1 cm.

Micro-scaffolds with BMPs may be useful to initiate local osteoinductivity (e.g. in fractured bone or for fusion of lumbar spines), thus facilitating bone formation. In addition, micro-scaffolds may act as a bulking agent to treat urinary stress incontinence. In summary, a straightforward technique has been developed to prepare injectable collagenous micro-scaffolds, which may be useful for localised tissue regeneration without the need for surgery.

REFERENCES

1. J.P.Foran, D.Patel, J.Brookes, and R.J.Wainwright. "Early mobilisation after percutaneous cardiac catheterisation using collagen plug (VasoSeal) haemostasis." *Br.Heart J* 69, no. 5(May 1993):424-29.
2. P.K.Sehgal and A.Srinivasan. "Collagen-coated microparticles in drug delivery." *Expert.Opin.Drug Deliv.* 6, no. 7(July 2009):687-95.
3. P.B.van Wachem, M.J.van Luyn, L.H.Olde Damink, P.J.Dijkstra, J.Feijen, and P.Nieuwenhuis. "Biocompatibility and tissue regenerating capacity of crosslinked dermal sheep collagen." *J Biomed.Mater.Res.* 28, no. 3(March 1994):353-63.
4. E.K.Yang, Y.K.Seo, H.H.Youn, D.H.Lee, S.N.Park, and J.K.Park. "Tissue engineered artificial skin composed of dermis and epidermis." *Artif.Organs* 24, no. 1(January 2000):7-17.
5. A.Berthold, K.Cremer, and J.Kreuter. "Collagen microparticles: carriers for glucocorticosteroids." *Eur.J Pharm.Biopharm.* 45, no. 1(January 1998):23-29.
6. M.Schlapp and W.Friess. "Collagen/PLGA microparticle composites for local controlled delivery of gentamicin." *J Pharm.Sci.* 92, no. 11(November 2003):2145-51.
7. W.S.Bartynski, G.V.O'Reilly, and M.D.Forrest. "High-flow-rate arteriovenous malformation model for simulated therapeutic embolization." *Radiology* 167, no. 2(May 1988):419-21.
8. H.Dumas, M.Tardy, M.H.Rochat, and J.L.Tayot. "Prilling process applied to collagen solutions." *Drug Development and Industrial Pharmacy* 18, no. 13(January 1992):1395-409.
9. F.Turjman, T.F.Massoud, H.V.Vinters, C.Ji, M.Tardy, G.Guglielmi, and F.Vinuela. "Collagen microbeads: experimental evaluation of an embolic agent in the rete mirabile of the swine." *AJNR Am J Neuroradiol.* 16, no. 5(May 1995):1031-36.
10. M.Sternlicht, S.F.Sales, J.R.Daniels, and A.Daniels. "Renal cisplatin chemoembolization with Angiostat, Gelfoam, and Ethiodol in the rabbit: renal platinum distributions." *Radiology* 170, no. 3 Pt 2(March 1989):1073-75.
11. J.S.Pieper, A.Oosterhof, P.J.Dijkstra, J.H.Veerkamp, and T.H.van Kuppevelt. "Preparation and characterization of porous crosslinked collagenous matrices containing bioavailable chondroitin sulphate." *Biomaterials* 20, no. 9(May 1999):847-58.
12. S.T.Nillesen, P.J.Geutjes, R.G.Wismans, J.Schalkwijk, W.F.Daamen, and T.H.van Kuppevelt. "Increased angiogenesis and blood vessel maturation in acellular collagen-heparin scaffolds containing both FGF2 and VEGF." *Biomaterials* 28, no. 6(February 2007):1123-31.
13. K.A.Faraj, T.H.van Kuppevelt, and W.F.Daamen. "Construction of collagen scaffolds that mimic the three-dimensional architecture of specific tissues." *Tissue Eng* 13, no. 10(October 2007):2387-94.
14. F.J.O'Brien, B.A.Harley, I.V.Yannas, and L.J.Gibson. "The effect of pore size on cell adhesion in collagen-GAG scaffolds." *Biomaterials* 26, no. 4(February 2005):433-41.

Chapter 7

“LYOPHILISOMES”: A NEW TYPE OF (BIO)CAPSULE

Paul J. Geutjes^{*1}
Willeke F. Daamen^{*1}
Herman T. van Moerkerk¹
Suzan T. Nillesen¹
Ronnie G. Wismans¹
Theo H. Hafmans^{1,2}
Bert L.P.W.J. van den Heuvel³
Arthur M.A. Pistorius⁴
Jacques H. Veerkamp¹
Jan C.M. van Hest⁵
Toin H. van Kuppevelt¹

^{1,2,3,4}Radboud University Nijmegen Medical Centre, Departments of
¹Biochemistry (280), ²Pulmonary Diseases (454), ³Paediatrics (656) and
⁴Biochemistry (286), P.O. Box 9101, 6525 GA Nijmegen, The Netherlands and
⁵Radboud University Nijmegen, Faculty of Sciences, ⁵Department of Organic
Chemistry, P.O. Box 9010, 6500 GL Nijmegen, The Netherlands

*These authors contributed equally to this work.

Advanced Materials 2007;19(5):673-77

INTRODUCTION

A number of techniques have been explored to prepare hollow structures (capsules) for biomedical applications. Liposomes (self-assembled vesicles composed of (phospho)lipids) represent the arch type of biological capsules (1) and are used *in vivo* in cancer therapy and systemic fungal infections. They are usually modified, e.g. by PEGylation, to avoid recognition as foreign bodies by the immune system (2). Another class of capsules, the polymersomes, (3) is based on synthetic monomers including man-made peptide/protein units such as poly-Lys backbones grafted with methoxypolyethylene glycol (4). The formation of both liposomes and polymersomes is largely driven by the amphiphilic nature of the compounds (5). Other methods for capsule formation that do not rely on amphiphilicity exist, e.g. vesicle templating, (6, 7) polyelectrolyte layer-by-layer assembly (8) and colloidosome fabrication (9, 10). Due to the procedures employed, synthetic rather than biological building blocks are used. For biomedical applications it would be advantageous if capsules could be prepared from the vast repertoire of (large) natural macromolecules, preferably without the need for amphiphilicity. One such example encompasses hollow microcapsules prepared by cavitation methods, e.g. spray-drying of aqueous albumin solutions (11). Capsules thus prepared are applied as contrast agents, but due to the high temperatures employed the biological activity of the proteins is likely diminished. Another example encompasses microcapsules prepared by the complex coacervation method (12) and interfacial polymerisation (13).

In this study, we present a general strategy to prepare biocapsules at low temperatures from a range of (large) biomolecules. The method is physical rather than chemical in nature, and amphiphilicity of the biomolecule is not essential. It is a general methodology that enables the preparation of a novel class of nano- to microscale capsules ("lyophilisomes") using a combined freezing, annealing and lyophilisation procedure. Model studies were performed using a solubilised form of elastin, an extracellular matrix protein that can easily be obtained in bulk quantities, and that shows autofluorescence which enables straightforward detection. The average molecular mass of the elastin preparation was about 1.1 MDa (for further characteristics of the elastin preparation, see Experimental). In a typical experiment, a solution of 2.0% elastin in 0.25 M acetic acid in water was fast frozen in liquid nitrogen (-196°C), incubated at -10 to -20°C for 3 h (annealing step), and lyophilised (for lyophiliser settings, see Fig. 1A). Such a freezing-annealing-lyophilisation regime resulted in globular structures ranging from 200 nm - 10 µm as revealed by scanning electron microscopy (SEM) (Fig. 1B). Further analysis by transmission electron microscopy using stabilised (vapour-crosslinked) preparations (see Experimental) revealed the capsule nature of these spheres (Fig. 1C). The walls of the capsules were smooth and the protein was distributed equally over the wall. The width of the wall was about 50-500 nm, depending on the size of the capsule. Using fluorescence-activated cell sorting, capsules could be separated according to size (Fig. 1D). Capsules could be prepared from a variety of macromolecules, including serum albumin (67 kDa) as an example of a spherical protein, type I collagen (280 kDa) as an example of a rod-like protein, and heparin (15 kDa) as an example of a highly negatively charged polysaccharide (Fig. 1E). This indicates that amphiphilicity is not required, in contrast to liposomes and polymersomes.

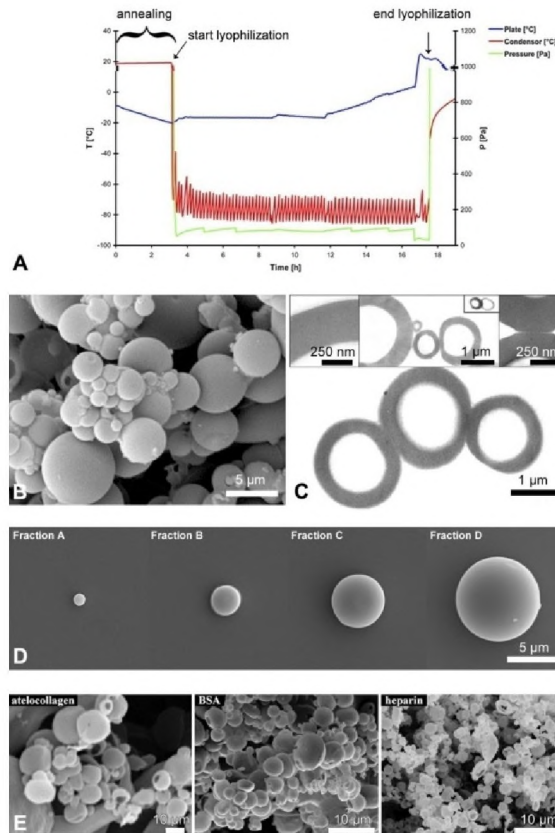


Fig. 1 Preparation and morphology of capsules. Elastin capsules were obtained by fast freezing of 2.0% elastin in 0.25 M acetic acid using liquid nitrogen (-196°C), followed by annealing at -10 to -20°C and lyophilisation. A) representative run of the standard lyophiliser program used for the preparation of elastin capsules. The sample is in contact with the plate. Please note that the pressure sensor can only accurately measure pressures below 1000 Pa. B) scanning electron micrograph (SEM), and C) transmission electron micrograph (TEM) of elastin capsules. Capsules displayed a smooth and round morphology. The left insert indicates the homogenous distribution of elastin throughout the capsule wall, the middle insert shows nanocapsules, and the right insert indicates plasticity of capsules as suggested when capsules are in contact with each other. D) SEM micrographs of capsules sorted according to size (A-D) using fluorescence-activated cell sorting. e, SEM micrographs of capsules prepared from 0.25% collagen (a rod-like protein), 0.25% bovine serum albumin (a globular protein), and 1.0% heparin (a highly negatively charged polysaccharide).

Fluorescent-labelled probes were applied to study if (macro)molecules could be incorporated in, and subsequently released from, the lumen and/or wall of the capsules (see Fig. 2A-C for fluorescent labelled dextrans). For the incorporation into the wall only, probes were added to the initial solution, prior to freezing. After capsule formation, probes were homogeneously incorporated into the wall with the lumen staying empty (Fig. 2A). To load the lumen of the capsule, probes were applied to pre-formed, vapour-crosslinked capsules (see Experimental), resulting in their presence in the lumen (Fig. 2A). After loading of the

lumen, the wall -which hardly contained the probe- could be sealed by further shell crosslinking. Hence it was possible to differentially incorporate substances into either the capsule wall and/or the capsule lumen. Likewise, we could incorporate antibodies in the wall and dextrans in the lumen, and (hydrophilic) dextrans in the wall and lipophilic DiOC18 molecules in the lumen. Incorporated probes could be released from the stabilised elastin capsules by digestion with the enzyme elastase (Fig. 2B, SEM and Fig. 2C, time resolved confocal laser scanning microscopy). Without elastase, no detectable release was observed for at least two weeks. To further explore if the biological activity of the biomolecules was preserved and not to a major extent affected by the used crosslinking methodology, see Experimental), enzymes were incorporated in the capsule wall and in the lumen. In one example, peroxidase-labeled IgG was incorporated in the wall and alkaline phosphatase-labelled IgG was positioned in the lumen. Both enzymes remained bioactive as shown by the conversion of chromogenic substrates into coloured reaction products (Fig. 2D, light microscopy).

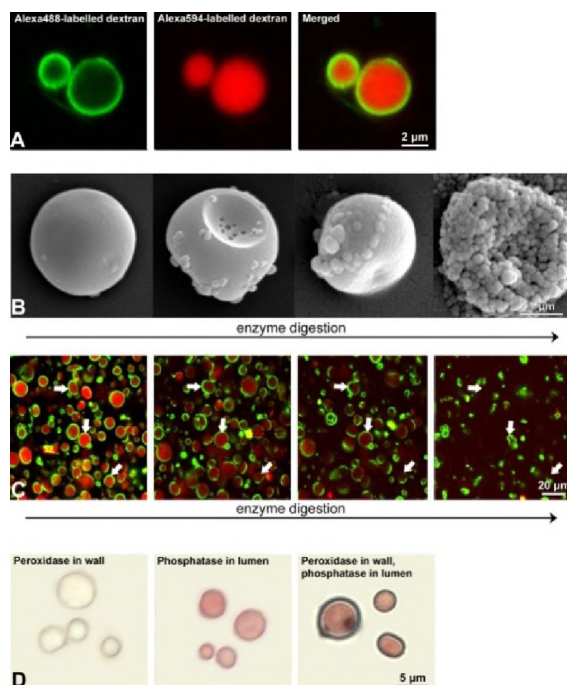


Fig. 2 Differential incorporation and release of compounds. A) a 10 kDa dextran probe labelled with Alexa Fluor488 (green) was specifically incorporated into the capsule wall followed by 24 h of vapour crosslinking, whereas a similar probe labelled with Alexa Fluor594 (red) was directed to the capsule lumen followed by 2 h of wet crosslinking (confocal laser scanning microscopy). B) upon degradation by 0.4 U/ml elastase, elastin capsules were perforated, and reassembled into nanospheres (scanning electron microscopy). C) treatment with 0.4 U/ml elastase released the (red) probe from the lumen, whereas the (green) probe was partially withheld in the wall. Arrows indicate capsules releasing their content in time (time resolved confocal laser scanning microscopy). D) peroxidase-labeled IgG was incorporated into the capsule wall followed by 24 h of vapour crosslinking, whereas alkaline phosphatase-labelled IgG was positioned in the capsule followed by 2 h of wet crosslinking.

To study the mechanism of capsule formation, we used fluorescence and freeze microscopy (Fig. 3, see also Fig. 4 for cartoon). Fast freezing in liquid N₂ induced a micro-phase separation between the bulk of the water (ice crystals) and an elastin/acetic acid/water compartment, typical for bi/ternary eutectic phase systems (14). The elastin was present in thin sheet-like structures (Fig. 3A; elastin detected on base of its autofluorescence). When the temperature of the frozen sample was increased to -10/-20°C and kept at that temperature for a period of time (annealing, Fig. 1A), macromolecular motion occurred and the sheets reassembled into spheres (Fig. 3B; the Supplementary Material shows a movie of this rearrangement).

This process is likely driven by globular structures being energetically more favourable than thin sheets (less surface interface). For the transition of spheres into capsules we propose that during lyophilisation a 3-dimensional analogy of the "coffee stain" mechanism occurs (Fig. 4A) (15). The coffee-stain mechanism explains the formation of solid, ring-like stains from solution droplets by capillary flow introduced by the larger evaporation of the solvent at the edge of the droplet compared to its interior. The solute is deposited as a solid ring providing that the contact line at the perimeter of the solution with the solid substrate is pinned. In our study, the lyophilisation process takes place at -20°C, which is above the eutectic point of an acetic acid in water mixture (-27°C) (14). At -20°C, most of the water is frozen (ice crystals), but the biomolecule/acetic acid/water compartment ("the melt") is present as a viscous fluid. In the proposed 3D analogy, the perimeter of the biomolecule-containing "melt" will be pinned, because it will freeze as a consequence of the subtraction of heat due to the sublimation of the bulk of ice crystals facing the "melt". Upon lyophilisation the biomolecules in the centre of the "melt" will be forced to the outer edge of the sphere where lyophilisation takes place. When all material (ice and acetic acid) is lyophilised, biomolecule capsules remain. This technology will most likely be generally applicable to both biological and synthetic polymers. Although this mechanism is hypothetical, some morphological observations are indicative for the 3D coffee stain theory. For example, capsules were observed with uneven wall thickness (probably due to unequal sublimation), resembling coffee stains with uneven wall thickness due to unequal evaporation (Fig. 4A) (16). Also, capsules were observed with a layered appearance of the capsule wall, indicative for wall formation by apposition growth, which also occurs in coffee stains that evaporate unevenly (data not shown).

The biocapsules may show great biomedical potential, firstly because of their ability to encapsulate both hydrophilic and lipophilic compounds, and secondly because the capsules can be prepared in large quantities from biological molecules that are biocompatible and biodegradable and which remain bioactive. Although not tested, scaling up the capsule production may be rather simple since the methodology works equally well when 1 ml volumes are applied. Additionally, by developing a 'droplet machine', many droplets can be fast frozen in liquid nitrogen and capsules can be prepared at high quantities. With the possibility to incorporate different biomolecules into the capsule wall and the capsule lumen, a two-way system may be prepared (Fig. 4B). This offers the construction of "smart" capsules, for instance those containing pre-active biomolecules (pro-drugs) in the lumen, offering a slow-release depot for e.g. therapeutics. Since capsules can be easily prepared in large quantities, applications in e.g. tissue engineering are also possible.

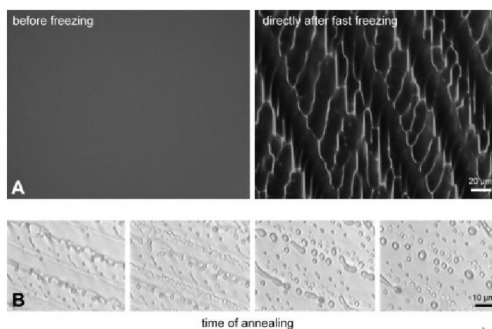


Fig. 3 Formation of elastin sheets and spheres by fast freezing and annealing evaluated by microscopical analysis. A) fast freezing. When a 2.0% elastin solution in 0.25 M acetic acid (left panel) was fast frozen in liquid nitrogen (right panel), it became organised in the form of sheets (fluorescence microscopy based on elastin's autofluorescence). B) annealing. When the frozen elastin preparation was incubated for 20 min at -40 to -18°C (i.e. above the eutectic point of acetic acid in water), spheres became apparent. In this specific example, frames were taken starting at -40°C ($t=0$ min, 1st frame), -29°C ($t=5$ min, 2nd frame), -22°C ($t=11$ min, 3rd frame) and -18°C ($t=20$ min, 4th frame).

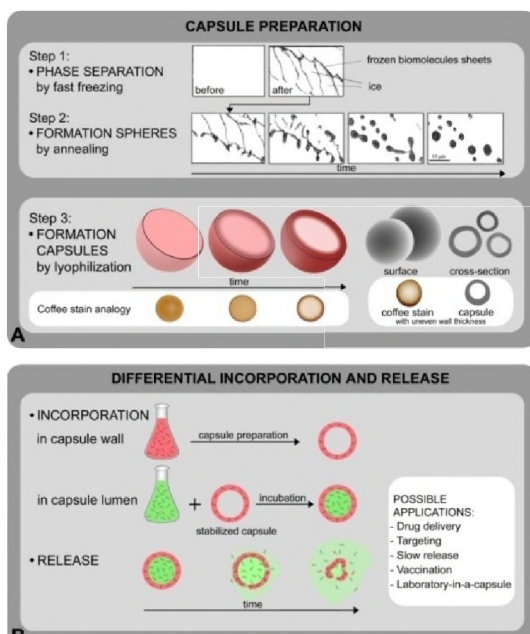


Fig. 4 Cartoon of proposed capsule formation and application. A) capsule formation. Capsule formation comprises a three-step procedure (freezing – annealing – lyophilisation). Fast freezing of biomolecules in solution (left upper panel) results in phase separation between water (the main solvent) and biomolecules which become organised into sheets (right upper panel). Annealing rearranges the sheets into spheres and lyophilisation transforms spheres into capsules, most likely due to a 3D analogy of the coffee stain mechanism (see text for further information). B) differential incorporation and release. Molecules (◡) are selectively incorporated in the capsule wall by adding them to the initial solution from which the capsules are made of. Molecules (◡) are incorporated in the capsule lumen by incubation with vapour-crosslinked capsules. The wall can optionally be sealed by crosslinking. Release can be triggered e.g. by digestion of the capsule with an appropriate enzyme.

In conclusion, we here present the preparation of a new class of capsules, dubbed "lyophilisomes". The preparation of these nano/microcapsules comprises three phases: micro-phase separation by fast freezing, structural rearrangement by annealing and the creation of a lumen by lyophilisation according to a 3D analogy of the coffee stain principle (Fig. 4A). Amphiphilicity does not seem to be required, thus expanding the type of molecules that can be used, including large biomolecules as we show here. Elastin was used as a model system, but the methodology works equally well with other bio(macro)molecules. The nature of the methodology offers flexibility since all three phases observed in capsule preparation can be influenced. Using this cheap and simple technology, a large range of new (bioactive) capsules may be anticipated.

EXPERIMENTAL

Preparation and characterisation of elastin

Insoluble elastin was isolated from equine ligamentum nuchae and solubilised by oxalic acid hydrolysis (17, 18). The solubilised elastin preparation was analysed by gel electrophoresis (SDS-PAGE, 4% gel, silver staining), and gel filtration chromatography [Sephacryl S-500 column material and the reference samples ferritin (0.88 MDa), dextran blue (2 MDa), and *Helix pomatia* haemocyanin (9 MDa)]. The average molecular mass of solubilised elastin was about 1,100 kDa. 2D gel electrophoresis showed that the solubilised elastin had an isoelectric point of around 6. Amino acid composition of insoluble elastin and solubilised elastin was similar for all amino acid residues, including desmosine and isodesmosine (both 0.5 ± 0.0 per 1000 amino acid residues) (19).

Preparation of capsules

The standard procedure for the preparation of capsules was to drop 20 μ l of a 2.0% (w/v) elastin in 0.25 M acetic acid solution in liquid nitrogen, incubate the frozen droplets at -10 to -20°C for about 3 h, and then lyophilise the sample in a Zirbus lyophiliser (Bad Grund, Germany) using the program plotted in Fig. 1a in the main text. Larger volumes (e.g. 1 ml) can be applied as well. Vapour crosslinking of elastin capsules was performed in vapour of 25% glutaraldehyde: 38% formaldehyde 1:1 for 24 h, optionally followed by wet crosslinking in 0.5% glutaraldehyde in phosphate buffer pH 7.4 for 2 h. Concentrations for type I collagen (Symatase Biomatériaux, Chaponost, France) and bovine serum albumin (Sigma, St. Louis, MO, USA) were 0.25% (w/v) and for heparin (Sigma) was 1.0% (w/v).

Incorporation of fluorescent probes into elastin capsules

Fluorescent probes were incorporated in the capsule wall by the addition of 50 μ g probe per ml 2.0% (w/v) elastin solution prior to freezing and lyophilisation. Fluorescent probes included Alexa Fluor594-labeled goat anti-mouse antibodies (150,000 Da) and Alexa Fluor488 or 594-labeled dextrans (10,000 Da). Capsule shells were crosslinked for 24 h by vapour crosslinking. Incorporation of fluorescent probes in the capsule lumen was performed by a 96 h incubation of vapour-crosslinked capsules in a solution of 50 μ g probe in either 1 ml MilliQ water (for dextrans) or 1 ml ethanol (for DiOC18; see below), followed by wet crosslinking, and three washings with MilliQ water or 100% ethanol to remove non-included probe. Probes included Alexa Fluor488 or 594-labeled dextran (10,000 Da) and 3,3'-diocadecyloxacarbocyanine perchlorate DiOC18 (882 Da), all from Molecular Probes Europe (Leiden, The Netherlands).

Incorporation of enzymes into elastin capsules

Peroxidase-labeled IgG (Sigma) was incorporated in the capsule wall by the addition of 100 µg enzyme per ml 2.0% (w/v) elastin solution prior to freezing and lyophilisation. Capsule shells were crosslinked for 24 h by vapour crosslinking. Alkaline phosphatase-labeled IgG (Dako, Glostrup, Denmark) was incorporated in the capsule lumen (100 µg enzyme per ml 50 mM Tris-HCl for 72 h at 4°C) followed by a 2 h wet crosslinking and washed three times with Tris-HCl. Enzyme activities were studied after reaction with Fast Red TR Salt for alkaline phosphatase followed by three washing steps with Tris-HCl, and a reaction with 3,3-diaminobenzidine tetrahydrochloride (DAB) for peroxidase followed by three washings with Tris-HCl (20).

Degradation studies using elastase

Enzymatic degradation of capsules containing fluorescent probes (Alexa Fluor488-labeled dextran in the capsule wall and Alexa Fluor594-labeled dextran in the capsule lumen) was assessed after incubation with elastase (Sigma) in 100 mM Tris-HCl pH 8.0 and analysed with time resolved confocal laser scanning microscopy (CLSM) and scanning electron microscopy (SEM). Specimens were treated with 0.4 U/ml elastase and analysed up to 30 min at 22°C.

Microscopical techniques

Scanning electron microscopy (SEM): Lyophilised samples were sputtered with gold and studied with a JEOL JSM-6310 SEM apparatus with an accelerating voltage of 15 kV. Wet samples first were critical point dried using liquid CO₂. Transmission electron microscopy (TEM): Vapour crosslinked samples (stabilised samples) were post-fixed with 0.5% glutaraldehyde in 10 mM PB (pH 7.4) for at least 24 h followed by 1% (w/v) osmium tetroxide in 0.1 M PB for 1 h. After a rinsing period of 3 h with 0.1 M phosphate buffer, samples were de-hydrated in an ascending series of ethanol in water solutions, embedded in epoxy resin (Epon 812). Sections (60 nm) were picked up on formvar-coated grids, post stained with lead citrate and uranyl acetate, and examined in a JEOL 1010 electron microscope. Fluorescence-activated cell sorting (FACS): The average size of the stabilised capsules was analysed by flow cytometry (Epics Elite flow cytometer, Coulter, Luton, UK). Capsules were gated according to their forward and side scattering patterns. Fractions were collected on poly-D-lysine coated coverslips and left to attach for 60 min. Coverslips were critical point dried, sputtered with gold, and studied by SEM. Fluorescence microscopy: Elastin preparations (2.0% (w/v) in 0.25 M acetic acid) were placed on a glass slide and studied before and after freezing in liquid nitrogen, using a fluorescence microscope with an I3 filter (Leica, DM 6000 B, Leica Microsystems, Wetzlar, Germany). Freeze microscopy: A droplet of 2.0% (w/v) elastin in 0.25 M acetic acid was put on a glass slide, frozen in liquid nitrogen and analysed in a -70°C precooled custom-built freeze microscope with temperature registration (RIVM National Institute for Public Health and the Environment, Bilthoven, The Netherlands). The temperature of the frozen sample was increased until a temperature of -18°C was reached. Confocal microscopy: Elastin capsules with incorporated fluorescent probes were deposited on poly-D-lysine coated coverslips. Confocal images were made at 488 nm and 594 nm with a BioRad MRC1024 confocal laser scanning microscope, equipped with an argon/krypton laser, using a 60x 1.4 NA oil objective and LaserSharp2000 acquisition software. Light microscopy: Capsules with incorporated enzymes were placed on a glass slide, stained as described above and studied using a Leica DM 6000 B microscope.

SUPPLEMENTARY MATERIAL

Movie showing annealing of frozen samples

The file [Daamen et al movie.avi](#) shows the change in morphology of 2.0% (w/v) elastin in 0.25 M acetic acid frozen in liquid nitrogen and incubated for 27 min at -70 to -18°C as analysed by freeze microscopy. In this process, spheres formed out of the thin sheets, suggesting that annealing is necessary to obtain globular structures.

REFERENCES

1. D.D.Lasic. "Novel applications of liposomes." *Trends Biotechnol.* 16, no. 7(July 1998):307-21.
2. H.Rosen and T.Abribat. "The rise and rise of drug delivery." *Nat.Rev.Drug Discov.* 4, no. 5(May 2005):381-85.
3. D.E.Discher and A.Eisenberg. "Polymer vesicles." *Science* 297, no. 5583(August 2002):967-73.
4. W.Wang, L.Tetley, and I.F.Uchegbu. "The level of hydrophobic substitution and the molecular weight of amphiphilic poly-L-lysine-based polymers strongly affects their assembly into polymeric bilayer vesicles." *J.Colloid Interface Sci.* 237, no. 2(May 2001):200-07.
5. M.Antonietti and S.Förster. "Vesicles and liposomes: A self-assembly principle beyond lipids." *Adv.Mater.* 15, no. 16(2003):1323-33.
6. D.H.W.Hubert, M.Jung, and A.L.German. "Vesicle templating." *Adv.Mater.* 12, no. 17(2000):1291-94.
7. M.Chen, L.Wu, S.Zhou, and B.You. "A method for the fabrication of monodisperse hollow silica spheres." *Adv.Mater.* 18,(2006):801-06.
8. C.S.Peyratout and L.Dahne. "Tailor-made polyelectrolyte microcapsules: from multilayers to smart containers." *Angew.Chem.Int.Ed.* 43, no. 29(July 2004):3762-83.
9. A.D.Dinsmore, M.F.Hsu, M.G.Nikolaides, M.Marquez, A.R.Bausch, and D.A.Weitz. "Colloidosomes: selectively permeable capsules composed of colloidal particles." *Science* 298, no. 5595(November 2002):1006-09.
10. P.F.Noble, O.J.Cayre, R.G.Alargova, O.D.Velev, and V.N.Paunov. "Fabrication of "hairy" colloidosomes with shells of polymeric microrods." *J.Am.Chem.Soc.* 126, no. 26(July 2004):8092-93.
11. A.D.Sutton, R.A.Johnson, P.J.Senior, and D.Heath. Preparation of diagnostic agents. 956875[5518709]. 1996. 15-3-1993. Ref Type: Patent
12. M.Tsung and D.J.Burgess. "Preparation and stabilization of heparin/gelatin complex coacervate microcapsules." *J Pharm.Sci.* 86, no. 5(May 1997):603-07.
13. E.Quevedo, J.Steinbacher, and D.T.McQuade. "Interfacial polymerization within a simplified microfluidic device: capturing capsules." *J Am.Chem Soc.* 127, no. 30(August 2005):10498-99.
14. J.Bartels, H.Borchers, H.Hausen, K.H.Hellwege, Kl.Schäfer, and E.Schmidt. *Landolt-Börnstein Zahlenwerte und funktionen aus physik, chemie, astronomie, geophysik und technik - II Eigenschaften der materie in ihren aggregatzuständen*, Berlin: Springer Verlag, 1962.
15. R.D.Deegan, O.Bakajin, T.F.Dupont, G.Huber, S.R.Nagel, and T.A.Witten. "Capillary flow as the cause of ring stains from dried liquid drops." *Nature* 389,(1997):827-29.
16. R.D.Deegan, O.Bakajin, T.F.Dupont, G.Huber, S.R.Nagel, and T.A.Witten. "Contact line deposits in an evaporating drop." *Phys.Rev.E* 62, no. 1 Pt B(July 2000):756-65.
17. W.F.Daamen, T.Hafmans, J.H.Veerkamp, and T.H.Van Kuppevelt. "Isolation of intact elastin fibers devoid of microfibrils." *Tissue Eng.* 11, no. 7-8(2005):1168-76.
18. S.M.Partridge, H.F.Davis, and G.S.Adair. "The chemistry of connective tissues. 2 - Soluble proteins derived from partial hydrolysis of elastin." *Biochem.J.* 61, no. 1(1955):11-21.
19. W.F.Daamen, T.Hafmans, J.H.Veerkamp, and T.H.Van Kuppevelt. "Comparison of five procedures for the purification of insoluble elastin." *Biomaterials* 22, no. 14(July 2001):1997-2005.
20. J.D.Bancroft and A.Stevens. *Theory and practice of histological techniques*, Edinburgh (UK): Churchill Livingstone, 1990.

Chapter 8

SUMMARY AND FUTURE DIRECTIONS

SAMENVATTING EN TOEKOMSTVISIE

SUMMARY

The general aim of tissue engineering and regenerative medicine is to restore or replace damaged tissues and organs by using biomaterials with or without cells. Biomaterials must have the capacity to become structurally integrated with the surrounding tissue, and initiate or restore local processes. Within regenerative medicine, different strategies with respect to biomaterials are known, e.g. the use of scaffolds, injectables, coatings and delivery devices.

The first part of this thesis describes the tools, preparation and evaluation of composite collagen-based biomaterials that create a specific microenvironment for tissue regeneration. The second part of this thesis describes the tools and potential clinical applications of injectable collagen to induce local hemostasis. The third part of this thesis describes the preparation of novel delivery vehicles for drugs/cells, based on natural matrix molecules.

PART 1: TOOLS, PREPARATION AND EVALUATION OF COLLAGEN-BASED BIOMATERIALS FOR TISSUE ENGINEERING

In **Chapter 1** an overview is given of the fundamental aspects of the preparation of collagen-based scaffolds for soft tissue engineering, in particular scaffolds composed of type I collagen, elastin, glycosaminoglycans and growth factors. The aim of tailor-made scaffolds for tissue engineering is to resemble the extracellular matrix composition of a specific tissue. Collagen has been used as a biological constituent for biomaterials, due to its biocompatibility and good mechanical and biological properties. Collagen-glycosaminoglycan scaffolds offer the opportunity to regulate cellular activities, and the binding and sustained release of growth factors (i.e. heparin-binding growth factors; VEGF, FGF-2 or EGF), resulting in a bio-active scaffold. The addition of growth factors to acellular scaffolds may increase angiogenesis. Therefore, large-scale production and purification of growth factors is desirable for tissue engineering. In **Chapter 2**, the cloning of rat recombinant VEGF-164, its expression in a *Pichia pastoris* expression system, and the production of large quantities of the growth factor using fermentation is described. The produced rat recombinant VEGF was shown to be biologically active. In **Chapter 3**, the rat VEGF was used to construct scaffolds with different combinations of type I collagen, heparin, rrFGF-2 and rrVEGF-164, and the tissue response after subcutaneous implantation in rats was evaluated. The combination of VEGF and FGF-2 resulted both in a larger area of blood vessels and a more developed vasculature in the a-cellular scaffolds.

PART 2: TOOLS AND POTENTIAL CLINICAL APPLICATIONS OF INJECTABLE COLLAGEN TO INDUCE LOCAL HEMOSTASIS

Collagen is biocompatible and biodegradable which allows remodelling in the host after implantation. These characteristics, in combination with its hemostatic activity, make collagen a good candidate for femoral artery pseudoaneurysm (PSA) treatment. **Chapter 4** describes the development of a porcine femoral PSA model using a one-step surgical procedure. The model involved the preparation of an arteriovenous shunt between the femoral artery and femoral vein, segmenting ~2 cm of the vein using proximal and distal ligatures. **Chapter 5** describes the preparation and characterisation of highly purified injectable fibrillar type I collagen and its evaluation in the PSA model. The outcome of this study indicated that sterilised injectable collagen can be prepared without major loss of its structural characteristics and platelet activity, and that *in vivo*, the injectable collagen formed a dense network

and triggered (partial) local hemostasis. Although optimisation is needed, injectable collagen fibrils may be useful for femoral PSA treatment.

PART 3: PREPARATION OF NOVEL DELIVERY VEHICLES, BASED ON NATURAL MATRIX MOLECULES: MICRO-CAPSULES AND MICRO-SCAFFOLDS

With respect to *in vivo* applications, it would be a major advantage if drug delivery vehicles or micro-carriers could be prepared from tissue derived molecules. In **Chapter 6** and **Chapter 7** the preparation of micro-capsules and micro-scaffolds from natural molecules is described. Both techniques rely on a combination of freezing/lyophilisation techniques. In the initial freezing step, the protein-water-acetic acid solution/suspension phase separates from the ice (water only). Differently sized micro-scaffolds (Chapter 6) can be prepared by pulverising frozen collagen suspensions under liquid nitrogen conditions using a cutting mill with defined sieve inserts and a subsequent lyophilisation step, followed by EDC/NHS crosslinking. Micro-scaffolds displayed an open porous network with lamellae formed after the freezing and freeze drying step. In case of microcapsules (Chapter 7), globules are formed during the freezing and annealing step of the process. In the subsequent lyophilisation step, ice sublimates resulting in dry protein with a defined capsule-like structure. The preparation of microcapsules was critically depended on annealing during freezing and protein concentration. The microcapsules show potential for *in vivo* targeting and drug delivery, whereas injectable micro-scaffolds can function as carrier for cells and effector molecules such as glycosaminoglycans and growth factors, thus allowing tissue regeneration without the need of surgery.

FUTURE DIRECTIONS

The use of specific growth factors in combination with collagen-based scaffolds is described in this thesis. Growth factors were shown to be key factors in acellular constructs. We found enhanced angiogenesis in collagen-based scaffolds combined with glycosaminoglycans, VEGF and FGF-2. It is highly plausible that the use of multiple growth factors may result in even more tissue specific regeneration. Since many tissues have a specific organisation (e.g. skin, bladder, urethra), special attention must be given to localisation, dose and release of the growth factors. In this respect, a possible application for lyophilisomes is to act as micro-containers for growth factors. This study showed that it is possible to incorporate different biomolecules into the capsule wall and/or lumen of the capsule. This two-way system offers the construction of “smart” capsules, for instance those containing biomolecules (growth factors) in the lumen and/or extracellular matrix molecules in the wall. This may generate a slow-release depot of signalling molecules in collagen-based scaffolds. In addition, injectable micro-scaffolds with both glycosaminoglycans and growth factors generate the possibility to enhance local tissue regeneration without surgery. The composition and structure of the injectable micro-scaffolds make them potential carriers to create a niche of growth factors and/or cells in damaged tissue, e.g. to induce local neovascularisation in ischemic tissue.

Another strategy which is described in this thesis is the use of collagen for local hemostasis to treat pseudoaneurysms (PSA). Although further research is needed, the outcome of the *in vivo* study indicated that injectable collagen may be an effective therapeutic alternative for the current PSA treatment. New collagen-based injectables may be necessary to improve its efficacy. Particularly for femoral PSA treatment, it might be attractive to combine collagen fibrils with thrombin to not only initiate the primary hemostasis but also induce the secondary (clotting factor mediated) hemostasis. In addition, the combination of contrast agents may assist in the proper follow-up after treatment. Depending on the clinical relevance, combinations of collagen-based material with other natural biomaterials may create new clinical applications, and have high potential in the field of tissue engineering and reconstructive medicine.

SAMENVATTING

Het algemene doel van weefseltechnologie en regeneratieve geneeskunde is om middels materialen, met of zonder cellen, beschadigde weefsels en organen te herstellen of te vervangen. Deze biomaterialen moeten de eigenschap hebben om in het omliggende weefsel te kunnen integreren en derhalve lokale processen te stimuleren of te herstellen. Met betrekking tot biomaterialen zijn er binnen de regeneratieve geneeskunde verschillende strategieën bekend, bijvoorbeeld het gebruik van dragermaterialen (matrices), injecteerbare materialen, coatings en afgiftesystemen.

Het eerste gedeelte van dit proefschrift beschrijft de benodigdheden, de bereiding en de evaluatie van op collageen gebaseerde biomaterialen, die de mogelijkheid bieden een specifieke micro-omgeving te creëren en zo voor weefselherstel te zorgen. Het tweede deel van dit proefschrift beschrijft de benodigdheden en de potentiële klinische toepassingen van injecteerbaar collageen voor lokale hemostase. Het derde onderdeel van dit proefschrift beschrijft het maken van nieuwe materialen die gebaseerd zijn op natuurlijke matrixmoleculen en die mogelijkheden bieden voor afgifte van medicijnen en/of cellen.

DEEL 1: BENODIGDHEDEN, BEREIDING EN EVALUATIE VAN OP COLLAGEEEN GEBASEERDE BIOMATERIALEN VOOR WEEFSELTECHNOLOGIE

In **hoofdstuk 1** wordt een overzicht gegeven van de fundamentele aspecten van de bereiding van op collageen gebaseerde matrices voor weefseltechnologie, bestaande uit collageen type I, elastine, glycosaminoglycanen en groeifactoren. Met deze op maat gemaakte dragermaterialen wordt de extracellulaire matrix van een bepaald type weefsel nabootst. Collageen wordt vaak gebruikt als hoofdbestanddeel van biomaterialen vanwege de biocompatibiliteit en de goede mechanische en biologische eigenschappen. Dragermaterialen bestaande uit collageen en glycosaminoglycanen bieden de mogelijkheid om het celgedrag en de afgifte van groeifactoren (heparine bindende groeifactoren zoals VEGF, FGF-2 of EGF) te reguleren, waardoor deze ook wel bioactieve dragermaterialen worden genoemd. De toevoeging van groeifactoren aan acellulaire dragermaterialen kan bijvoorbeeld de bloedvat-ingroei stimuleren. Daarom is een grootschalige productie en zuivering van dergelijke groeifactoren binnen de weefseltechnologie zeer gewenst. In **hoofdstuk 2** wordt het kloneren van recombinant rat VEGF-164, de expressie in het *Pichia pastoris* expressiesysteem en het grootschalig produceren van deze groeifactor middels fermentatie beschreven. Het geproduceerde recombinant rat VEGF blijkt biologisch actief te zijn. In **hoofdstuk 3** wordt de bereiding van dragermaterialen met verschillende combinaties van type I collageen, heparine, FGF-2 en VEGF-164 beschreven en worden deze materialen na subcutane implantatie in ratten geëvalueerd. De combinatie van VEGF en FGF-2 stimuleert de ontwikkeling van grotere en beter ontwikkelde bloedvaten in acellulaire dragermaterialen.

DEEL 2: BENODIGDHEDEN EN MOGELIJKE KLINISCHE TOEPASSINGEN VAN INJECTEERDARE COLLAGEEEN PREPARATEN VOOR LOKALE HEMOSTASE

Collageen is biocompatibel en biologisch afbreekbaar, waardoor herstel in het lichaam na implantatie mogelijk wordt gemaakt. Deze eigenschappen, in combinatie met de hemostatische activiteit, maakt collageen een goede kandidaat voor de behandeling van femorale pseudoaneurysma (PSA). **Hoofdstuk 4** beschrijft de ontwikkeling van een femoraal PSA

varkensmodel, gebruikmakend van één chirurgische ingreep. Een arterioveneuze shunt wordt aangelegd tussen de *arteria femoralis* en *vena femoralis*, in combinatie met het segmenteren van ~2 cm vene middels proximale en distale knopen. **Hoofdstuk 5** beschrijft de bereiding en karakterisatie van hoogwaardig gezuiverd injecteerbaar fibrillair collageen type I en de toepasbaarheid ervan in het PSA model. Uit deze studie blijkt dat injecteerbaar collageen gesteriliseerd kan worden zonder al te veel verlies van de structurele eigenschappen en bloedplaatjesactiviteit. Na toediening *in vivo*, vormt het injecteerbare collageen een compact netwerk en induceert (gedeeltelijk) de lokale hemostase. Hoewel optimalisatie nodig is, zou injecteerbaar collageen een alternatief kunnen bieden voor de behandeling van femorale PSA.

DEEL 3: BEREIDING VAN NIEUWE AFGIFTESYSTEMEN OP BASIS VAN NATUURLIJKE MATRIX MOLECULEN: MICROCAPSULES EN MICRODRAGERS.

Met betrekking tot *in vivo* toepassingen zou het een groot voordeel zijn als afgiftesystemen en microdragers uit natuurlijke moleculen gemaakt kunnen worden. In **hoofdstuk 6** en **hoofdstuk 7** wordt de bereiding van microcapsules en microdragers uit natuurlijke moleculen beschreven. Beide technieken zijn gebaseerd op een combinatie van vries- en vriesdroogtechnieken. De initiële bevroingsstap zorgt voor een fasescheiding resulterend in een eiwit-azijnzuur-water mengsel en ijs (water alleen). Microdragers van verschillende grootte (hoofdstuk 6) kunnen worden bereid door de collageensuspensie in vloeibare stikstof in te vriezen, te verpulveren in een machine met verschillende zeefgroottes, te vriesdrogen en uiteindelijk te crosslinken middels EDC/NHS. De microdragers vormen dan een open en poreus netwerk met lamellen. In geval van microcapsules (hoofdstuk 7), worden er tijdens het invriezen en incuberen kleine bolletjes gevormd. In de daaropvolgende vriesdroogstap sublimeert het ijs hetgeen resulteert in droog eiwit met een gedefinieerde bolstructuur. De bereiding van microcapsules is afhankelijk van de eiwitconcentratie en de incubatietijd tijdens het invriezen. De microcapsules zouden mogelijk toegepast kunnen worden voor gereguleerde medicijnafgifte *in vivo*. De injecteerbare microdragers kunnen mogelijk worden gebruikt voor het lokaal toedienen van cellen en effectormoleculen, zoals glycosaminoglycanen en groeifactoren, waardoor weefselregeneratie zonder een invasieve ingreep mogelijk wordt gemaakt.

TOEKOMSTVISIE

In dit proefschrift wordt het gebruik van specifieke groeifactoren in combinatie met collageene dragermaterialen voor toepassing in regeneratieve geneeskunde beschreven. Uit dit onderzoek bleek dat groeifactoren belangrijke factoren zijn voor acellulaire constructen. In deze studie observeerden we dat de bloedvatvorming wordt bevorderd als collageen dragermaterialen worden gecombineerd met glycosaminoglycanen, VEGF en FGF-2. Het is aanmerkelijk dat ook bij gebruik van andere weefselgerelateerde groeifactoren er een meer weefsel specifieke regeneratie wordt geïnduceerd. Aangezien veel weefsels een specifieke organisatie hebben (bijv. huid, blaas, urethra), moet er meer aandacht worden besteed aan de locatie, dosering en afgifte van deze groeifactoren. Een mogelijkheid is om lyophilisates als microcontainers voor groeifactoren te gebruiken. Dit onderzoek heeft aangetoond dat het mogelijk is om verschillende biomoleculen in de wand en/of lumen van de capsules te lokaliseren. Deze twee-weg strategie biedt de mogelijkheid om "slimme" capsules te maken, bijvoorbeeld capsules met biomoleculen (groeifactoren) in het lumen en/of extracellulaire matrix moleculen in de wand. In combinatie met op collageen gebaseerde dragers zouden deze capsules voor een langzame en gecontroleerde afgifte van dergelijke signaalmoleculen kunnen zorgen. Daarnaast hebben injecteerbare microdragers in combinatie met glycosaminoglycanen en groeifactoren de mogelijkheid om lokaal de weefselregeneratie te stimuleren zonder gebruik te maken van een chirurgische ingreep. Door de samenstelling en structuur van de injecteerbare micro-dragers zijn het in potentie goede materialen voor het lokaal aanbrengen van groeifactoren en/of cellen in beschadigd weefsel, bijvoorbeeld voor het stimuleren van neovascularisatie in ischemisch weefsel.

Een andere strategie die in dit proefschrift is beschreven, is het gebruik van collageen als hemostatisch middel voor de behandeling van pseudoaneurysma (PSA). Het *in vivo* onderzoek heeft aangetoond dat het injecteerbare collageen een mogelijk therapeutisch alternatief is voor de behandeling van PSA, hoewel verder onderzoek noodzakelijk is. Nieuwe injecteerbare collageenpreparaten zijn nodig om de effectiviteit te verbeteren. Vooral voor femorale PSA behandeling kan het aantrekkelijk zijn om collageenfibrillen te combineren met thrombine, om zo naast de primaire bloedstolling ook de secundaire stolling (stollingsfactor gemedieerde stolling) te stimuleren. Bovendien zou een combinatie met een contrast-middel ervoor kunnen zorgen dat de preparaten beter te volgen zijn in het lichaam, wat zowel het onderzoek als de behandeling kan vereenvoudigen.

In zijn algemeenheid kan gesteld worden dat collageene materialen in combinatie met andere natuurlijke biomaterialen veel potentie hebben voor weefseltechnologie en reconstructieve geneeskunde en gebruikt kunnen worden voor nieuwe klinische toepassingen.

Chapter 9

AUTHOR INFORMATION:

CURRICULUM VITAE

LIST OF PUBLICATIONS

DANKWOORD

COLOUR FIGURES

CURRICULUM VITAE

Paul Geutjes werd geboren op 27 juni 1977 te Wijchen, en behaalde in 1993 zijn MAVO diploma aan de Scholengemeenschap te Wijchen. Hij heeft na de Middelbare Laboratorium Opleiding (MLO, '93-'97) en de Hogere Laboratorium Opleiding (HLO, '97-'00) Biomedische gezondheidswetenschappen (BMW, '00-'03) gestudeerd aan het Universitair Medisch Centrum St Radboud te Nijmegen.

In 2004 is hij als junior onderzoeker begonnen bij de afdeling Biochemie, Nijmegen Centre for Molecular Life Sciences (NCMLS), Universitair Medisch Centrum St Radboud te Nijmegen (Prof. dr. R.E. Brock, Dr. T.H. van Kuppevelt). Hier heeft hij onderzoek gedaan naar de ontwikkeling van nieuwe methodieken en modellen voor weefseltechnologie. Dit onderzoek kende een commerciële kant, aangezien een deel van zijn project in directe samenwerking met het Nijmeegse bedrijf Aap bio implants - EMCM BV werd uitgevoerd. De resultaten van het promotieonderzoek staan in dit proefschrift beschreven. Tijdens zijn promotieonderzoek was hij betrokken bij diverse onderwijstaken en het begeleiden van studenten en stagiaires. Tevens heeft hij zijn onderzoeksresultaten mogen presenteren op zowel nationale als internationale congressen.

Tegenwoordig werkt hij aan een post-doc project bij de afdeling Urologie, Universitair Medisch Centrum St Radboud te Nijmegen (Prof. dr. W.F. Feitz) en coördineert het weefseltechnologisch onderzoek voor het ontwikkelen van nieuwe behandelingsmethodieken voor aangeboren afwijkingen (Soft Tissue Engineering for Congenital birth defects, www.EuroSTEC.eu). In 2007 heeft hij een NWO Casimir subsidie mogen ontvangen om in een bedrijf met cleanroom faciliteiten (Aap bio implants - EMCM BV) een productielijn voor tissue engineering constructen op te starten.

LIST OF PUBLICATIONS

Articles

Geutjes PJ, Daamen WF, Buma P, Feitz WF, Faraj KA, van Kuppevelt TH. From molecules to matrix: construction and evaluation of molecularly-defined bioscaffolds. *Adv Exp Med Biol.* 2006;585:279-95. Review.

Nillesen STM, Geutjes PJ, Wismans RG, Schalkwijk J, Daamen WF, van Kuppevelt TH. Increased angiogenesis in acellular scaffolds by combined release of FGF2 and VEGF. *J Control Release.* 2006;116(2):e88-90.

Nillesen STM, Geutjes PJ, Wismans RG, Schalkwijk J, Daamen WF, van Kuppevelt TH. Increased angiogenesis and blood vessel maturation in acellular collagen-heparin scaffolds containing both FGF2 and VEGF. *Biomaterials.* 2007;28(6):1123-31.

Daamen WF*, Geutjes PJ*, van Moerkerk HT, Nillesen STM, Wismans RG, Hafmans TH, van den Heuvel LPWJ, Pistorius AMA, Veerkamp JH, van Hest JCM, van Kuppevelt TH. "Lyo-philisomes": a new type of (bio)capsules. *Adv Mat.* 2007;19(5):673-77 *Equally contributed.

Geutjes PJ*, Nillesen STM*, Lammers G, Daamen WF, van Kuppevelt TH. Expression, production and biological activity analyses of recombinant rat VEGF-164. *Protein Expr Purif.* 2010;69(1):76-82. *Equally contributed.

Geutjes PJ, van der Vliet JA, Faraj KA, de Vries N, van Moerkerk HT, Wismans RG, Hendriks T, Daamen WF, van Kuppevelt TH. An animal model for femoral artery pseudoaneurysms. *J Vasc Inter Radiol.* 2010;21(7):1078-83.

Geutjes PJ, van der Vliet JA, Faraj KA, de Vries N, van Moerkerk HT, Wismans RG, Hendriks T, Daamen WF, van Kuppevelt TH. Preparation and characterisation of injectable fibrillar type I collagen and evaluation for pseudoaneurysm treatment in a pig model. *J Vasc Surg.* 2010 In press.

Geutjes PJ, Faraj KA, Daamen WF, van Kuppevelt TH. Preparation of different sized porous collagen type I micro-scaffolds. *J Tissue Eng Regen Med.* 2010 In press.

Nuininga JE, Koens MJW, Tiemessen DM, Oosterwijk E, Daamen WF, Geutjes PJ, van Kuppevelt TH, Feitz WF. Urethral reconstruction of critical defects in rabbits using molecularly-defined tubular type I collagen biomatrices: key issues in growth factor addition. *Tissue Eng Part A.* 2010 In press.

Hosper NA, Eggink AJ, Roelofs LAJ, Wijnen RMH, van Luyn MJA, Bank RA, Harmsen MC, Geutjes PJ, Daamen WF, van Kuppevelt TH, Tiemessen DM, Oosterwijk E, Crevels AJ, Blokkx WAM, Lotgering FK, van den Berg PP, Feitz WF. Intra-uterine tissue engineering of full thickness skin defects in a fetal sheep model. *Biomaterials.* 2010;31(14):3910-9.

Koens MJW, Geutjes PJ, Faraj KA, Hilborn J, Daamen WF, van Kuppevelt TH. Organ-specific tubular collagen scaffolds for tissue engineering applications. *Conditionally accepted.*

Karaj KA*, Brouwer KM*, Geutjes PJ, Versteeg EM, Wismans RG, Deprest JA, Chajra H, Tiemessen DM, Feitz WF, Oosterwijk E, Daamen WF, van Kuppevelt TH. The effect of ethylene oxide sterilisation, beta irradiation and gamma irradiation on collagen fibril-based scaffolds. Evaluation of biological, physical and chemical parameters. *Submitted*. *Equally contributed.

Brouwer KM, van Rensch P, Harbers VEM, Geutjes PJ, Koens MJW, Wijnen RMH, Daamen WF, van Kuppevelt TH. Construction of collagenous scaffolds with a radial pore structure for tissue engineering. *Submitted*.

Book chapters

Farhat WA, Geutjes PJ. Artificial biomaterials for urological tissue engineering. *Biomaterials and Tissue Engineering in Urology 2009*.

Daamen WF, Faraj KA, Koens MJW, Lammers G, Brouwer KM, Uijtdewilligen PJE, Nillesen STM, Roelofs LA, Nuininga JE, Geutjes PJ, Feitz WF, van Kuppevelt TH. Extracellular matrix-based scaffolds from scratch. *The Handbook of Intelligent Scaffold for Regenerative Medicine 2009*.

Patents

Daamen WF, Geutjes PJ, van Kuppevelt TH. Method for obtaining hollow particles. *Patent pending P27948EP00*.

DANKWOORD

Dus dit was promoveren... Nu ik eindelijk op mijn promotie terug kan kijken kom ik tot de volgende belangrijke conclusie; promoveren doe je niet alleen! Daarom wil ik bij deze iedereen bedanken die ook maar enige bijgedragen heeft geleverd of interesse heeft getoond in mijn proefschrift.

In het bijzonder wil ik mijn promotor Prof. dr. Roland Brock en copromotoren Dr. Toin van Kuppevelt, Dr. Willeke Daamen en Dr. Daan van der Vliet bedanken.

Beste Roland, bedankt voor de mogelijkheid tot promotieonderzoek binnen jouw afdeling. Bedankt voor het vertrouwen en dat je mijn promotor wilde zijn.

Beste Toin, ontzettend bedankt dat ik binnen jouw sectie de mogelijkheid heb gehad om te promoveren. Het was een aardige klus maar het is uiteindelijk goed gekomen. Ik heb jouw flexibiliteit altijd erg gewaardeerd. Met name in het laatste jaar van mijn promotie waarbij je accepteerde dat ik parttime voor EuroSTEC ging werken. Tijdens de artikelbesprekingen hadden we de nodige discussies. In sommige gevallen eindigde deze in een nieuw en eigenaardig experiment, gecombineerd met een dosis humor. Ik heb ook goede herinneringen aan de vele bezoeken bij verschillende bedrijven. In de trein de laatste nieuwtjes bespreken en dan nog even checken hoe het thuis gaat. Ik hoop dat we nog bij vele tissue engineering projecten mogen samenwerken.

Beste Willeke, jij ook ontzettend bedankt voor de begeleiding. Wat begon met het begeleiden van mijn stage ging al snel over tot het begeleiden van mijn promotie. Jouw ontelbare e-mails, telefoontjes, besprekingen, nagekeken versies hebben mede voor dit succes gezorgd. Bedankt dat je naast je drie kids en de dagelijkse werkzaamheden toch nog wat uurtjes voor me hebt weten te vinden. Ik hoop dat ook wij nog bij vele projecten mogen samenwerken.

Beste Daan, ondanks je overvolle agenda maakte je tijd voor me. Tussen je klinische taken door opereren op het CDL. Ik ben nog steeds onder de indruk van je chirurgische expertise, het harde werken en je dosis nuchterheid. Bedankt voor de soepele samenwerking.

De leden van de manuscriptcommissie, Prof. dr. John Jansen, Prof. dr. Ruud Bank en Prof. dr. Pieter Buma, wil ik bedanken voor het snel beoordelen van mijn proefschrift.

De medewerkers van sectie Matrix Biochemie wil ik bedanken voor de fijne samenwerking. In het bijzonder wil ik bedanken;

Herman, tussen de experimenten door hadden we regelmatig onze dagelijkse gesprekken. Naast het bespreken van de wereldproblematiek en de laatste klussen in huis, deelde jij ook jouw oerdegelijke Biochemische kennis. Jouw nuchterheid zette mij altijd weer over tot relativering, met name met jouw bekende woorden 'geen probleem!'. Bedankt voor de fijne samenwerking.

Kaeuis, of het nu ging om pulveriseren, zuiveren of het maken van scaffolds, je was altijd bereid om advies te geven of te helpen. Tijdens de experimenten op het CDL heb je vele malen naast me gestaan en bij Aap – EMC bio implants BV hebben we veel overleg gehad. Je maakte regelmatig tijd voor een praatje wat ik altijd erg heb gewaardeerd.

Arie (*Arpe*), de man met de grote glimlach. Door jou werden mijn lachspieren regelmatig getriggerd. Ook al werden de moppen en versprekingen vaak hergebruikt, je zorgde toch altijd voor die heerlijke schater. Met je vele reisverhalen, foto's en films nam je me regelmatig op reis. Bedankt voor je ondersteuning.

Nu dan mijn mede junior onderzoekers, Nicole, Suzan, Mieke, Joost, Tessa, Martin, Gerwen, Peter, Xander, Katrien en Etienne. We hebben veel lief en leed gedeeld. Ik heb goede herinneringen aan de gezamenlijke congressen in Papendal, NBTE en DPTe meetings, lab uitjes en de kerstdiners en discoavondjes. De foto's (en filmpjes) die daar zijn gemaakt spreken boekdelen... Succes bij het afronden van jullie promotie en/of verdere carrière.

Natuurlijk wil ik ook de andere (ex)collega's van sectie Matrix Biochemie bedanken voor hun bijdrage aan het proefschrift en de super gezellige sfeer op het lab; Elly, Els, Ronnie, Gerdy, Toon, Cindy, Marianne en de diehard SQ-laaf gangers Theo, Paul J. en Guido.

Verder wil ik iedereen van het CDL bedanken voor de enthousiaste hulp bij de experimenten. Hiervan wil ik een aantal mensen extra noemen; Alex H., Wilma, Jeroen M, Connie, Geertje, Mathieu, Hennie, Conrad, Maikel, Jeroen de B, Janneke, Henk en Leo. Jullie flexibiliteit en natuurlijk ook gezelligheid heb ik altijd erg gewaardeerd.

Directe begeleiders van Aap – EMCM bio implants BV (Noes de Vries, Rimmert Wolters, Alina Bergshoeff en Henriette Valster) wil ik bedanken voor hun input gedurende mijn promotie-onderzoek. Tijdens de vele maandelijkse meetings hebben jullie mij de commerciële 'ins en outs' bijgebracht. Dit maakte mijn promotietraject uniek.

Er zijn ook een aantal studenten die aan dit proefschrift een steentje hebben bijgedragen. Bedankt voor jullie inzet en interesse in het onderzoek gedurende mijn promotie; Lobke Gierman, Antoinette van Laarhoven en Saskia Heffener.

Prof. dr. Wout Feitz, Dr. Egbert Oosterwijk, Prof. dr. Jack Schalke en Prof. dr. Peter Mulders wil ik bedanken voor hun steun, geduld en vertrouwen bij het afronden van mijn proefschrift. Ook de andere collega's en stagiaires van de afdeling Urologie (en foetale research groep) wil ik bedanken voor de interesse en de nodige geestelijke bijstand.

I would like to thank Dr. Benjamin Herbage and Dr. Hanane Chajra (Symatase Biomatériaux, Chaponost, France) for purifying bovine fibrillar type I collagen (RTEN001) according to our protocols.

Cor van Ingen (Rijksinstituut voor Volksgezondheid en Milieu te Bilthoven) wil ik bedanken voor het gebruik van de vriesdroogmicroscop.

Ik heb de contacten met de samenwerkende afdelingen altijd erg gewaardeerd. Afdeling Biomaterialen; tijdens gezamenlijke congressen heb ik met Dennis, Lise, Corrine, Jeroen, Frank, Wouter, Joop, Sander en Edwin een hoop gezelligheid meegemaakt. Afdeling Orthopedie; Willem, bedankt voor de technische ondersteuning bij de displacement experimenten. De heren René, Gerjon, Eric en Prof. dr. Pieter Buma wil ik bedanken voor de samenwerking en de mooie gesprekken. Helaas hebben we dat ene artikelje niet meer kunnen afronden. Onder het genot van een bakkie nog maar eens bespreken?

Afdeling Hematologie; Dr. Waander van Heerde wil ik bedanken voor de ondersteuning bij de trombocyten aggregatie testen.

Afdeling Celbiologie; Huib en Jack wil ik bedanken voor de technische ondersteuning.

Afdeling Nucleaire Geneeskunde; 'de bollenman' wil met name Prof. dr. Otto Boerman, Annemarie, Cathelijne, Gerben, Maarten, Annemieke, Huub en Erik bedanken voor hun hulp en interesse. Helaas hebben de eindeloze labelingsexperimenten niet in een wetenschappelijk artikel mogen resulteren.

Mijn ex-medestudenten (MLO/HLO/universiteit), budblaffers/trekvogels en oud-huisgenoten mogen bij dit dankwoord niet ontbreken. Door jullie heb ik een geweldige studententijd gehad waarop ik nu nog altijd met veel plezier op terugkijk. Ook al heeft iedereen het erg druk, jullie hebben altijd interesse getoond.

Gosse en Bas, ook jullie bedankt voor onze vriendschap en de vele gesprekken. Ik kijk uit naar ons volgende stapavondje, al zegt mijn lever iets anders... Erik en Terry, al sinds de middelbare school hebben we lief en leed gedeeld. Jullie hebben altijd interesse getoond waarvoor ik erg dankbaar ben. Mario en Rick, jullie waren en zijn verantwoordelijk voor de nodige ontspanning. Bedankt voor het aanhoren van de vele onderzoeksverhalen en jullie nuchtere adviezen zoals bijvoorbeeld; "jongen, neem toch eens een dag vrij". Bedankt dat jullie mijn vrienden zijn.

Dennis (*Linkie*), bedankt voor je interesse en ondersteuning in de afronding van mijn proefschrift. Zonder jou had ik hier niet gestaan, want jij was degene die me heeft overgehaald om BMW te gaan studeren. Tof dat je altijd de moeite neemt om op een congres af te spreken of naar Nederland te komen. Ik ben blij dat je mijn vriend en paranif bent.

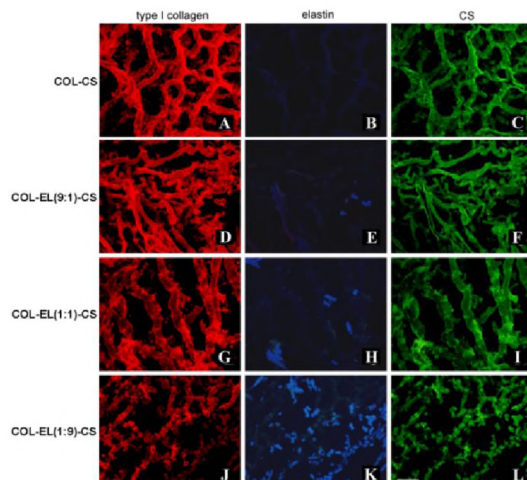
Beste (schoon)familie en vrienden, bedankt voor jullie interesse en het luisterende oor voor de frustrerende momenten die wetenschappelijk onderzoek doen soms bij mij opriepen. Joepie (UP Reclame Ravenstein), fijn dat je met het drukwerk hebt geholpen.

Mijn ouders wil ik bedanken voor de enorme steun, interesse en vertrouwen. Jullie stonden altijd klaar en zorgde voor van alles en nog wat; hulp bij de verbouwing, hulp na de geboorte van Lisa en Hanne, ophalen/wegbrengen, dingetjes regelen, etc. Zonder jullie was het nooit gelukt. Ontzettend bedankt!

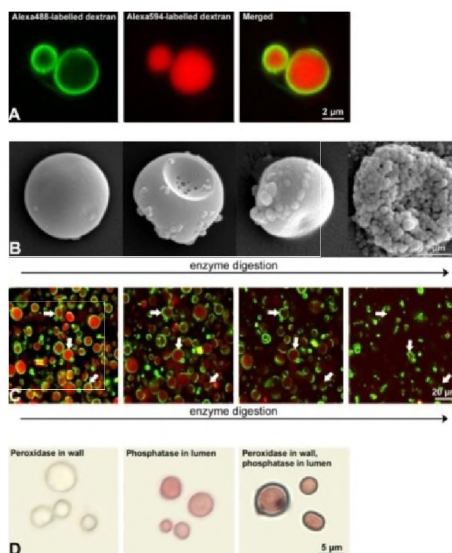
Ha broer, beste Frank, ik ben ontzettend trots dat jij mijn paranif bent. Wie had dat gedacht. Bedankt voor je interesse en nuchterheid tijdens mijn onderzoek. Nee, er wordt niet getoverd op het lab, dat was toch echt een magneetroerder...

Lisa en Hanne, terwijl jullie op één oor lagen te slapen zat papa weer eens te typen... Jullie vrolijkheid zorgde voor de ultieme ontspanning waardoor het onderzoek makkelijker te relativeren was. Ik hoop jullie nog heel lang mee te mogen maken.

Leonie, jij hebt natuurlijk een hele grote bijdrage geleverd. Je zorgde voor de mentale ondersteuning en dat de thuissituatie op de meest drukke momenten draaiende bleef. Ondanks dat het soms niet mee viel, gaf je me de tijd en ruimte om mijn ding te kunnen doen. Je verdient ontzettend veel credits voor het volbrengen van de promotie. Ontzettend bedankt dat je er altijd voor ons bent.



Chapter 1. Fig 4 Immunostaining of scaffolds containing variable amounts of collagen and elastin with covalently attached chondroitin sulfate using immunostaining for type I collagen (red) and CS (green), whereas elastin was analysed by UV optics (blue). Bar is 50 μ m. COL=collagen, EL=elastin, CS=chondroitin sulphate. Figure modified with permission from Daamen *et al.* (5).



Chapter 7. Fig. 2 Differential incorporation and release of compounds. A) a 10 kDa dextran probe labelled with Alexa Fluor488 (green) was specifically incorporated into the capsule wall followed by 24 h of vapour crosslinking, whereas a similar probe labelled with Alexa Fluor594 (red) was directed to the capsule lumen followed by 2 h of wet crosslinking (confocal laser scanning microscopy). B) upon degradation by 0.4 U/ml elastase, elastin capsules were perforated, and reassembled into nanospheres (scanning electron microscopy). C) treatment with 0.4 U/ml elastase released the (red) probe from the lumen, whereas the (green) probe was partially withheld in the wall. Arrows indicate capsules releasing their content in time (time resolved confocal laser scanning microscopy). D) peroxidase-labeled IgG was incorporated into the capsule wall followed by 24 h of vapour crosslinking, whereas alkaline phosphatase-labelled IgG was positioned in the capsule followed by 2 h of wet crosslinking.